# Time-Varying Volatility Models and Indices: A GARCH Option Pricing Approach

by

**Pierre Johan Venter**

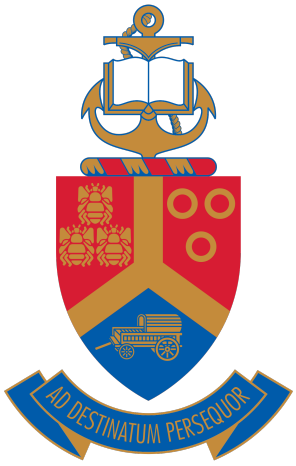


A thesis submitted to the Faculty of Natural and Agricultural Sciences in the fulfilment of the requirements for the degree of

Philosophiae Doctor

in

Actuarial Science

at the

University of Pretoria

**Supervisor: Prof. Eben Maré**

16-May-2022

# Abstract

In this thesis, the generalised autoregressive conditional heteroskedasticity (GARCH) option pricing model is applied to illiquid markets, volatility indices and in a modern derivative pricing framework. Chapter 2 provides empirical support for the use of a volatility index to obtain a more accurate GARCH option pricing model (applied to the South African equity market). In Chapter 3, the analysis (GARCH option pricing and volatility indices) is extended to FX markets. Empirical results show that asymmetry is an important factor to consider when modelling FX volatility indices.

The aim of Chapter 4 is to quantify the effect of asymmetry in the cryptocurrency market. Furthermore, the accuracy of the GARCH option pricing model applied to cryptocurrencies is also considered. Results indicate that the GARCH option pricing model produces reasonable price discovery, and that asymmetric effects are not significant when pricing cryptocurrency options. Chapter 5 focuses on the construction of a cryptocurrency volatility index, the models in Chapter 4 are used as a basis. The term structure of the GARCH generated volatility indices are consistent with expectations. Furthermore, short term volatility tends to increase when large jumps occur in the underlying asset.

In Chapter 6, the Heston–Nandi futures option pricing model is applied to Bitcoin (BTC) futures options. The model prices are compared to market prices to give an indication of the pricing performance. In addition, a multivariate Bitcoin futures option pricing methodology based on a multivatiate GARCH model is developed. The empirical results show that a symmetric model is a better fit when applied to Bitcoin futures returns, and also produces more accurate option prices compared to market prices for two out of three expiry dates considered.

Chapter 7 focuses on the pricing of volatility index options respectively. In Chapter 7, the GARCH option pricing model is applied to the Standard and Poor's 500 (S&P500) Volatility Index (VIX) option pricing. The different GARCH models are fitted to VIX futures returns. The results show that the symmetric GARCH model with skewed Student-$t$ errors is the best performing model, and that the GARCH option pricing model provides reasonable price discovery when applied to the VIX.

In Chapter 8, the standard Black model and Heston-Nandi futures options pricing model are applied to the hedging of VIX futures options. The hedge performance is compared based on the stability of the profit and loss distribution (P&L) of the hedged portfolio. Empirical results show that the Heston-Nandi futures option pricing model is more reliable when applied to hedging of VIX futures options.

The focus of Chapter 9 is the application of the GARCH model to the pricing of collateralised options in the South African equity market. Symmetric GARCH and nonlinear asymmetric GARCH (AGARCH) models are considered. The models are used to price fully collateralised and zero collateral options (European, Asian, and lookback options). The effect of collateral is illustrated by the difference between zero collateral and fully collateralised option price surfaces. Finally, the effect of asymmetry is shown by the difference between the symmetric and asymmetric GARCH option price surfaces.

Finally, a closed-form expression for a collateralised European option in the presence of counterparty credit risk and stochastic volatility is derived in Chapter 10. The model is applied to S&P500 index options. The option prices obtained are consistent with expectations, default risky options are cheaper than options with no counterparty credit risk, and fully collateralised options are more expensive when compared to zero collateral options. The effect of correlation is tested by plotting the default risky at-the-money (ATM) option price for different levels of correlation. The results indicate that correlation has an insignificant impact when pricing using the calibrated parameters.

# Acknowledgements

I owe a debt of gratitude to many people who have guided and supported me during the writing of my PhD thesis.

- First and foremost, I would like to express my deepest thanks to my supervisor, Prof Eben Maré. Thank you for your excellent guidance and patience. Your immense knowledge and experience has encouraged me in all the time of my academic research and also in daily life.
- I would like to express my sincere gratitude to my good friend and colleague, Alexis Levendis, for many meaningful discussions and also proofreading this thesis.
- I would like to thank my beautiful wife Chalté. Thank you for your endless support, encouragement, and understanding during this journey. Without you, this would not have been possible.
- I have been blessed with wonderful parents (Johan and Linda). Thank you for everything you have done for me and especially for your support and encouragement during my PhD studies. Without you, I would not be who I am today.

# Dedication

*This work is dedicated to our close friend, Prof Coenraad Labuschagne*

*(16-May-1958 to 10-Jul-2017)*

# Publications From This Thesis

## Journal Articles

The following articles were published in the following peer-reviewed, accredited journals:

- Venter, P.J. and Maré, E., 2020. GARCH option pricing models in a South African equity context. *ORiON, 36(1),* pp. 1-17.
- Venter, P.J. and Maré, E., 2020. GARCH Generated Volatility Indices of Bitcoin and CRIX. *Journal of Risk and Financial Management, 13(6),* pp. 1-15.
- Venter, P.J., Maré, E. and Pindza, E., 2020. Price discovery in the cryptocurrency option market: A univariate GARCH approach. *Cogent Economics & Finance, 8(1),* pp. 1-9.
- Venter, P.J. and Maré, E., 2021. GARCH Option Pricing and Implied FX Volatility Indices. *Studies in Economics and Econometrics, 13(6),* pp. 1-15.
- Venter, P.J. and Maré, E., 2022. Price Discovery in the Volatility Index Option Market: A Univariate GARCH Approach. *Finance Research Letters, 44,* 102069.
- Venter, P.J. and Maré, E., 2021. Univariate and Multivariate GARCH Models Applied to Bitcoin Futures Option Pricing. *Journal of Risk and Financial Management,* 14(6), p.261.
- Venter, P.J. and Maré, E., 2022. Pricing Collateralised Options in the Presence of Counterparty Credit Risk: An Extension of the Heston-Nandi Model. *South African Statistical Journal, 56(1),* pp.37-51.

# Contents



# List of Tables



# List of Figures



# List of Theorems



# List of Definitions



# Notation

| | |
|---|---|
| $S_t$ | Underlying asset price at time $t$ |
| $X_t$ | FX rate at time $t$ |
| $F_{t,T}$ | Futures price at time $t$ with expiry at time $T$ |
| $h_t$ | Conditional variance at time $t$ |
| $VRP_{t,\tau}$ | $\tau$-period variance risk premium at time $t$ |
| $RV_{t,\tau}$ | $\tau$-period realised variance at time $t$ |
| $\Sigma_t$ | Conditional covariance matrix at time $t$ |
| $SAVI_t$ | SAVI at time $t$ |
| $\mathbb{E}_t^Q[\cdot]$ | Conditional expectation under measure $Q$ |
| $V_t$ | Price of a derivative at time $t$ |
| $\tilde{V}_t$ | Price of a credit risky derivative at time $t$ |
| $DF(t,T)$ | Discount factor used to discount a cashflow from time $T$ to time $t$ |
| $K$ | Strike price |
| $s_K$ | Quoted spread of a spread option |
| $\sigma$ | Implied volatility |
| $T$ | Expiry date |
| $\tilde{\tau}$ | Random default time |
| $r$ | Risk-free rate |
| $r_R$ | Repurchase agreement rate |
| $r_C$ | Collateral rate |
| $r_F$ | Funding rate |
| $r^{(d)}$ | Domestic rate |
| $r^{(f)}$ | Foreign rate |
| $R_{j,t,T}$ | Futures return of asset $j$ at time $T$ with expiry at time $T$ |
| $\Phi(\cdot)$ | Cumulative normal distribution function |
| $L_R(\cdot)$ | Log-likelihood function based on historical returns |
| $L_V(\cdot)$ | Log-likelihood function based on the historical volatility index |
| $L_{RV}(\cdot)$ | Joint likelihood based on historical returns and volatility index |
| $L_{FX}(\cdot)$ | Log-likelihood function based on historical FX returns |
| $L_{HN}(\cdot)$ | Heston-Nandi log-likelihood function based on historical returns |

| | |
|---|---|
| $L_M(\cdot)$ | Multivariate Log-likelihood function based on historical returns |
| $W_t$ | Standard Brownian motion |
| $RMSE_t$ | Root mean squared error at time $t$ |
| $f(\cdot)$ | Cumulant generating function of the Heston-Nandi futures model |
| $f_{BS}(\cdot)$ | Cumulant generating function in the Black-Scholes framework |
| $f_P(\cdot)$ | Cumulant generating function in the Piterbarg framework |
| $f_{PD}(\cdot)$ | Cumulant generating function in the credit risky Piterbarg framework |

# Abbreviations

| | |
|---|---|
| AGARCH | Asymmetric GARCH |
| AIC | Akaike information criterion |
| ARCH | Autoregressive conditional heteroskedasticity |
| ARIMA | Autoregressive integrated moving average |
| ATM | At-the-money |
| BEKK | Baba, Engle, Kraft and Kroner |
| BTC | Bitcoin |
| CBOE | Chicago Board Options Exchange |
| CCC | Constant conditional correlation |
| CIR | Cox–Ingersoll–Ross |
| CIVETS | Columbia, Indonesia, Vietnam, Egypt, Turkey and South Africa |
| CME | Chicago Mercantile Exchange |
| CRIX | Cryptocurrency Index |
| DCC | Dynamic conditional correlation |
| EGARCH | Exponential GARCH |
| FTSE | Financial Times Stock Exchange |
| FX | Foreign exchange |
| GARCH | Generalised ARCH |
| GDP | Gross domestic product |
| GFC | Global Financial Crisis |
| GJR-GARCH | Glosten, Jagannathan, and Runkle GARCH |
| IGARCH | Integrated GARCH |
| JSE | Johannesburg Stock Exchange |
| LRNVR | Locally risk-neutral valuation relationship |
| MAE | Mean absolute error |
| P&L | Profit and loss |
| RMSE | Root mean squared error |
| S&P500 | Standard and Poor's 500 |
| SAVI | South African Volatility Index |
| SIC | Schwarz information criterion |
| SR-SARV | Square-root stochastic autoregessive volatility |

| | |
|---|---|
| TGARCH | Threshold-GARCH |
| USD | United States Dollar |
| VIX | CBOE Volatility Index |
| VXST | Short term VIX |
| ZAR | South African Rand |

# Preamble

The purpose of the preamble is to outline the foundation of the main theory applied in this thesis. The preamble is divided into two sections, the first section considers the introductory theory in which time-varying volatility models are introduced. The second section focuses on volatility indices and introduces the volatility risk premium.

## Introductory Theory

The main method applied in this thesis is a time series approach to derivative pricing. The fundamental concepts of financial time series are discussed in this section. These fundamental concepts form a basis for the theory that is applied and extended in this thesis. McNeil et al. (2015) outlined the stylised facts of financial returns as follows:

1. Return series show little serial correlation (the correlation between a time series and lagged values of itself) and returns are not identically and independently distributed.
2. Squared or absolute returns indicate signs of profound serial correlation.
3. The conditional expectation of returns is close to zero.
4. Volatility varies over time.
5. Extreme returns appear in clusters.
6. Return series show signs of leptokurtosis.

Conventional wisdom among financial modelling researchers and practitioners is that most financial models assume that returns are not normally distributed. To illustrate this concept, the Financial Times Stock Exchange/Johannesburg Securities Exchange (FTSE/JSE) Top40 returns are plotted below. In addition, simulated returns from a normal distribution (with the same mean and variance as the Top40 returns) are plotted below.

Figure 1: Financial returns

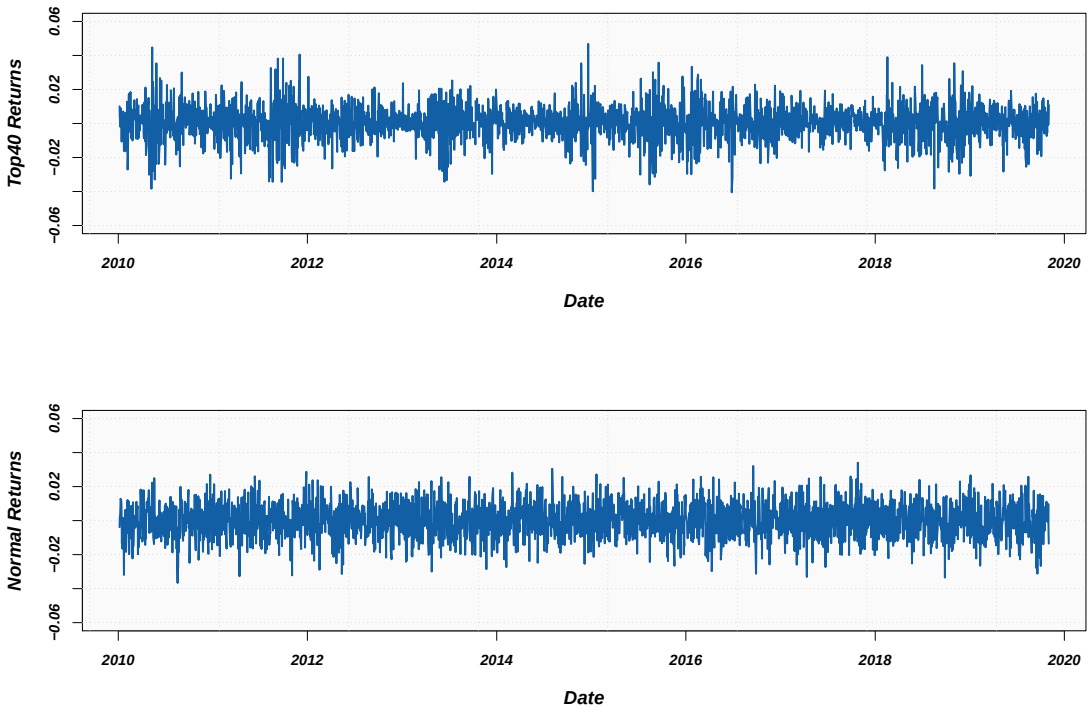


From the above, it is clear that the normal distribution does not sufficiently capture three important stylised facts: volatility varies over time, extreme returns appear in clusters, and leptokurtosis.

In this thesis, we focus on the modelling of volatility in discrete time for the purpose of pricing derivative instruments. As shown above, assuming normally distributed returns is not necessarily realistic, and therefore a different approach is required. A possible solution is the use of an autoregressive conditional heteroskedasticity (ARCH) process. Before defining an ARCH process, the concept of strict stationarity is required, which is defined as:

**Definition 1: Strict stationarity**

A time series $Y_t$ $(t \in \mathbb{Z})$ is strictly stationary if

$$(Y_{t_1}, ..., Y_{t_n}) = (Y_{t_1+k}, ..., Y_{t_n} + k)$$

for all $t_1, ..., t_n, k \in \mathbb{Z}$

McNeil et al. (2015) define an ARCH process as follows:

**Definition 2: ARCH process**

Let $Z_t$ be a strict white noise process with mean zero and variance equal to one. The process $Y_t$ is an ARCH($p$) process if it is strictly stationary and if it satisfies, for all $t \in \mathbb{Z}$ and some strictly positive values process $h_t$, the equations

$$Y_t = h_t Z_t,$$

$$h_t = \alpha_0 + \sum_{i=1}^{p} \alpha_i Y_{t-i}^2,$$

where $\alpha_0 > 0$ and $\alpha_i \geq 0$, $i = 1, ..., p$.

Asteriou and Hall (2015) explain that a major drawback of the ARCH specification is that it behaves more like a moving average rather than an autoregression. Danielsson (2011) also explains that a long lag length required for the ARCH model to capture the impact of historical returns on current volatility. This gave rise to the generalised ARCH (GARCH) model by Bollerslev (1986). According to McNeil et al. (2015) a GARCH process is defined as follows:

**Definition 3: GARCH process**

Let $Z_t$ be a strict white noise process with mean zero and variance equal to one. The process $Y_t$ is a GARCH($p, q$) process if it is strictly stationary and if it satisfies, for all $t \in \mathbb{Z}$ and some strictly positive values process $h_t$, the equations

$$Y_t = h_t Z_t,$$

$$h_t = \alpha_0 + \sum_{i=1}^{p} \alpha_i Y_{t-i}^2 + \sum_{i=1}^{q} \beta_i h_{t-i},$$

where $\alpha_0 > 0$, $\alpha_i \geq 0$, $i = 1, ..., p$, and $\beta_j \geq 0$, $j = 1, ..., q$.

A GARCH process can capture the presence of volatility clustering, leptokurtosis, and the time varying nature of volatility. In this thesis, the GARCH model (and extensions thereof) is applied to financial derivative pricing and volatility indices. Volatility indices are introduced in the next section.

## Volatility indices

Conventional wisdom among quantitative finance researchers is that the Chicago Board Options Exchange (CBOE) Volatility Index (VIX) is the most popular and most widely used volatility index. According to Hao and Zhang (2013), VIX reflects investors' expectation of volatility of the Standard and Poor's 500 (S&P500) Index over the next 30 days.

The time series of the S&P500 index level and returns from 1990 to the end of 2021 are plotted below:

Figure 2: S&P500 Index

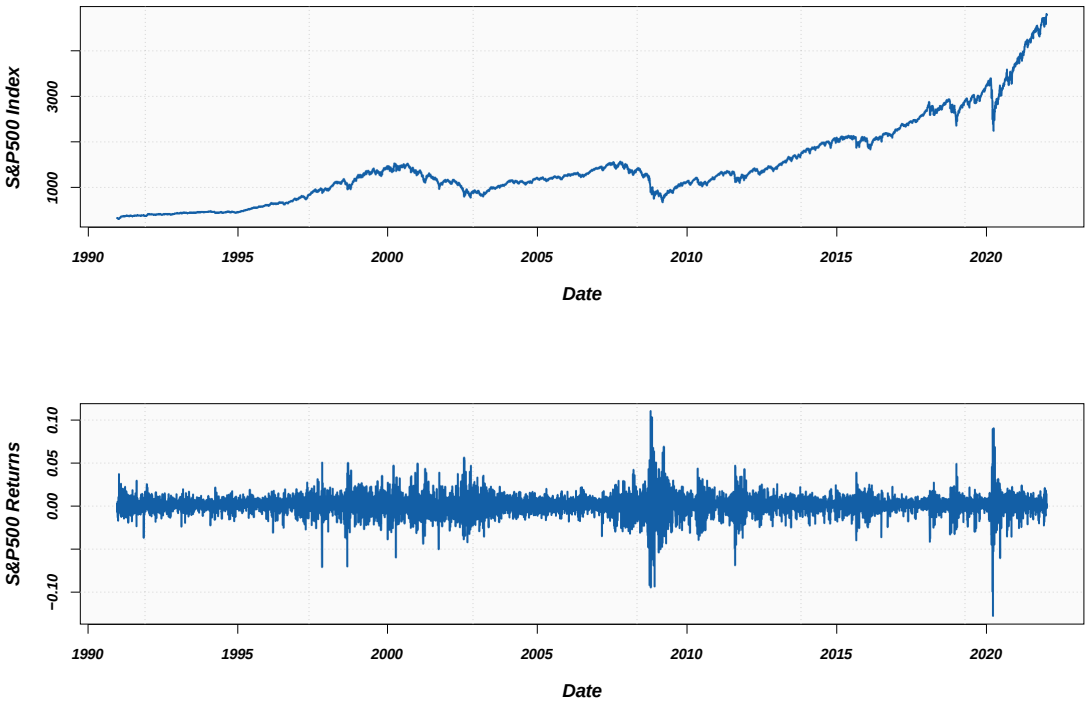


From the above, it seems that volatility has a tendency to vary over time, and that extreme returns appear in clusters (especially during financial crises). This is consistent with the stylised facts of financial returns (Cont, 2001). As mentioned previously, the GARCH option pricing model can capture the stylised facts of financial returns. However, option pricing takes place under the risk-neutral measure. The GARCH option pricing model by Duan (1995) takes this into account by incorporating a volatility risk premium (the difference between implied and realised volatility). This implies that the model can be calibrated under the real-world measure.

To illustrate the concept, the implied volatility (assumed to be the VIX), the expected

realised volatility (assumed to be the 22 day GARCH forecast), and the volatility risk premium (the difference between implied volatility and expected realised volatility) of the S&P500 Index are plotted below:

Figure 3: S&P500 volatility and risk premium

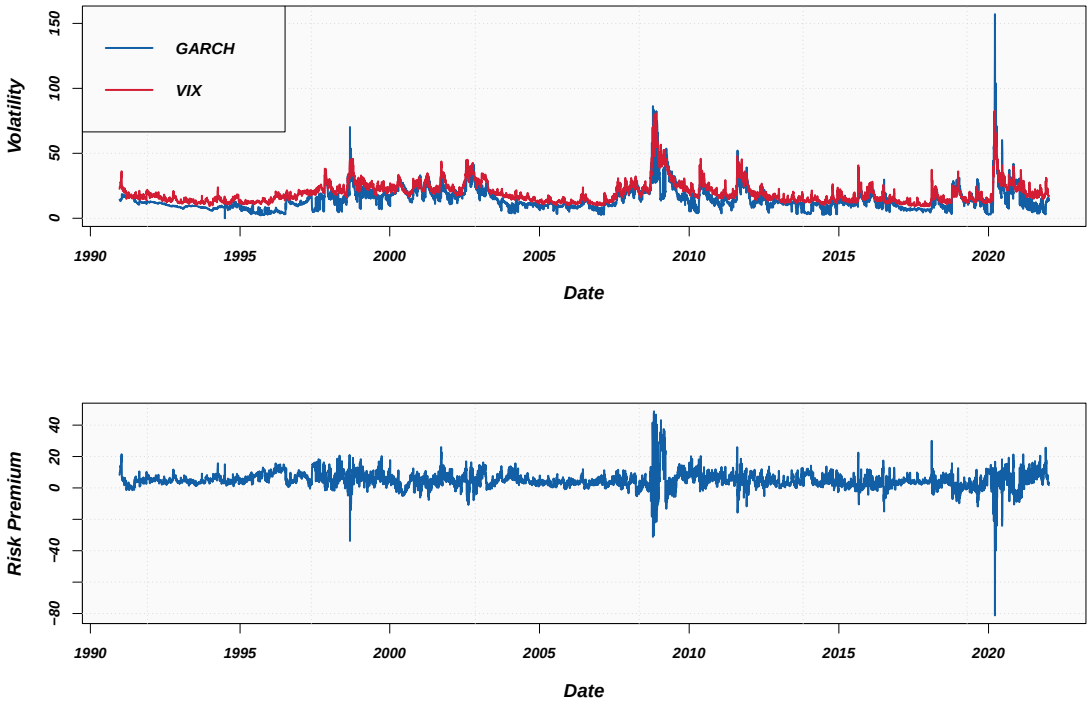


From the above, the volatility risk premium remains relatively stable. However, the risk premium tends to be negative at the beginning of crisis periods. The descriptive statistics are reported in the table below.

Table 1: Descriptive statistics: volatility risk premium

| | Risk premium |
|---|---|
| Mean | 4.8795 |
| Median | 4.4118 |
| Maximum | 48.8037 |
| Minimum | -81.1893 |
| Std. Dev. | 5.3429 |
| Skewness | -0.1199 |
| Kurtosis | 23.0034 |
| Observations | 8097 |
| Jarque-Bera | 135014.6 |

The volatility risk premium is positive on average, and not normally distributed (based on the Jarque-Bera statistic). The volatility risk premium also shows signs of leptokurtosis. The risk premium is discussed in more detail in Chapter 3.

# Chapter 1

# Introduction

The focus of this thesis is the application of the GARCH option pricing model to illiquid markets (South African and crypto asset markets), volatility indices, and derivative pricing after the Global Financial Crisis (GFC). This chapter is divided into three sections. The first considers the objectives and research questions, the second focuses on the research question, and finally the thesis structure is outlined.

## 1.1 Aims and objectives

The aim of this thesis is to contribute to the existing literature on the GARCH option pricing model in the context of volatility indices, illiquid markets (for price discovery), and modern derivative pricing frameworks (after the GFC). More specifically, the use of volatility indices to obtain more accurate pricing when applying the GARCH option pricing model (applied to equity and also extended to foreign exchange markets), and constructing a volatility index in the absence of a well-established derivatives market. Investigating model performance when applied to option pricing in illiquid markets, and the pricing and hedging of volatility index options. Finally, extending existing models to a modern derivative pricing framework that is suitable for post-GFC pricing (more realistic assumptions and takes additional factors into account, *i.e.,* collateral and counterparty credit risk).

The objective of Part I is the modelling of South African volatility indices using the GARCH option pricing model as a basis. By making use of both symmetric and asymmetric GARCH models, our aim is to show which GARCH model is the most accurate when modelling South African volatility indices (this is done by comparing the model implied volatility index to the actual volatility index). We will also illustrate the importance of asymmetric volatility in the South African market. The application of the GARCH option pricing model equity volatility indices is well-documented in the literature (see *e.g.,* Hao and Zhang, 2013), Part I also aims to extend this idea to the foreign exchange (FX) market.

In order to contribute to the existing literature on the GARCH option pricing model applied to price discovery, the focus of Part II is the application of the GARCH option pricing model to cryptocurrencies. This will give an indication of the pricing performance

when applied to a new asset class that does not have an established derivatives market. In addition to price discovery, a cryptocurrency volatility index is also considered. Finally, II also focuses on price discovery of multivariate cryptocurrency options.

In Part III, volatility index futures returns are modelled directly using different GARCH models and different assumptions for the error distribution. This will indicate which GARCH model and error distributional assumption is most appropriate when modelling volatility index futures returns. In addition, III also considers the hedge performance of the GARCH option pricing model when compared to a classical approach. This will illustrate whether a more realistic assumption that incorporates time varying volatility, volatility clustering, and leptokurtosis improves hedge performance when applied to volatility index options.

Financial markets have changed substantially since the GFC. The models used for the pricing of financial derivatives now need to take additional factors into account that were not necessary in previous years. Part IV aims to extend the existing GARCH option pricing model to take these additional factors (*i.e.,* collateral and counterparty credit risk) into account. The research questions are outlined in the next section. In addition, the effect of collateral and asymmetry is also considered.

## 1.2 Research questions

The aims and objectives outlined in the section above give rise to multiple research questions. The main research questions are listed below:

1. *Can volatility indices be used to obtain more accurate GARCH option pricing models when applied to the South African market, and can this be extended to different asset classes?*

2. *Does the GARCH option pricing model produce reasonable price discovery when applied to a new asset class, can it be used to construct a reasonable volatility index, and can the model be used for the pricing of multivariate options?*

3. *Which GARCH model and error distributional assumption is most reliable when pricing volatility index options, and does GARCH outperform classical methods when applied to hedging volatility index options?*

4. *What is the effect of collateral and asymmetry on vanilla and exotic options in a GARCH option pricing framework, and can the GARCH option pricing framework be extended to account for collateral and counterparty credit risk?*

The thesis structure is outlined in the next section.

## 1.3 Thesis structure

The different parts of this thesis are outlined below:

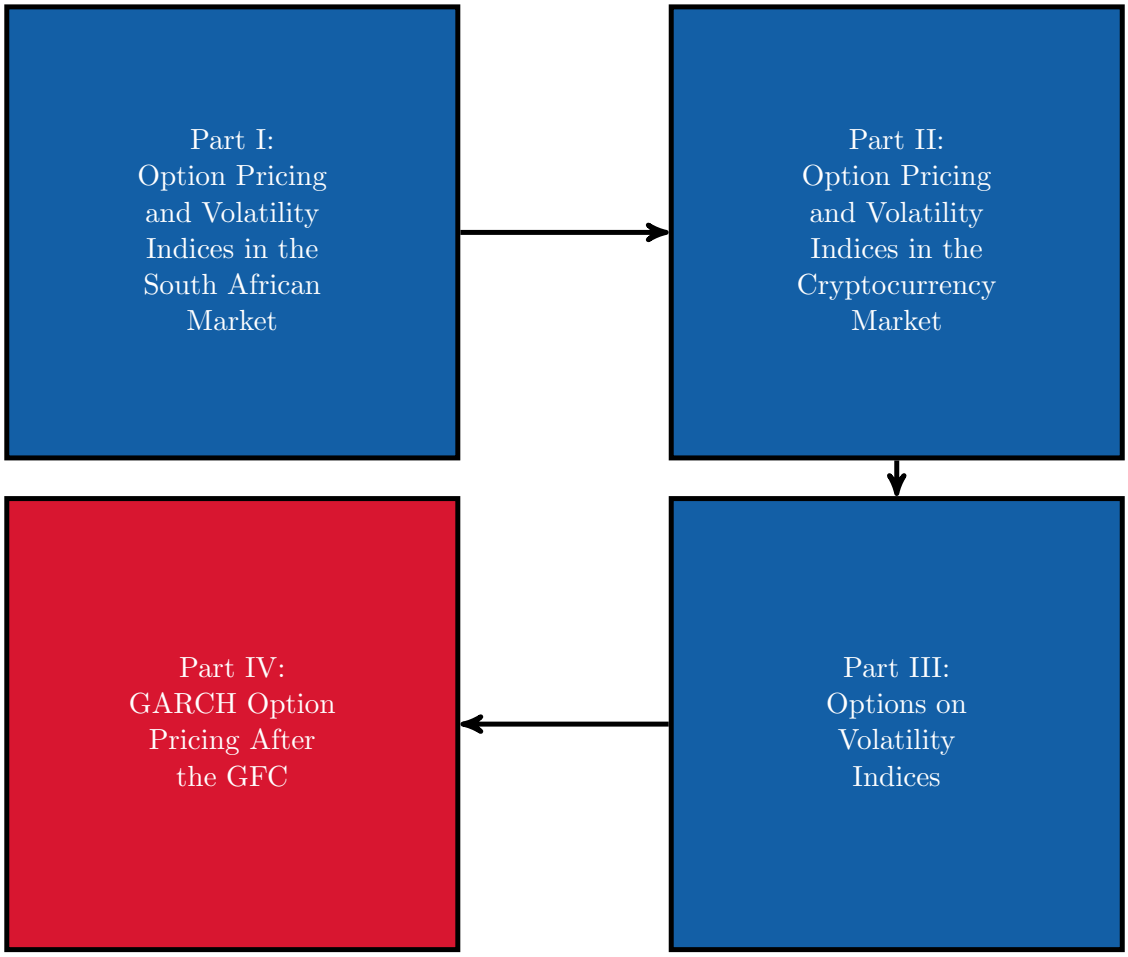


For the most part, Part IV can be read independently of Parts I to III. The subsections below discuss the different parts of this thesis in more detail.

### 1.3.1 Option pricing and volatility indices in the South African market

Part I consists of the following chapters:

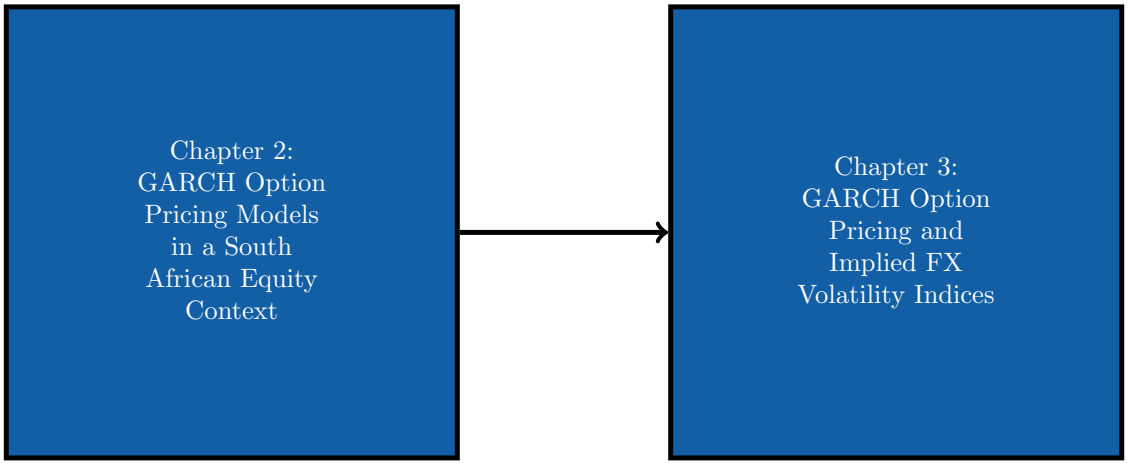


According to Flint and Maré (2017), a problem that financial modelling practitioners are often faced within a South African markets context, is an illiquid options market. The market standard for the pricing of vanilla options is the model by Black and Scholes (1973) (and extensions of the model, which are considered in Part III), which requires implied volatility (not always observable in illiquid markets) as an input. A possible solution to this problem is the use of historical data. However, implied volatility is a forward looking measure.

Another possible solution to the problem of pricing options in illiquid markets is the use of a volatility index. Kotzé et al. (2009) explain that a volatility index captures the market's expectation (forward looking) of volatility for a specified period. The South African Volatility Index (SAVI) is a measure of the market's expectation of three month volatility. Option pricing models based on both historical data and a volatility index can also be considered as a possible solution. This idea is explored in a South African equity context in Chapter 2. The work by Hao and Zhang (2013) is extended to the South African market to determine whether making use of the SAVI can improve the pricing performance of the GARCH option pricing model.

Most studies that consider volatility indices and variance risk premia, focus on equity indices. Duan and Wei (1997) extended the GARCH option pricing model to FX options. Using this model as a basis, the work by Hao and Zhang (2013) is extended to the FX market in Chapter 3. The GARCH-implied FX volatility indices are estimated for both South Africa (SAVI Dollar) and the United States (Euro VIX) to consider both a developed and emerging market. Furthermore, the FX variance risk premium is also considered in Chapter 3. Essentially, the work on variance risk premiums by Fassas and Papadamou (2018) is extended to the FX market. Chapter 3 concludes part I on option pricing and volatility indices in the South African market.

### 1.3.2 Option pricing and volatility indices in the cryptocurrency market

The following chapters are included in Part II:

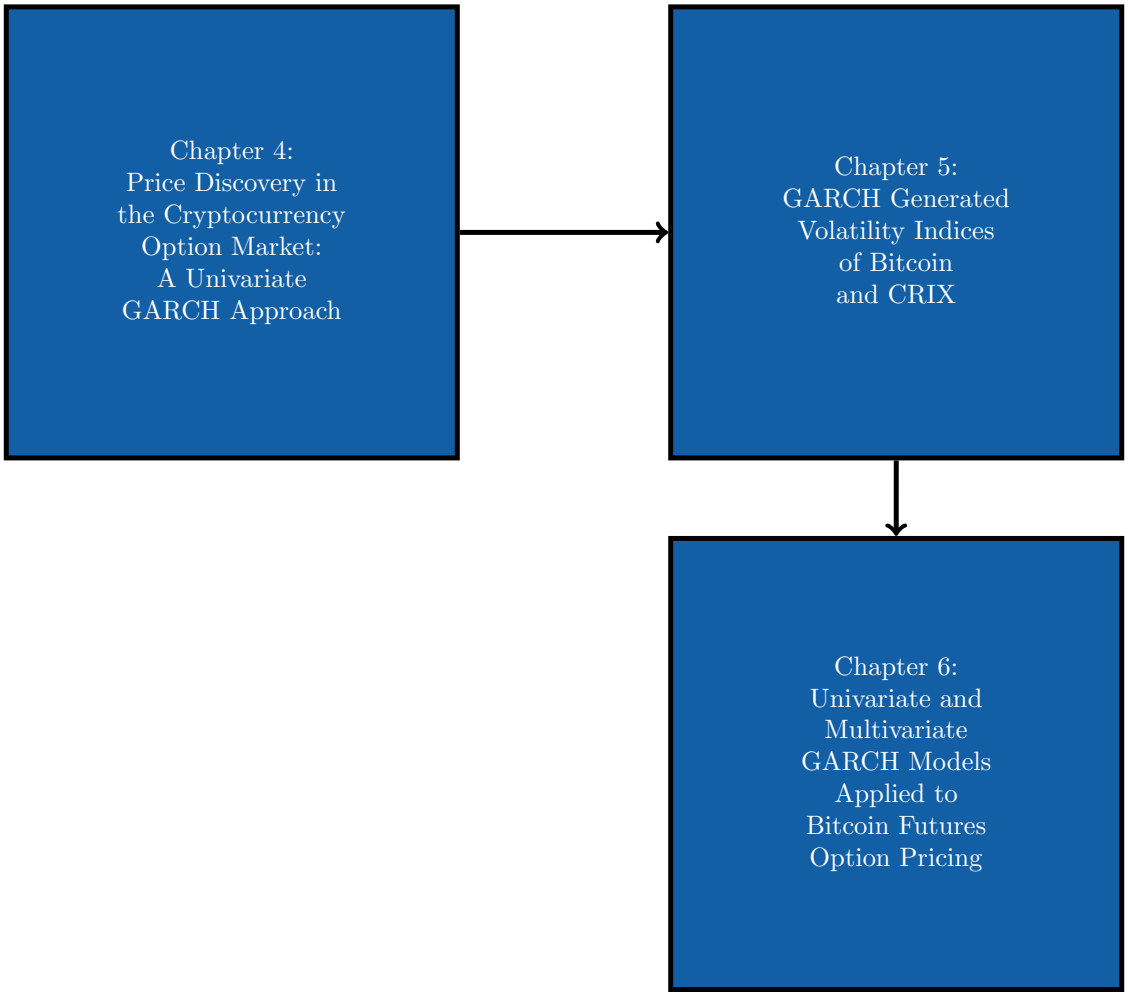


In addition to pricing derivatives in an illiquid market, financial modelling practitioners are faced with a similar problem when a new asset class is introduced. Cryptocurrencies are a good example of a new asset class that does not have a well-established derivatives market. In this case, the GARCH option pricing model is calibrated to historical returns only, given that a cryptocurrency volatility index has not yet been developed. The GARCH option pricing model (both symmetric and asymmetric conditional variance processes) is applied to Bitcoin (BTC) and Cryptocurrency Index (CRIX) historical returns in Chapter 4 to illustrate the effect of asymmetry in an option pricing context. Previous studies on cryptocurrency volatility (*e.g.,* Dyhrberg, 2016) rely heavily on statistical tests and do not consider option pricing.

In addition to the effect of asymmetry, the pricing performance of the GARCH option pricing model is also tested in Chapter 4 by comparing model prices to BTC market option prices. This will give an indication of whether the GARCH option pricing model produces reasonable price discovery. As mentioned previously, a cryptocurrency volatility index has not yet been developed. To address this problem, using the best performing

model in Chapter 4, the GARCH-implied BTC and CRIX volatility indices are estimated in Chapter 5. Volatility indices are based on option prices, and are therefore risk-neutral. The GARCH option pricing model is ideal in this case as the model is estimated under the real-world measure, but the same parameters are required for the risk-neutral price process (required for the GARCH-implied volatility index).

Alexander and Heck (2020) explain that crypto-asset futures are often exposed to significant basis risk, which makes crypto-asset futures spread options an attractive product. This idea is explored in Chapter 6. Previous chapters focus on the modelling of spot dynamics, Chapter 6 considers the futures price process. The model by Heston and Nandi (2000) was extended to futures options by Li (2019a). This work was used as a basis to test the pricing performance of the model when applied to BTC futures options. Rombouts and Stentoft (2011) derived the risk-neutral dynamics of the spot prices processes for a general class of multivariate heteroskedasticity models. This work is extended to multivariate futures options. Chapter 6 concludes Part II on option pricing and volatility indices in the cryptocurrency market.

### 1.3.3 Options on volatility indices

Part III consists of the following:

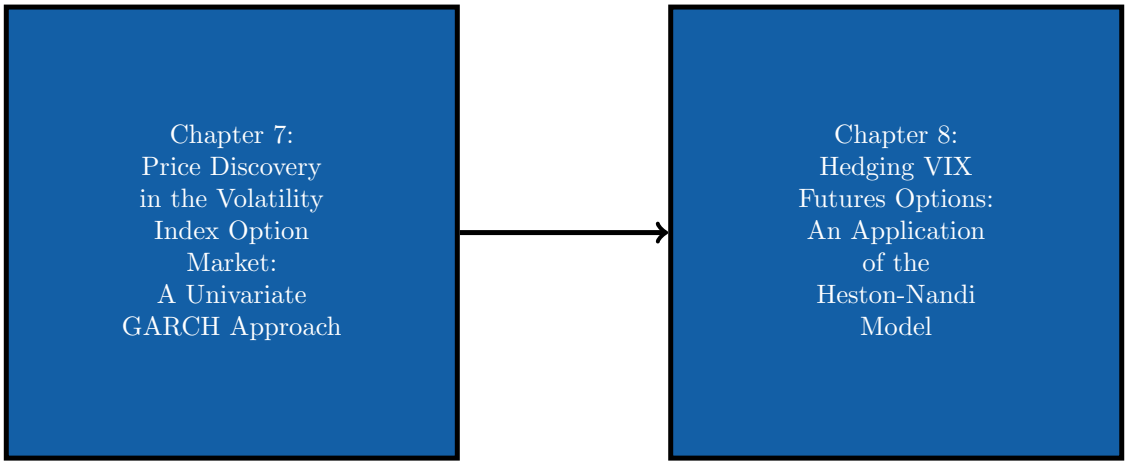


The chapters outlined previously focus on the use of volatility indices to obtain more accurate prices, or the construction of a volatility index in the absence of a well-established derivatives market. However, derivatives on volatility indices are not considered in previous chapters. In this case, the volatility index becomes the underlying asset. The use of volatility index derivatives for the hedging of volatility risk has become very popular in recent years. The pricing and hedging of volatility index derivatives is the focus of Part III.

The focus of Chapter 7 is price discovery in the volatility index option market. Currently, options on the SAVI (and other volatility indices) do not actively trade, and there-

fore a different approach is required. GARCH models are applied to the pricing of volatility index options in Chapter 7. Conventional wisdom among financial modelling researchers and practitioners is that the assumption of a Gaussian distribution when modelling financial returns is not necessarily realistic. Therefore, different distributional assumptions (that take skewness and kurtosis into account) are also considered. The GARCH models are applied to CBOE VIX option pricing. According to Fernandes et al. (2014), the CBOE has published the VIX since 1993. The VIX is calculated using near term (30 calendar days) volatility implied by options on the S&P500 index. Furthermore, the VIX is based on a model-free estimator of implied volatility and therefore does not rely on a particular option pricing framework. VIX options actively trade, and therefore the pricing performance can be determined by comparing model prices to market prices.

The VIX is not a tradeable asset. However, futures and options on VIX do trade. Literature focusing on the pricing of VIX options is well-documented in the literature. However, not many studies have considered the hedging of VIX options. By making use of a similar approach to Alexander and Nogueira (2004) (applied different option pricing models to the hedging of equity options) and Lassance and Vrins (2018) (tested the hedge performance of the Heston-Nandi model applied to equity options), the hedge performance of the Heston-Nandi futures option pricing model (applied in Chapter 6) applied to VIX options is considered in Chapter 8. This chapter concludes Part III on volatility index options. The next part focuses on modern pricing frameworks.

### 1.3.4 GARCH option pricing after the GFC

As mentioned previously, Part IV can be read independently of Part I to III (for the most part). The following chapters are included in Part IV:

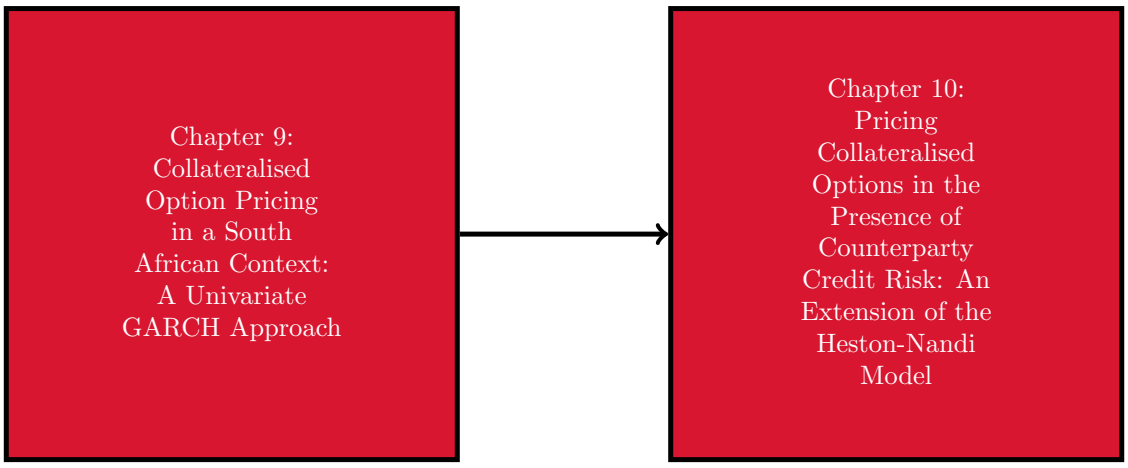


The GFC has changed financial markets permanently, especially financial derivatives. Before the GFC, the model by Black and Scholes (1973) was considered the market standard. However, the GFC has shown that numerous additional factors that need to be considered.

This has forced quantitative finance researchers and practitioners to develop a new pricing framework. Modern derivative pricing frameworks and the GARCH option pricing model are the focus of Part IV.

An important assumption required for the Black and Scholes (1973) framework is the existence of a constant and unique risk-free rate. The collapse of large financial institutions has shown that this is not necessarily a realistic assumption. Furthermore, an important factor that is often required in today's market is the posting of collateral. Piterbarg (2010) extended the Black and Scholes (1973) model to price derivatives in the presence of collateral. The model relaxes the assumption of a risk-free rate.

Labuschagne and Von Boetticher (2017) were the first to extend the GARCH option pricing model to the Piterbarg (2010) framework, for the pricing of collateralised options in the South African market. In Chapter 9 the work by Labuschagne and Von Boetticher (2017) is extended to different GARCH processes (symmetric and asymmetric), and also exotic options. The overall purpose is to illustrate the effect of collateral and asymmetry in a South African equity market context.

An obvious shortcoming of Chapter 9 is that the model still requires an important assumption made by Black and Scholes (1973) and Piterbarg (2010), which is no counterparty credit risk. This is clearly a strong assumption given defaults during the GFC. A more realistic approach is considered in Chapter 10. Von Boetticher (2017) extended the work by Heston and Nandi (2000) to the Piterbarg (2010) framework. However, the model by Von Boetticher (2017) assumes no counterparty credit risk. In addition, Wang (2017) extended the model by Heston and Nandi (2000) to the pricing of options in the presence of counterparty credit risk in the Black and Scholes (1973) framework (assumes a constant risk-free rate). By making use of ideas presented in Von Boetticher (2017) and Wang (2017), Chapter 10 extends the Heston-Nandi model to the pricing of options in the presence of collateral and counterparty credit risk. This chapter concludes Part IV on GARCH option pricing and modern derivative pricing frameworks. Finally, concluding remarks and areas for future research are outlined in Chapter 11.

# Part I

# Option Pricing and Volatility Indices in the South African Market

# Chapter 2

# GARCH Option Pricing Models in a South African Equity Context

## 2.1 Introduction

In modern finance, asset volatility is synonymous with an asset's risk. Financial modelling researchers and practitioners, therefore, face the issue of finding a reliable estimate of volatility. Soczo (2003) explains that historical data can be used to estimate current and future levels of volatility. However, this assumes that the future will be like the past, which is not necessarily a realistic assumption.

Financial researchers (see, *e.g.,* McNeil et al., 2015) have demonstrated that volatility is not constant, *i.e.,* it changes substantially over time. Furthermore, financial time series exhibit periods of high or low volatility; this phenomenon is known as clustering. There also appears to be mean reversion in volatility, *i.e.,* periods of unusually high or low volatility tend to be followed by reversion to more normal behaviour (see, *e.g.,* Cont, 2001). In equity markets, volatility typically increases when stock prices decrease; this is often referred to as the leverage effect.

When it comes to the topic of time-varying volatility in discrete time, most financial modelling researchers will agree that the GARCH model is the most widely used. A wide range of different GARCH processes have been introduced in the literature (see, *e.g.,* Francq and Zakoian, 2019). An important factor to consider when modelling conditional volatility is the effect of asymmetry. According to Asteriou and Hall (2015), symmetric volatility models assume that positive and negative shocks have the same effect on volatility, which is also not necessarily a realistic assumption. Therefore, we test the performance of both symmetric and asymmetric GARCH models when modelling the conditional variance.

GARCH model parameters are usually estimated using historical returns of an asset price, by making use of the maximum likelihood method. The fitted GARCH model can then be used to obtain a forward looking estimate of volatility. A different approach is to make use of a volatility index. In this chapter, the so-called SAVI is used. As explained by Kotzé et al. (2009), the SAVI was introduced in 2007 for the purpose of measuring

the expected three-month volatility based on the FTSE/JSE Top40 index. During times of higher uncertainty (*e.g.,* financial crises), the SAVI index increases substantially (in direct analogy with the CBOE VIX, which measures investors' expectations of volatility of the S&P500 index). Equity volatility indices serve as important financial indicators, measuring the level of risk in markets, while also exhibiting predictive power for index returns (see, *e.g.,* Huskaj and Larsson, 2016).

In this chapter,[1] three different univariate GARCH processes are used to model the implied SAVI index. By making use of an approach similar to Hao and Zhang (2013), three different log-likelihood functions are considered for the estimation of the GARCH option pricing model parameters to determine the best performing GARCH model when compared to the historical SAVI. Furthermore, the accuracy of estimated GARCH option pricing models is tested by comparing the model option prices to market prices (consistent with Hunzinger et al., 2014). The rest of this chapter is structured as follows: Section 2.2 focuses on the methodology, thereafter the empirical results are presented in Section 2.3, and finally the main findings are summarised in Section 2.4.

## 2.2 Methodology

This section is divided into four subsections. The first focuses on GARCH models in finance. The second subsection considers the application of GARCH models to option pricing. Thereafter, the theoretical framework of the GARCH-implied SAVI is considered. Finally, the data and estimation methods used in this study are discussed.

### 2.2.1 GARCH models in finance

A large proportion of models used in finance assume constant volatility. A good example of this is the classical Black-Scholes (see *e.g.,* Wilmott, 2007) model used for option pricing. As mentioned previously, the GARCH model is clearly the most popular when modelling volatility in discrete time. According to McNeil et al. (2015), GARCH models capture two important stylised facts of financial time series, namely leptokurtosis and volatility clustering.

The application of GARCH models to solve financial problems is well-documented in the literature. According to Duncan and Liu (2009), the mean model of a typical GARCH model takes the following form:

$$\ln\left(\frac{S_t}{S_{t-1}}\right) = \mu + \epsilon_t, \tag{2.1}$$

where $S_t$ is the price of the underlying asset at time $t$, $\mu$ remains constant over time, and the error term, $\epsilon_t$, is assumed to be normally distributed with mean zero and conditional variance $h_t$, where $h_t$ is some GARCH process. The conditional variance when modelled

[1] This chapter is based on a paper (Venter and Maré , 2020b) published in *ORiON*.

using a GARCH(1,1) process is given by,

$$h_t = \alpha_0 + \alpha_1 \epsilon_{t-1}^2 + \beta_1 h_{t-1}, \tag{2.2}$$
$$\alpha_0 > 0,\ \alpha_1, \beta_1 \geq 0,\ \alpha_1 + \beta_1 \leq 1,$$

where the parameters $\alpha_0$, $\alpha_1$, and $\beta_1$ are typically estimated using the maximum likelihood method (to be discussed in Section 2.2.4).

When the variance equation is modelled using the symmetric GARCH(1,1) process, the assumption is that volatility will have the same reaction to positive and negative shocks. However, this is not necessarily a realistic assumption. Glosten et al. (1993) therefore include an indicator function to capture the asymmetric nature of positive and negative shocks. The (Glosten, Jagannathan, and Runkle) GJR-GARCH(1,1) model takes the following form:

$$h_t = \alpha_0 + \alpha_1 \epsilon_{t-1}^2 + \beta_1 h_{t-1} + \gamma \mathbf{1}_{\{\epsilon_{t-1}<0\}} \epsilon_{t-1}^2, \tag{2.3}$$
$$\alpha_0, \alpha_1 > 0,\ \beta_1 \geq 0,\ \alpha_1 + \gamma \geq 0,\ \gamma < 2(1 - \alpha_1 - \beta_1),$$

where the indicator function, $\mathbf{1}_{\{\epsilon_{t-1}<0\}}$ takes a value of one when shocks are negative, and zero otherwise.

The third model considered in this study is the asymmetric GARCH (AGARCH) model that has the following form (see Alexander, 2008):

$$h_t = \alpha_0 + \alpha_1 (\epsilon_{t-1} - \gamma)^2 + \beta_1 h_{t-1}, \tag{2.4}$$
$$\alpha_0 > 0,\ \alpha_1, \beta_1 \geq 0,\ (1 + \gamma^2)\alpha_1 + \beta_1 \leq 1,$$

where the parameter $\gamma$ captures asymmetric effects. If $\gamma > 0$, then $(\epsilon_{t-1} - \gamma)^2$ will result in larger negative shocks. Furthermore, when modelling volatility on equity returns, $\gamma$ is usually positive, while $\gamma$ is usually negative for commodities.

An important factor to consider when modelling volatility using different GARCH type models, is the goodness of fit. Ahmad and Ping (2014) explained that the goodness of fit of symmetric and asymmetric GARCH models can be compared using the Akaike information criterion (AIC) and Schwarz information criterion (SIC). The AIC and SIC are given by,

$$AIC = -2 \ln L + 2k$$
$$SIC = -2 \ln L + k \ln N,$$

where $L$ is the maximised value of the likelihood function, $k$ is the number of estimated parameters, and $N$ is the sample size. Oberholzer and Venter (2015) applied symmetric and asymmetric GARCH models to a range of different JSE indices to determine the most reliable model. Their empirical results based on the AIC and SIC indicated that the GJR-GARCH(1,1) model is the most reliable model when modelling Top40 volatility.

Conventional wisdom amongst finance researchers and practitioners is that there is a positive relationship between risk and return. However, the mean model specified in

Equation 2.1 does not reflect this. Asteriou and Hall (2015) explain that this can be captured by making use of the GARCH-in-mean model, where the conditional mean is a function of the conditional variance (or standard deviation). An example of a GARCH-in-mean specification is given by,

$$\ln\left(\frac{S_t}{S_{t-1}}\right) = \mu + \lambda h_t + \epsilon_t,$$

where $\mu$ remains constant over time, $\lambda$ is the coefficient of the conditional variance $h_t$, which is some GARCH process, and $\epsilon_t$ is assumed to be normally distributed with mean zero, and variance $h_t$.

Hansen and Lunde (2005) compared the predictive ability of 330 GARCH type models, with the GARCH(1,1) model as the benchmark model. Their findings indicated that the GARCH(1,1) is highly robust, and that it is difficult to find an alternative model that shows consistent outperformance. Hence, the GARCH(1,1) model is used as a benchmark model in this study. Furthermore, Oberholzer and Venter (2015) showed that the GJR-GARCH(1,1) model is superior when modelling Top40 returns, which is consistent with the results found in Flint et al. (2014). However, this was based on historical data only. Therefore the performance of the GJR-GARCH(1,1) applied to Top40 option pricing is considered in this study. Finally, according to Hsieh and Ritchken (2005), the application of the AGARCH(1,1) model to option pricing is superior at removing pricing biases from pricing residuals and should be considered by traders and risk managers. Therefore the AGARCH(1,1) model is included in this study. GARCH models applied to financial option pricing is considered in the next subsection.

### 2.2.2 GARCH models applied to option pricing

Duan (1995) explains that when using a GARCH process to model the log-returns of an asset, the following is assumed,

$$\ln\left(\frac{S_t}{S_{t-1}}\right) = r + \lambda\sqrt{h_t} - \frac{1}{2}h_t + \epsilon_t,$$

and

$$\epsilon_t = \sqrt{h_t}z_t,$$

where $r$ is the unique risk-free rate (continuously compounded), and $\lambda$ is the constant unit risk premium. Furthermore, $z_t$ is assumed to be identically and independently distributed with mean zero and variance equal to one under the real-world measure $P$.

Wilmott (2007) explains that the value of an option can be shown to be the expectation of the discounted future payoff under the risk-neutral measure ($Q$). Consider the following definition from Duan (1995):

**Definition 4: Locally risk-neutral valuation relationship**

A pricing measure $Q$ satisfies the locally risk-neutral valuation relationship (LRNVR) if the measure $Q$ is absolutely continuous with respect to measure $P$, $S_t/S_{t-1}$ is log-normally distributed, with conditional expectation and variance under the risk-neutral measure

$$\mathbb{E}^Q\left[\frac{S_t}{S_{t-1}} \mid \mathcal{F}_{t-1}\right] = \exp\{r\}, \tag{2.5}$$

and

$$\mathbb{V}ar^Q\left[\ln\left(\frac{S_t}{S_{t-1}}\right) \mid \mathcal{F}_{t-1}\right] = \mathbb{V}ar^P\left[\ln\left(\frac{S_t}{S_{t-1}}\right) \mid \mathcal{F}_{t-1}\right],$$

almost surely with respect to measure $P$, where $\mathcal{F}_t$ is the information set available at time $t$.

To simplify notation, the conditional expectation at time $t$ is denoted by $\mathbb{E}_t[\cdot]$. The above definition allows us to derive the following theorem:

**Theorem 1: Risk-neutral asset price dynamics under GARCH**

Under pricing measure $Q$, the LRNVR implies

$$\ln\left(\frac{S_t}{S_{t-1}}\right) = r - \frac{1}{2}h_t + \xi_t, \tag{2.6}$$

where

$$\xi_t = \sqrt{h_t}z_t^*,$$

and $z_t^*$ is a standard normal random variable under the risk-neutral measure $Q$. This implies that,

$$\xi_t|\mathcal{F}_{t-1} \sim \mathcal{N}(0, h_t).$$

*Proof.* Given that $S_t/S_{t-1}$ is log-normal under measure $Q$, it can be written as,

$$\ln\left(\frac{S_t}{S_{t-1}}\right) = \mu_t + \xi_t, \tag{2.7}$$

where $\mu_t$ is the conditional mean, and $\xi_t$ is a $Q$-normal random variable, with conditional

mean zero and variance $h_t$. This follows that

$$\begin{aligned}\mathbb{E}_t^Q\left[\frac{S_t}{S_{t-1}}\right] &= \mathbb{E}_t^Q\left[\exp\left\{\mu_t+\xi_t\right\}\right]\\ &= \exp\left\{\mu_t+\frac{1}{2}h_t\right\}\end{aligned}$$

by the LRNVR, $h_t = \mathbb{V}ar^Q\left[\ln\left(\frac{S_t}{S_{t-1}}\right) \mid \mathcal{F}_{t-1}\right] = \mathbb{V}ar^P\left[\ln\left(\frac{S_t}{S_{t-1}}\right) \mid \mathcal{F}_{t-1}\right]$. Furthermore, because Equation 2.5 holds, it follows that

$$\mu_t = r - \frac{1}{2}h_t.$$

This completes the proof. □

Theorem 2 focuses on the case where $h_t$ follows a GARCH(1,1) process.

**Theorem 2: GARCH(1,1) risk-neutral dynamics**

If $h_t$ takes on a GARCH(1,1) specification, the LRNVR implies

$$h_t = \alpha_0 + \alpha_1\left(\xi_{t-1} - \lambda\sqrt{h_{t-1}}\right)^2 + \beta_1 h_{t-1}. \tag{2.8}$$

*Proof.* By making use of Equations 2.5 and 2.7, it is clear that

$$r + \lambda\sqrt{h_t} - \frac{1}{2}h_t + \epsilon_t = r - \frac{1}{2}h_t + \xi_t,$$

which suggests that

$$\epsilon_t = \xi_t - \lambda\sqrt{h_t}.$$

If the above is substituted into Equation 2.2, Equation 2.8 is obtained. This completes the proof. □

It is clear from the above that irrespective of how the conditional variance ($h_t$) is specified, the variable $\epsilon_t$ is always replaced by $\xi_t - \lambda\sqrt{h_t}$. The GJR-GARCH(1,1), and AGARCH(1,1) processes under the risk-neutral measure $Q$ are given by:

$$\begin{aligned}h_t &= \alpha_0 + \alpha_1(\xi_{t-1} - \lambda\sqrt{h_{t-1}})^2\left[\alpha_1 + \gamma\mathbf{1}_{\{\xi_{t-1}<0\}}\right] + \beta_1 h_{t-1} \text{ and}\\ h_t &= \alpha_0 + \alpha_1\left(\xi_{t-1} - \lambda\sqrt{h_{t-1}} - \gamma\sqrt{h_t}\right)^2 + \beta_1 h_{t-1},\end{aligned}$$

respectively. Furthermore, the stationarity constraints of the GARCH(1,1), GJR-GARCH(1,1), and AGARCH(1,1) processes are given by,

$$\alpha_1(1+\lambda^2)+\beta_1<1,$$
$$\alpha_1(1+\lambda^2)+\beta_1+\gamma\left[\frac{\lambda}{\sqrt{2\pi}}\exp\left\{-\frac{\lambda^2}{2}\right\}+(1+\lambda^2)\Phi(\lambda)\right]<1,$$
$$\alpha_1[1+(\lambda+\gamma)^2]+\beta_1<1$$

respectively, where $\Phi(\cdot)$ denotes the cumulative normal distribution function.

In this study, Monte Carlo simulation is used to price European options. Given the estimated parameters ($\alpha_0$, $\alpha_1$, $\beta_1$, $\gamma$ and $\lambda$), the current value of the underlying asset ($S_0$), and the unique risk-free rate ($r$), options can be priced using the GARCH(1,1) model by using the following algorithm at the current time $t=0$ (the initial risk-neutral variance $\sigma_0$ and the initial value of $\xi_0$ are assumed to be the unconditional variance and zero respectively).

For a European call option that expires at time $T$, with strike $K$, the Monte Carlo price is given by

**Algorithm 1: GARCH(1,1) Monte Carlo option pricing**

Step 1: Generate $(z_{1,1},...,z_{M,T})\sim\mathcal{N}(0,1)$ where $M$ is the number of simulations.

Step 2: Compute $h_{j,t}=\alpha_0+\alpha_1(\xi_{j,t-1}-\lambda\sqrt{h_{j,t-1}})^2+\beta h_{j,t}$, where $\xi_{j,t}=\sqrt{h_{j,t}}\times z_{j,t}$ for $t=1,...,T$.

Step 3: Compute $S_{j,t}=S_{j,t-1}\exp\left\{r-\frac{1}{2}h_{j,t}+\xi_t\right\}$, for $t=1,...,T$.

Step 4: Repeat steps 2 and 3 $M$ times.

Step 5: The option price is equal to the discounted payoff function applied to the underlying:

$$V_t=DF(t,T)\frac{1}{M}\sum_{j=1}^{M}\max\left\{S_{j,T}-K,0\right\},$$

where $DF(t,T)$ is a discount factor used discount a cash flow from time $T$ to time $t$.

The conditional variance process in the algorithm changes when using the GJR-GARCH(1,1) or AGARCH(1,1) model. The GARCH-implied SAVI is considered in the next subsection.

### 2.2.3 GARCH-implied SAVI

As mentioned, the SAVI reflects investors' expectations of volatility of the Top40 in the following three calendar months, which is given by,

$$\left(\frac{SAVI_t}{100}\right)^2 = \mathbb{E}_t^Q\left[\frac{1}{\tau_0}\int_t^{t+\tau_0}\tilde{h}_s ds\right],$$

where $\tau_0$ is equal to three calendar months (assumed to be 63 trading days), $\tilde{h}_s$ is the instantaneous annualised variance of the Top40 returns, and $\mathbb{E}_t^Q[\cdot]$ denotes the conditional expectation at time $t$, under the risk-neutral measure. In this chapter, the SAVI is calculated as the expected average of the variance in the $n$ subperiods of the following three calendar months,

$$\left(\frac{SAVI_t}{100}\right)^2 = \frac{1}{n}\sum_{k=1}^{n}\mathbb{E}_t^Q\left[\tilde{h}_{t+\frac{k\times\tau_0}{n}}\right].$$

Daily data is used to estimate the implied SAVI, hence $n = \tau_0$, as explained by Hao and Zhang (2013). Furthermore, when estimating the implied SAVI using daily data, a proxy for $SAVI_t$ in terms of daily variance is required. This is given by,

$$\vartheta_t = \frac{1}{n}\sum_{k=1}^{n}\mathbb{E}_t^Q[h_{t+k}],$$

where $\vartheta_t = \frac{1}{252}\left(\frac{SAVI_t}{100}\right)^2$ almost surely.

In order to derive the GARCH-implied SAVI, $\xi_t$ in Equation 2.6 is assumed to be a square-root stochastic autoregessive volatility (SR-SARV) process of order one. SR-SARV models are characterised by the autoregressive nature of the stochastic variance, hence the variance depends on the previous values (lags) of itself. The general form of the conditional variance (given the information set $J_t$, available at time $t$) of a SR-SARV process is given by,

$$\mathcal{P}_t = \Omega + \Gamma\mathcal{P}_{t-1} + \upsilon_t,$$

where $\Omega$ is a constant, $|\Gamma| < 1$, and the error term $\mathbb{E}[\upsilon_t|J_t] = 0$. For more information on SR-SARV processes, the interested reader is referred to Meddahi and Renault (2004). Hao and Zhang (2013) showed that if $\xi_t$ follows an SR-SARV process, the implied volatility index (in terms of daily variance) implied by the GARCH(1,1), GJR-GARCH(1,1), and AGARCH(1,1) models have an analytical formula, which takes the following form:

$$\vartheta_t = \zeta + \psi h_t,$$

where

$$\zeta = \frac{\Omega}{1-\gamma}(1-\psi),$$
$$\psi = \frac{1-\Gamma^n}{n(1-\Gamma)}.$$

The estimated SAVI of the GARCH(1,1), GJR-GARCH(1,1) and AGARCH(1,1) models are obtained using the general form above.

### 2.2.4 Data and estimation methods

In this study, daily data from 1-Jan-2010 to 19-Apr-2019 are used, the dataset was obtained from the Thomson Reuters Datastream databank. As mentioned previously, GARCH model parameters are usually estimated using maximum likelihood. According to Christoffersen et al. (2013), GARCH models used for option pricing can be estimated using the maximum likelihood method (based on historical returns), by making use of loss functions (errors between the GARCH-implied option prices and market option prices are minimised) or models can be calibrated to both historical returns and market option prices.

Hao and Zhang (2013) estimate GARCH models using three different likelihood functions to estimate the GARCH models, ultimately to estimate the GARCH-implied VIX. The first likelihood function is based on historical returns only, the second is based on the historical VIX only, and the final function is a joint likelihood function based on historical returns and the historical VIX. Christoffersen et al. (2013) explain that estimation methods based on both historical returns and option prices, or in this case implied volatility, are better than methods based on option prices only, because they ensure that the model is consistent with historical returns and the market's expectations of the future.

In this study, by making use of a similar approach to Hao and Zhang (2013), three different likelihood functions are used to estimate GARCH model parameters, ultimately to estimate the GARCH-implied SAVI. The best performing GARCH model is determined by comparing the GARCH-implied SAVI to the historical SAVI, and by comparing GARCH-implied option prices to market option prices.

The GARCH parameters based on returns only are estimated by maximising the following log-likelihood function (Hao and Zhang, 2013),

$$\ln L_R = -\frac{N}{2}\ln(2\pi) - \frac{1}{2}\sum_{t=1}^{N}\left(\ln h_t + \left[\ln\frac{S_t}{S_{t-1}} - r - \lambda\sqrt{h_t} + \frac{1}{2}h_t\right]^2 / h_t\right),$$

or equivalently, by minimising

$$-2\ln L_R = N\ln(2\pi) + \sum_{t=1}^{N}\left(\ln h_t + \left[\ln\frac{S_t}{S_{t-1}} - r - \lambda\sqrt{h_t} + \frac{1}{2}h_t\right]^2 / h_t\right),$$

where $N$ is the number of historical returns in the estimation period. For the log-likelihood function based on the historical SAVI, the following is assumed regarding the relationship between the market and GARCH-implied SAVI,

$$SAVI_t^{Mkt} = SAVI_t^{Imp} + \varepsilon_t,\ \varepsilon_t \sim i.i.d.\mathcal{N}(0, \varsigma^2).$$

The log-likelihood function based on the historical SAVI is given by (Hao and Zhang, 2013),

$$\ln L_V = -\frac{N}{2}(2\pi\hat{\varsigma}^2) - \frac{1}{2\hat{\varsigma}^2}\sum_{t=1}^{N}\left(SAVI_t^{Mkt} - SAVI_t^{Imp}\right)^2, \tag{2.9}$$

where $\varsigma^2$ is estimated with sample variances $\hat{\varsigma}^2$. In this case, the following function is minimised,

$$-2\ln L_V = N(2\pi\hat{\varsigma}^2) + \frac{1}{\hat{\varsigma}^2}\sum_{t=1}^{N}\left(SAVI_t^{Mkt} - SAVI_t^{Imp}\right)^2.$$

Finally, the joint log-likelihood function based on returns and the SAVI is given by:

$$\ln L_{RV} = \ln L_R + \ln L_V. \tag{2.10}$$

For the non-linear constrained optimisation required to estimate the GARCH model parameters, the `fmincon` function in Matlab is used, this is based on the interior-point algorithm. The empirical results are discussed in the next section.

## 2.3 Empirical results

In this section, the performance of the GARCH(1,1), GJR-GARCH(1,1), and AGARCH(1,1) option pricing models in a South African equity context are considered. The goodness of fit of the different likelihood functions for each GARCH model is compared based on the AIC and SIC, and the performance of the models (the GARCH-implied SAVI compared to the historical SAVI) is compared based on the mean absolute error (MAE), and root mean squared error (RMSE). The information criteria and performance metrics are reported in Tables 2.1 and 2.2 below:

Table 2.1: GARCH model information criteria

| Log-likelihood function | GARCH(1,1) | | GJR-GARCH(1,1) | | AGARCH(1,1) | |
|---|---|---|---|---|---|---|
| | AIC | SIC | AIC | SIC | AIC | SIC |
| $\ln L_R$ | -6.4264 | -6.4168 | -6.4628 | -6.4508 | **-6.4776** | **-6.4656** |
| $\ln L_V$ | 6.5748 | 6.5844 | 7.4713 | 7.4833 | **5.4206** | **5.4326** |
| $\ln L_{RV}$ | -0.8559 | -0.8463 | **-0.9288** | **-0.9168** | -0.6642 | -0.6522 |

Table 2.2: GARCH-implied SAVI performance metrics

| Log-likelihood function | GARCH(1,1) | | GJR-GARCH(1,1) | | AGARCH(1,1) | |
|---|---|---|---|---|---|---|
| | MAE | RMSE | MAE | RMSE | MAE | RMSE |
| $\ln L_R$ | 3.4729 | 4.4200 | 3.7126 | 4.6570 | 3.0943 | 3.9850 |
| $\ln L_V$ | 3.6869 | 4.6287 | 3.2764 | 4.0218 | **1.9028** | **2.5157** |
| $\ln L_{RV}$ | **2.0112** | **1.986** | **1.9860** | **2.6060** | 2.5785 | 3.3930 |

In Table 2.1, the values in bold indicate the best fitting model for the respective log-likelihood function. The bold values in Table 2.2 indicate the log-likelihood function that produces the best performing GARCH model in estimating the SAVI.

The AIC and SIC clearly show that the asymmetric models produce a better fit when modelling Top40 returns; this is consistent with the findings of Oberholzer and Venter (2015). The performance metrics indicate that the joint log-likelihood function (historical returns and SAVI) produces the best performing model for the GARCH(1,1), and the GJR-GARCH(1,1) model. The log-likelihood function based on the historical SAVI ($\ln L_V$) produces the best performing AGARCH(1,1) model.

When the performance of the three GARCH option pricing models is considered, the AGARCH(1,1) model is the best performing model when modelling the implied SAVI. This implies that incorporating asymmetric effects improves performance when modelling implied volatility in the South African equity market, which is consistent with the information criterion. The coefficients of the best performing GARCH(1,1), GJR-GARCH(1,1) and AGARCH(1,1) model are reported in Table 2.3 below:

Table 2.3: GARCH model coefficients

| Coefficient | GARCH(1,1) | GJR-GARCH(1,1) | AGARCH(1,1) |
|---|---|---|---|
| $\alpha_0$ | 3.79E-07 | 3.58E-07 | 4.08E-07 |
| $\alpha_1$ | 0.0171 | 0.0029 | 0.015 |
| $\beta_1$ | 0.9825 | 0.9841 | 0.9775 |
| $\gamma$ | - | 0.0233 | 4.2273 |
| $\lambda$ | 0.1539 | 0.0695 | -3.5230 |

The asymmetry coefficient of the GJR-GARCH(1,1) and AGARCH(1,1) indicates that volatility of the Top40 returns reacts differently to positive and negative shocks, this is also consistent with previous findings in the literature. Furthermore, the $\gamma$ coefficient of the AGARCH(1,1) model is positive; this is consistent with expectations (positive for equity returns, Alexander, 2008). The coefficients in Table 2.3 were used to produce the line graphs below. Figure 2.1 illustrates the GARCH-implied SAVI (of the best performing models) and historical SAVI over time.

Figure 2.1: GARCH-implied SAVI

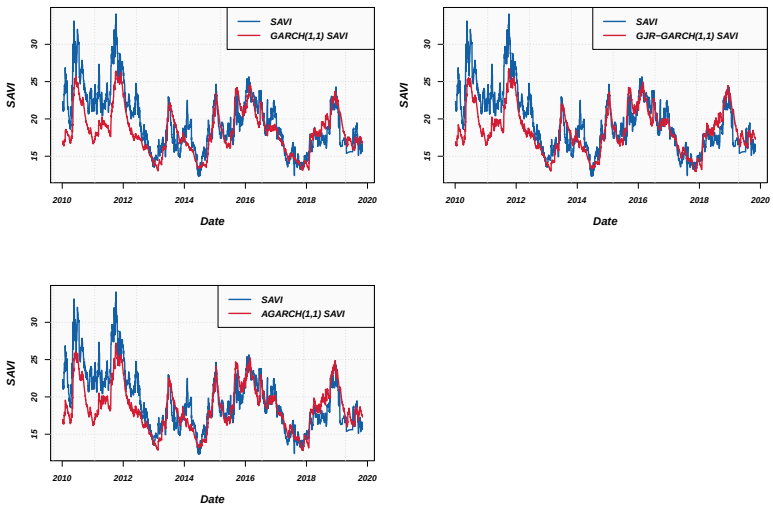


Figure 2.1 indicates that the GARCH-implied SAVI is similar for each model and that the models perform fairly well when compared to the historical SAVI.

The best performing GARCH(1,1), GJR-GARCH(1,1), and AGARCH(1,1) are used to price European options on the Top40; the model prices are compared to the JSE prices to test the pricing performance of each model. Monte Carlo simulation is used to obtain risk-neutral sample paths. Sample paths of each model are plotted in Figure 2.2 below:

Figure 2.2: Risk-Neutral Sample Paths

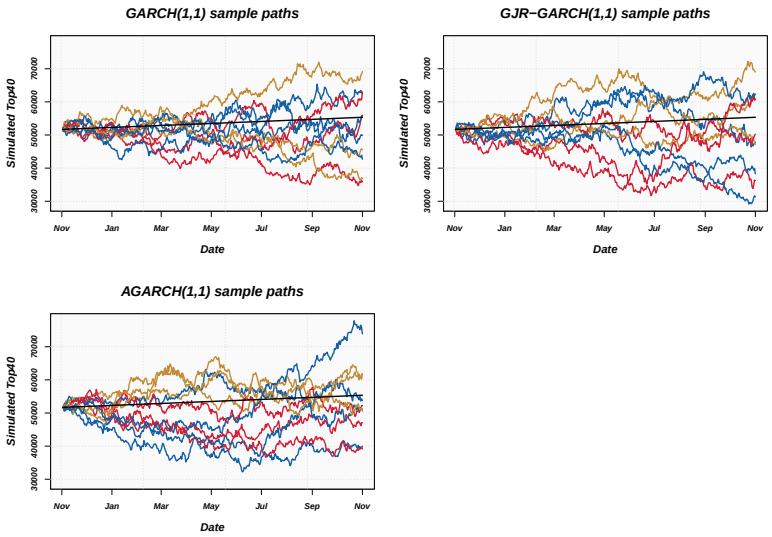

The sample paths in Figure 2.2 indicate how the simulated spot price varies over time. The black line in each subplot represents the expected value under the risk-neutral measure. This illustrates the concept of risk-neutrality.

To show the convergence of the Monte Carlo prices, we show the JSE price as well as three standard deviation error bounds of each relevant model, plotted across the number of simulations in Figure 2.3 below. The prices are for a 72-day European call option with strike $K = 41\ 251.27$ (moneyness=1.2). Furthermore, the interest rate used to simulate the spot price is consistent with the JSE forward curve (published by the JSE), the expected payoff is discounted using the 91-day Treasury bill rate.

Figure 2.3: GARCH Monte Carlo Option Prices

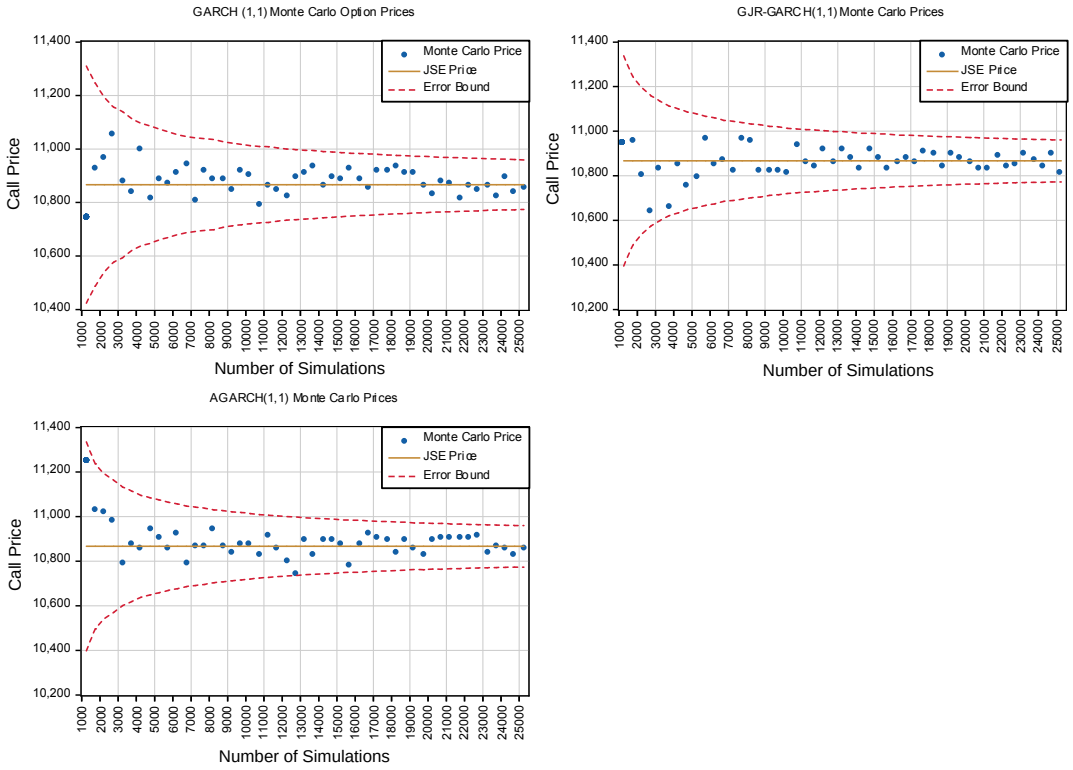


To test the pricing performance of each model, the model prices of nine 72-day European call options are compared to market prices published by the JSE (on 9 April 2019). The moneyness levels are equally spaced between 0.6 and 1.4. The GARCH option prices were calculated using 1 000 000 sample paths. The implied model prices and JSE prices are plotted in Figure 2.4 below:

Figure 2.4: Implied call option prices

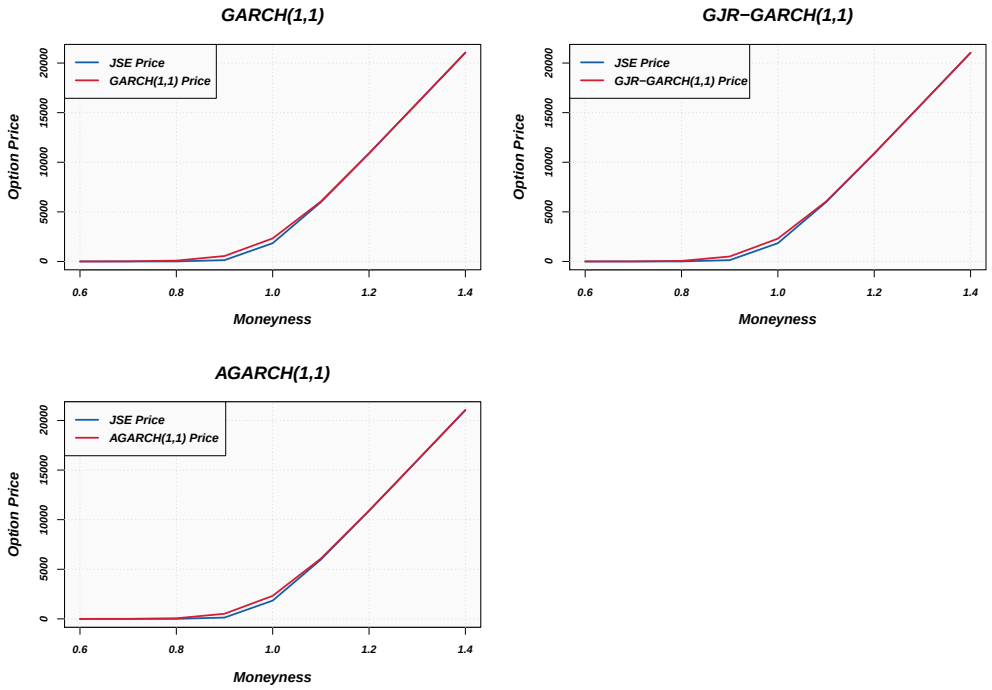


Figure 2.4 indicates that the GARCH option pricing models perform well when compared to market option prices. The pricing performance metrics and computation time (seconds required to price nine 72-day European call options) of each model are reported in Table 2.4 below:

Table 2.4: Pricing performance metrics and computation time

| Model | RMSE | MAE | Computation Time |
|---|---|---|---|
| GARCH(1,1) | 191.4070 | 104.5114 | 225.5 |
| GJR-GARCH(1,1) | 184.0239 | 99.6803 | 281.3 |
| AGARCH(1,1) | **180.2461** | **97.5269** | 275.9 |

The RMSE and and MAE are calculated based on the ZAR (South African Rand) values of the option prices. The pricing performance metrics indicate that the AGARCH(1,1) model is the most accurate, followed by the GJR-GARCH(1,1) model, and finally the GARCH(1,1) model. The results are consistent with the implied SAVI performance metrics. However, the difference between the pricing performance of the symmetric GARCH(1,1) model and the asymmetric models is marginal. Furthermore, the computation time indicates that the time required to price options using the GARCH(1,1) is

slightly less than the other models; this is due to the fact that the latter model does not include a term modelling asymmetry.

## 2.4 Summary

The use of volatility indices has grown in recent times. These indices are used to aid in the prediction and measurement of financial conditions as well as stress situations in the markets (Huskaj and Larsson, 2016). In recent work, Bollerslev et al. (2015) highlighted the use of volatility indices and the variance risk premium to predict aggregate stock market returns. While many studies have been performed using the CBOE VIX, we consider the SAVI index.

In this chapter, three different GARCH models were used to model the GARCH-implied SAVI. The symmetric GARCH(1,1), the asymmetric GJR-GARCH, and AGARCH(1,1) models. Furthermore, three different log-likelihood functions were considered in the model parameter estimation. The first based on historical returns data only, the second based on the historical SAVI, and finally a joint likelihood function based on the historical returns and SAVI. This is based on the work by Hao and Zhang (2013).

The goodness of fit of each model was compared based on the AIC and SIC. The information criteria indicated that the asymmetric models provide a better fit when compared to the symmetric GARCH(1,1) model, this is consistent with previous findings in the literature (Oberholzer and Venter, 2015, Flint et al., 2014). The accuracy of each model was tested by comparing the GARCH-implied SAVI to the historical SAVI.

Regarding the log-likelihood functions, for the GARCH(1,1) and GJR-GARCH(1,1) the joint likelihood function based on historical returns and the historical SAVI produces the best performing model. The log-likelihood function based on the historical SAVI produces the best performing AGARCH(1,1) model. Finally, when the performance of all models are considered, the empirical results showed that the asymmetric AGARCH(1,1) is the best performing model when modelling the GARCH-implied SAVI.

The pricing performance of the GARCH option pricing models was compared based on the GARCH-implied prices when compared to (72-day) market traded European option prices. The results were consistent with the GARCH-implied SAVI results; this indicates that the use of asymmetric GARCH option pricing models improves the model performance in the South African equity market. However, the improvement is marginal. The use of asymmetric models is more computationally intensive. Therefore our results are in line with Hansen and Lunde (2005), the GARCH(1,1) model is highly robust and that it is difficult to find an alternative model that shows consistent outperformance.

This chapter indicates that the use of volatility indices in a South African equity context improves pricing performance. However, the focus was on equity options only. The next chapter extends the analysis to the FX market. Furthermore, the FX volatility indices of South Africa and the United States of America are considered.

# Chapter 3

# GARCH Option Pricing and Implied FX Volatility Indices

## 3.1 Introduction

In this chapter,[1] the GARCH option pricing analysis applied in Chapter 2 is extended to the FX market. FX turnover exceeds $8.3 trillion daily according to the most recent BIS Triennial Central Bank survey (BIS , 2019). Currency movements are therefore studied intensively by market participants as leading indicators of macro-economic stress based on their immense liquidity, especially the United States Dollar (USD), Euro, Pound Sterling and Japanese Yen. According to Dimitriou and Kenourgios (2013), studies that examine the behaviour of currency markets during high volatility periods are rare.

Baruník et al. (2017) explain that currency volatility is an important factor to consider for various market participants; on the FX market volatility affects decisions to hedge open foreign exchange positions and may also increase the idiosyncratic risk that diminishes gains from international portfolio diversification.

It is interesting to view ZAR against other emerging market peers. Figure 3.1 below demonstrates average daily turnover (BIS , 2019) per currency as a percentage of nominal GDP (gross domestic product) detailing the ZAR liquidity. The ZAR is frequently viewed as one of the most liquid currencies in the world and seen as an emerging market proxy - this makes the ZAR of interest in any currency related analysis.

[1] This chapter is based on a paper (Venter and Maré, 2021) that appeared in *Studies in Economics and Econometrics.*

Figure 3.1: Average daily turnover per currency as a percentage of nominal GDP

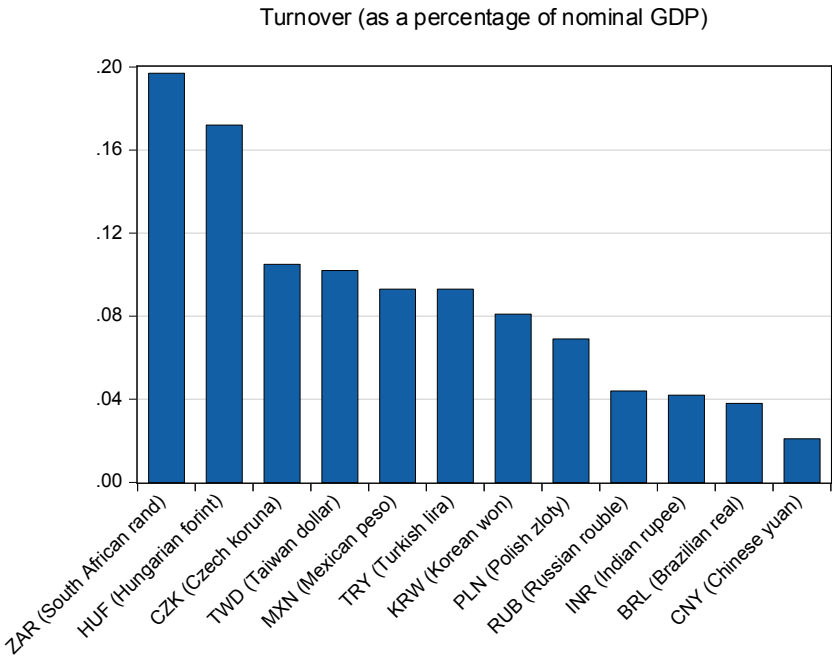


As mentioned previously, the use of volatility indices (fear indices), have become very popular in recent years. According to Alexander et al. (2015), a wide range of volatility indices on different asset classes have been developed. Furthermore, these volatility indices are constructed using European options. As explained, volatility indices reflect investors' expectations of future realised volatility (in this case, volatility in the FX market).

The focus of this study is on the modelling of FX volatility indices, both a developed market (USD to the Euro, referred to as the Euro VIX) and an emerging market (ZAR to USD, referred to as the SAVI Dollar) are considered. As mentioned previously, the ZAR is considered due to the fact that it is highly liquid compared to its peers. According to Alexander et al. (2015), the Euro VIX and SAVI Dollar are based on one-month and three-month expected volatility respectively.

In this chapter, the GARCH-implied volatility approach by Hao and Zhang (2013) (also applied in Chapter 2) is extended to FX options. Hence, volatility indices are obtained using the GARCH option pricing model, and not the model-free approach used by the CBOE and the JSE.

The remainder of this chapter is structured as follows: Section 3.2 reviews the recent and relevant literature, Section 3.3 focuses on the theoretical framework, the data and estimation methods are discussed in Section 3.4, the empirical results are presented in

Section 3.5, and finally the main findings are summarised.

## 3.2 Literature review

Variance risk premia is a well-researched topic. Carr and Wu (2019) estimated the variance risk premium using the risk-neutral expected variance, also known as the variance swap rate. This rate is approximated using a particular portfolio of options. Carr and Wu (2019) propose that the variance risk premium is equal to the difference between the realised variance, and the synthetic variance swap rate. The empirical analysis consisted of an investigation of the historical behaviour of the variance risk premium on five stock indices, and five individual stocks. The results show that the variance risk premiums are strongly negative.

According to Fassas and Papadamou (2018), implied volatility reflects not only uncertainty in the market, but also investors' risk aversion. Hence the risk aversion component reflects the investors' compensation for bearing risk and can be measured by the variance risk premium. Fassas and Papadamou (2018) estimate the variance risk premium by taking the difference between an implied volatility index, and realised volatility in the equity market (this approach is extended to the FX market in this study). Empirical evidence shows that the risk premium is negative on average, indicating that the variance risk premium is priced in.

Research based on FX option pricing and volatility indices is well-documented. The empirical performance of the FX GARCH option pricing model was considered by Bhat and Arekar (2016). The pricing performance during turbulent times of exchange-traded currency options (USD for Indian Rupee), using the FX GARCH option pricing model and the Black-Scholes model, was compared. The empirical results indicate that the Black-Scholes model performs better than the FX GARCH option pricing model. However, it is also noted that the FX GARCH option pricing model is free of the strike price and maturity biases associated with the Black-Scholes model.

Kanniainen et al. (2014) used historical data of the CBOE VIX to improve the pricing performance of the GARCH option pricing model when applied to options on the S&P500 index. The method is based on joint maximum likelihood estimation, which incorporates both historical returns of the underlying asset and the level of the volatility index. The empirical results indicate that the joint maximum likelihood method is superior when the pricing performance is compared to the model when calibrated to historical returns only.

In the previous chapter, the work by Hao and Zhang (2013) was applied to the South Arican equity market. The overall conclusion is that the SAVI can be used to obtain more accurate option prices. In this chapter, this work is extended to the FX market by making use of the FX GARCH option pricing model derived by Duan and Wei (1997). The theoretical framework applied in this chapter is outlined in the next section.

## 3.3 Theoretical framework

In this section, the theory of the variance risk premium and GARCH option pricing model applied to FX options is discussed. This section is divided into two parts; the first focuses on the variance risk premium, and the second on the option pricing framework. The theoretical aspects of the GARCH-implied SAVI is discussed in Section 2.2.3.

### 3.3.1 Variance risk premium

In this chapter, a similar approach to Fassas and Papadamou (2018) is followed. According to Della Corte et al. (2016), the $\tau$-period (in days) variance risk premium is formally defined as:

$$VRP_{t,\tau} = \mathbb{E}^P[RV_{t,\tau}] - \mathbb{E}^Q[RV_{t,\tau}],$$

where $RV_{t,\tau}$ is the $\tau$-period realised variance at time $t$. Furthermore, the expectation of the $\tau$-period realised volatility under $P$ is given by:

$$\mathbb{E}^P[RV_{t,\tau}] = \frac{252}{\tau}\sum_{i=0}^{\tau}\left[\ln\left(\frac{X_{t-i}}{X_{t-i-1}}\right)\right]^2,$$

where $X_t$ is the exchange rate at time $t$.

Fassas and Papadamou (2018) define the risk-neutral expectation of the realised variance as the squared implied volatility index ($IV_t^2$). Hence, the variance risk premium is given by:

$$VRP_{t,\tau} = 100 \times (RV_{t-1,\tau} - IV_{t-1})$$

The US FX variance risk premium is estimated using the Euro VIX. To estimate the South African FX variance risk premium, the SAVI Dollar is used. The FX GARCH option pricing model is outlined in the next subsection.

### 3.3.2 FX GARCH option pricing model

In this study, the following is assumed regarding the FX log-returns under the real-world measure $P$:

$$\ln\left(\frac{X_t}{X_{t-1}}\right) = r^{(d)} - r^{(f)} + \lambda\sqrt{h_t} - \frac{1}{2}h_t + \epsilon_t \tag{3.1}$$
$$\epsilon_t|\mathcal{F}_{t-1} \sim \mathcal{N}(0, h_t),$$

where $r^{(d)}$ and $r^{(f)}$ are the domestic and foreign rates respectively. In order to price options written on the exchange rate $X_t$, the risk-neutral dynamics are required. Duan and Wei (1997) define the equilibrium pricing measure as follows:

**Definition 5: Equilibrium pricing measure**

An equilibrium price measure $Q_d$ for the domestic market satisfies the LRNVR if for any asset value (measured in domestic currency $X_t^{(d)}$), the following conditions are satisfied:

1. $Q_d$ is mutually continuous with respect to $P$;
2. $\frac{X_t^{(d)}}{X_{t-1}^{(d)}}$ is log-normally distributed under $Q_d$;
3. $\mathbb{E}_t^{Q_d}\left(\frac{X_t^{(d)}}{X_{t-1}^{(d)}}\right) = \exp\{r^{(d)}\}$ almost surely under $P$; and
4. $\mathbb{V}ar^{Q_d}\left(\ln \frac{X_t^{(d)}}{X_{t-1}^{(d)}}|\mathcal{F}_t\right) = \mathbb{V}ar^{P}\left(\ln \frac{X_t^{(d)}}{X_{t-1}^{(d)}}|\mathcal{F}_t\right)$ almost surely under $P$.

If the exchange rate follows the dynamics specified in 3.1, and if the equilibrium price measure satisfies the LRNVR, Duan and Wei (1997) show that the risk-neutral dynamics are given by,

$$\ln\left(\frac{X_t}{X_{t-1}}\right) = r^{(d)} - r^{(f)} - \frac{1}{2}h_t + \xi_t, \tag{3.2}$$

where

$$\xi_t = \epsilon_t + \lambda\sqrt{h_t}|\mathcal{F}_t \sim \mathcal{N}(0, h_t).$$

Given the risk-neutral dynamics of $h_t$, risk-neutral realisations of $X_t$ (Equation 3.2) can be simulated, option prices are equal to the expected discounted payoff. In this chapter, the same univariate GARCH processes that were estimated in Chapter 2 are applied. The real-world and risk-neutral dynamics of these models are outlined in Section 2.2.2.

## 3.4 Data and estimation

In this study, the Euro VIX and SAVI Dollar are estimated using univariate GARCH models. The dataset consists of daily data for the 91-day Treasury bill rates for each currency, the ZAR/USD exchange rate, the USD/EUR exchange rate, the SAVI Dollar index, and the Euro VIX index. The dataset was obtained from Bloomberg. Three different maximum likelihood methods are considered for the estimation of the GARCH-implied volatility indices, this is based on the work by Hao and Zhang (2013).

The first maximum likelihood method makes use of historical data only, the log-likelihood function is given by,

$$\ln L_{FX} = -\frac{N}{2}\ln 2\pi - \frac{1}{2}\sum_{t=1}^{N}\left(\ln h_t + \left[\ln\frac{X_t}{X_{t-1}} - (r^{(d)} - r^{(f)}) - \lambda\sqrt{h_t} + \frac{1}{2}h_t\right]^2 / h_t\right).$$

The second log-likelihood function relies on the assumption that the difference between the GARCH-implied volatility index and the market volatility index is normally distributed (consistent with Equation 2.9). Finally, a joint likelihood considered (consistent with Equation 2.10). The empirical results are considered in the next section.

## 3.5 Empirical results

In this section, the empirical results of the estimated variance risk premium and the univariate GARCH-implied volatility indices are reported. This section is divided into two subsections; the first focuses on the variance risk premium, and the second on the GARCH-implied volatility indices.

### 3.5.1 Variance risk premium

The descriptive statistics of the ZAR and USD variance risk premium are reported in Table 3.1 below:

Table 3.1: Descriptive statistics: variance risk premia

| | ZAR FX | USD FX |
|---|---|---|
| Mean | -0.0988 | -0.2453 |
| Median | -0.2487 | -0.2113 |
| Maximum | 2.8529 | 1.0952 |
| Minimum | -3.9815 | -2.2577 |
| Std. Dev. | 0.8336 | 0.4052 |
| Skewness | 0.4269 | -0.6901 |
| Kurtosis | 4.3585 | 5.3170 |
| Jarque-Bera | 262.8042 | 790.0604 |

The descriptive statistics in Table 3.1 indicate that the both the ZAR and USD variance risk premium are negative on average. This indicates that the variance risk premium is captured in FX market option prices, this is consistent with findings by Fassas and Papadamou (2018). Furthermore, the Jarque-Bera statistic indicates that both series are not normally distributed. Finally, the variance risk premium of the ZAR FX market is more volatile when compared to the USD market. This is consistent with expectations due to South Africa being an emerging market.

To illustrate how the variance risk premium varies over time, the real-world variance, risk-neutral variance and variance risk premium for each currency is plotted in Figures 3.2 and 3.3.

Figure 3.2: ZAR FX variance risk premium

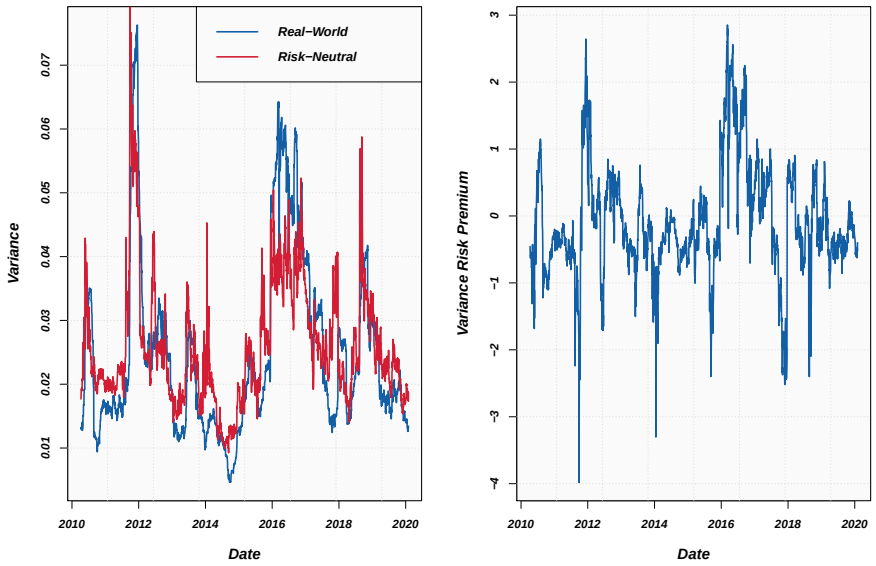


Figure 3.3: USD FX variance risk premium

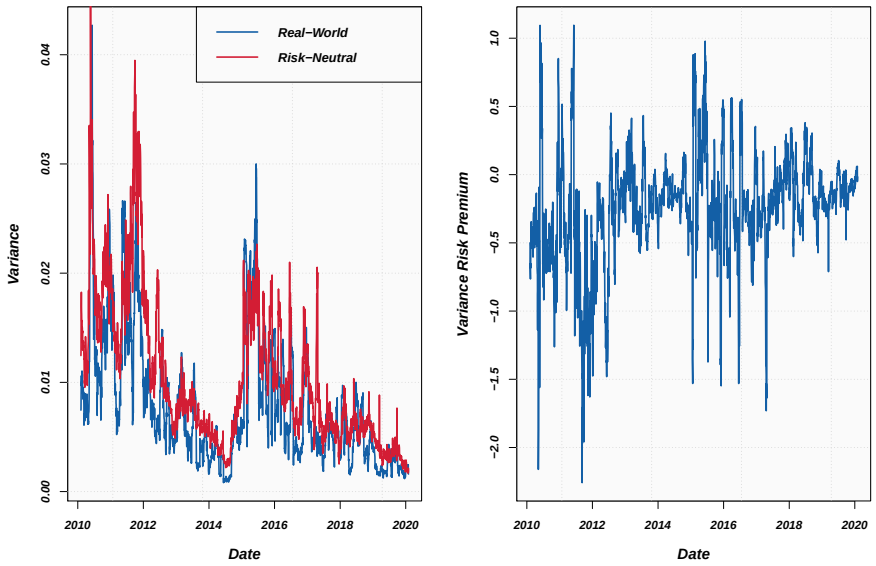


As expected, the line graphs indicate that the ZAR is the more volatile of the two curren-

cies. Furthermore, the variance risk premium tends to decrease at lower levels of volatility. Hence, during periods of low volatility, investors require less compensation for taking risk, which is consistent with expectations.

### 3.5.2 GARCH-implied FX volatility indices

In this subsection, the different univariate GARCH models and maximum likelihood methods are compared for the GARCH-implied SAVI Dollar and the Euro VIX. The different univariate GARCH models and maximum likelihood methods are compared based on the RMSE and the MAE. The performance metrics for the GARCH-implied SAVI Dollar and Euro VIX are reported in the Tables 3.2 and 3.3.

Table 3.2: GARCH-implied SAVI Dollar performance metrics

| Likelihood function | GARCH(1,1) | | GJR-GARCH(1,1) | | AGARCH(1,1) | |
|---|---|---|---|---|---|---|
| | RMSE | MAE | RMSE | MAE | RMSE | MAE |
| $L_R$ | 1.4921 | 1.9865 | 1.3308 | 1.7482 | 1.1861 | 1.5906 |
| $L_V$ | 1.1054 | 1.4818 | 1.7962 | 2.2575 | 2.1918 | 2.8332 |
| $L_{RV}$ | **1.0753** | **1.4652** | **1.0439** | **1.4088** | **1.0375** | **1.3776** |

Table 3.3: GARCH-implied Euro VIX performance metrics

| Likelihood function | GARCH(1,1) | | GJR-GARCH(1,1) | | AGARCH(1,1) | |
|---|---|---|---|---|---|---|
| | RMSE | MAE | RMSE | MAE | RMSE | MAE |
| $L_R$ | 1.2746 | 1.8100 | 1.2681 | 1.7560 | 1.3589 | 1.8746 |
| $L_V$ | **1.0163** | **1.4243** | 1.0608 | 1.4825 | **1.0180** | **1.4337** |
| $L_{RV}$ | 1.1266 | 1.5278 | **0.9934** | **1.4037** | 1.0220 | 1.4454 |

The best performing maximum likelihood method is indicated in bold in Tables 3.2 and 3.3. When the SAVI Dollar performance metrics are considered, it is clear that the joint log-likelihood function performs best. Furthermore, the AGARCH(1,1) is the best performing univariate GARCH model. When the Euro VIX is considered, the log-likelihood function based on the difference between the market and GARCH-implied volatility index seems to be the most reliable. The GJR-GARCH model is the best performing model when modelling the GARCH-implied Euro VIX. The best performing models are plotted in Figures 3.4 and 3.5.

Figure 3.4: GARCH-implied SAVI Dollar

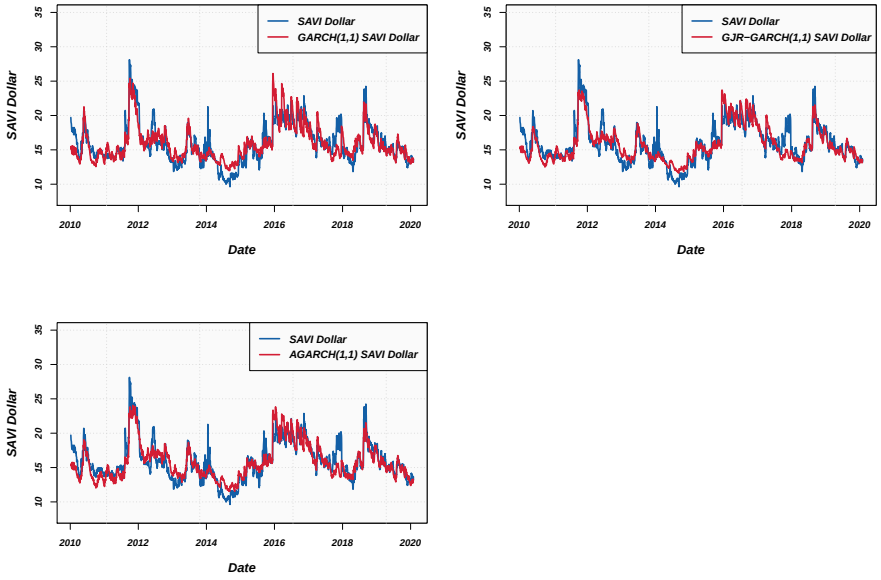


Figure 3.5: GARCH-implied Euro VIX

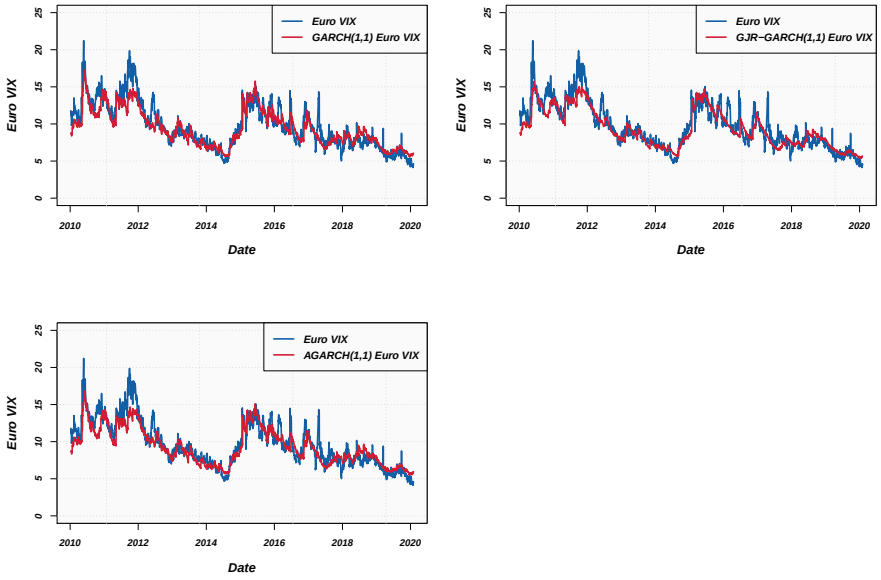


In most instances, the univariate GARCH models perform well for both the SAVI

Dollar and the Euro VIX. Furthermore, asymmetry is an important factor to consider in both markets. The asymmetric GJR-GARCH and AGARCH models outperform the symmetric GARCH model in most cases. Finally, the maximum likelihood method based on historical data only does not sufficiently capture the variance risk premium, this is consistent with the outputs by Hao and Zhang (2013).

## 3.6 Summary

Foreign currency markets frequently serve as early warning systems for macroeconomic shocks and market stresses owing to their significant volumes traded. An implementation of GARCH option pricing models is extended to create volatility indices for the EUR and ZAR against the USD yielding a powerful method to examine forward looking volatility risk premia for currencies. This has application to trading and investment strategies as well as forward looking exchange rate forecasts and asset pricing models.

The empirical results indicate that the ZAR is the more volatile of the two currencies. Furthermore, the variance risk premium tends to decrease at lower levels of volatility, which is consistent with expectations. Furthermore, the joint likelihood method based on historical data and the difference between the market and GARCH-implied volatility index is the most reliable for the SAVI Dollar. When the Euro VIX is considered, the log-likelihood function based on the difference between the market and GARCH-implied volatility index seems to be the most reliable. The maximum likelihood method based on historical data only does not sufficiently capture the variance risk premium, this is consistent with other findings in the literature.

The empirical results also show that asymmetry is an important factor to consider when modelling FX volatility indices using univariate GARCH models, this is the case for both the SAVI Dollar and the Euro VIX. This is also consistent with the South African equity market (Chapter 2). This chapter concludes Part I on option pricing and volatility indices in the South African market. Thus far, the estimated models have relied on the existence of a volatility index and therefore an established derivatives market is required. The focus of Part II is implied volatility in the cryptocurrency market (*i.e.,* pricing in the absence of an established derivatives market).

# Part II

# Option Pricing and Volatility Indices in the Cryptocurrency Market

# Chapter 4

# Price Discovery in the Cryptocurrency Option Market: A Univariate GARCH Approach

## 4.1 Introduction

Cryptocurrencies, and especially BTC, have gained a lot of attention in recent years. A problem that the cryptocurrency market is currently facing, is that it does not have a well-established derivatives market. This implies that there is no consensus regarding the pricing of options and other derivatives based on cryptocurrencies. According to Barnes (2018), cryptocurrencies have no intrinsic value. Barnes (2018) further explains that cryptocurrencies have prices, which are generally unrelated to economic events and determined by interaction between supply and demand.

Madan et al. (2019) explain that the cryptocurrency derivatives market is a young market and therefore different pricing methodologies are required for price discovery. Madan et al. (2019) found that models that incorporate stochastic volatility generally perform well when applied to the pricing of cryptocurrency options. A possible solution is to rely on historical data; this was considered by Hou et al. (2018) for the pricing of BTC and CRIX options, with the focus on a stochastic volatility model with correlated jumps.

In this chapter,[1] the GARCH option pricing model is applied to BTC and CRIX. We consider symmetric and asymmetric GARCH models to assess the impact of asymmetric effects on the implied volatility of cryptocurrencies. In a similar study, Dyhrberg (2016) made use of univariate GARCH models (symmetric and asymmetric) to assess the financial asset capabilities of BTC. The empirical results of this study indicate that the volatility of BTC reacts similarly to positive and negative news. However, the focus of this chapter is on symmetric and asymmetric effects of cryptocurrencies in an option pricing context, and how option prices can be obtained in the absence of a well-established derivatives market

[1] A previous version of this chapter appears as a publication (Venter et al., 2020) in *Cogent Economics and Finance.*

(by making use of historical data).

The rest of this chapter is structured as follows. In Section 4.2 the recent and relevant literature is considered. Section 4.3 focuses on the theoretical framework. In Section 4.4, the statistical properties of the dataset and estimation method is considered. Section 4.5 focuses on the empirical results, and Section 4.6 summarised the main findings.

## 4.2 Literature review

This section focuses on recent and relevant literature, and is divided into three subsections. The first subsection focuses on cryptocurrency indices, the second reviews relevant literature based on volatility models applied to cryptocurrencies, finally studies based on cryptocurrency derivatives are considered.

### 4.2.1 Cryptocurrency indices

According to Chu et al. (2017), with the exception of BTC, there is not much literature focused on the application of GARCH models to cryptocurrencies. Therefore, the CRIX is also considered in this chapter. According to Abboud (2017), there have been several attempts to construct a cryptocurrency index. Most cryptocurrency index attempts make use of empirical models from traditional financial markets with arbitrary parameters fitted to cryptocurrencies. The indices include capitalisation weighted indices like CRIX, Bletchley, TaiFu30, Crypto30, LBI, Smith + Crown SCI. Furthermore, capped capitalisation indices include: CRYPTO20, CCX30, and BIT20. Finally, the smoothed capitalisation weighted index, such as the CCI30.

According to Kim et al. (2019) the CRIX is comparable to the S&P500 index (reflection of the current state of the US market) because it gives an indication of the current state of the cryptocurrency market. Furthermore, Kim et al. (2019) explain that the CRIX provides a statistically backed (the number of constituents is determined by the explanatory power that each cryptocurrency has over market movements, this is based on the Akaike information criterion) market measure, which distinguishes it from other cryptocurrency indices. Therefore, the CRIX is used in this study to give an indication of the volatility of the cryptocurrency market as a whole. The CRIX was also used as a proxy for the cryptocurrency market by Elendner et al. (2018), Klein et al. (2018), and Hafner (2020).

### 4.2.2 Cryptocurrency volatility modelling

Cryptocurrency volatility modelling has gained a lot of attention in recent years (as mentioned previously, most of this work has been based on BTC). In an attempt to forecast BTC risk, Agyarko et al. (2019) made use of univariate symmetric and asymmetric GARCH models. Their empirical results indicate that the symmetric GARCH(1,1) model provides the best fit. This is also consistent with the argument by Hansen and Lunde (2005), it is difficult to find a model that consistently outperforms the GARCH(1,1) model because it is highly robust and parsimonious. With regard to forecasting risk, Agyarko et

al. (2019) explain that no model clearly emerged as superior. Therefore, the study indicates that it is reliable to use the best fitted model when forecasting volatility (symmetric GARCH, in the case of BTC).

In a recent study, Kurihara and Fukushima (2018) made use of different univariate GARCH models to analyse BTC volatility. Both symmetric and asymmetric GARCH models were considered. The overall conclusion is that there is not much difference when symmetric and asymmetric GARCH models are compared, and that traders should consider both short and long term volatility when examining BTC prices. In a similar study, Katsiampa (2017) considered a wide range of univariate GARCH models for the modelling of BTC volatility. In this study, the best fitting model was determined using the Akaike, Bayesian and Hannan-Quinn information criterion. Their empirical results indicate that the autoregressive component GARCH model is the best performing model. This highlights the importance of both short and long run volatility components of the conditional variance.

Chen et al. (2018) performed an econometric analysis of the CRIX for portfolio investment. The empirical analysis included the application of autoregressive integrated moving average (ARIMA), univariate GARCH, and multivariate GARCH models. Their empirical results illustrate that the GARCH(1,1) model is sufficient to explain the heteroskedasticity of the CRIX. Chen et al. (2018) also consider alternate GARCH specifications. To capture the leverage effect (negative relationship between return shocks and subsequent shocks to volatility) the exponential GARCH (EGARCH) model was estimated. However, McAleer and Hafner (2014) show that leverage is not possible for the EGARCH model. Chen et al. (2018) conclude that the symmetric GARCH(1,1) model with a Student-$t$ error distribution is the best performing univariate model when applied to the CRIX.

In order to determine the effect weather has on the cryptocurrency market, Kathiravan et al. (2019) made use of a GARCH(1,1) model, Johansen cointegration, and a Granger causality test. The Coinbase index was used as a proxy for the cryptocurrency market in this study. The GARCH analysis showed that temperature is the only weather factor that is statistically significant when modelling cryptocurrency volatility.

To give an indication of the best performing volatility model when applied to the cryptocurrencies market (not focused on BTC only), Chu et al. (2017) applied 12 GARCH models (eight different error distributions) to the seven most popular cryptocurrencies. The models were compared based on the goodness of fit, forecasting performance, and acceptability of value-at-risk estimates. Their empirical results indicate that the normal distribution provides the best fitting GARCH model in most cases. Furthermore, the symmetric integrated GARCH(1,1) (IGARCH(1,1)) model with normal innovation was the best fitting model for most cryptocurrencies.

In a recent study, Hafner (2020) made use of GARCH models to test for the existence of speculative bubbles in the cryptocurrency market. The empirical analysis made use of eleven of the largest cryptocurrencies and the CRIX. The estimated parameters of the GARCH models indicate that volatility clustering is important and significant when modelling cryptocurrency volatility and, unlike equities, cryptocurrencies do not have asymmetric news impact curves. More specifically, the asymmetry terms of asymmetric

GARCH models are generally statistically insignificant when applied to cryptocurrencies, this is consistent with other findings in the literature (see *e.g.* Baur and Dimpfl, 2018). According to Hafner (2020), there is general evidence that speculative bubbles exist in cryptocurrency markets.

Gyamerah (2019) made use of the symmetric GARCH(1,1), threshold-GARCH(1,1) (TGARCH(1,1)), and IGARCH(1,1) models to model the volatility of BTC returns. With regards to the error distribution, Gyamerah (2019) considered the Student-$t$, generalised error, and normal inverse Gaussian distributions. The different models were compared based on the AIC and SIC. Their empirical results indicate that the asymmetric TGARCH(1,1) model with a normal inverse Gaussian error distribution is the best fitting model when modelling volatility of BTC returns. This implies that incorporating asymmetry in the GARCH model specification, and skewness and kurtosis in the error distribution, can improve the fit of a GARCH model when applied to BTC.

In order to determine the best performing model when forecasting exchange rate and cryptocurrency (BTC, Ethereum, and Dash) volatility, Peng et al. (2018) made use of the following univariate GARCH models: GARCH(1,1), EGARCH(1,1) and the GJR-GARCH(1,1) model. Three different error distributions were considered: normal, Student-$t$, and skewed Student-$t$ distributions. In addition, a support vector regression GARCH(1,1) model was also estimated. Their empirical results show that the support vector regression GARCH(1,1) model is superior when compared to the other models considered. Furthermore, when the traditional GARCH models are compared, the GJR-GARCH(1,1) performed slightly better when compared to the symmetric GARCH(1,1) and EGARCH(1,1) models. The different error distributions yielded similar results. This illustrates that different GARCH specifications can offer better results when applied to exchange rate and cryptocurrency volatility.

### 4.2.3 Cryptocurrency derivatives

According to Madan et al. (2019), the BTC derivatives market is a young, but growing market. Shi and Shi (2019) explain that BTC futures were introduced in 2012, this was done to provide investors with additional trading tools for BTC. In 2014 more BTC derivatives such as BTC swaps and options emerged. Karkkainen (2018) analysed BTC futures using vector autoregressive and vector error correction models. The author's empirical results indicate that futures lead price discovery in the BTC market. This is consistent with existing literature of futures-spot market price discovery.

To illustrate how cryptocurrency derivatives can be used, Sebastião and Godinho (2019) investigated the hedging properties of BTC futures. The authors considered an equal and opposite hedge, as well as optimal hedge ratios estimated using the ordinary least squares, and dynamic conditional correlation GARCH approach. The hedge effectiveness was determined by comparing the variance, semivariance, and expected shortfall of the hedged portfolio to the unhedged position. Their empirical results show that BTC futures are effective hedge instruments for BTC and also other cryptocurrencies.

Madan et al. (2019) made use of option price data collected from various unregulated exchanges to construct various BTC volatility surfaces. Furthermore, different Markov

models were calibrated to the volatility surfaces to determine the best performing model. The empirical results indicate that the classical Black-Scholes model does not capture the volatility surface well and that models including some notion of stochastic volatility perform better. However, the GARCH option pricing model was not considered.

In a recent study, Pagnottoni (2020) made use of a neural network approach for the pricing of BTC options, where the classical models, namely the trinomial tree model, Monte Carlo simulation, and finite difference methods were used as input layers. The empirical results show that BTC option prices are overpriced when classical methods are considered, and that the use of the neural network model significantly improves pricing performance.

Hou et al. (2018) mentioned that research based on cryptocurrency derivatives is limited despite its necessity, and that cryptocurrency derivatives trading on unregulated exchanges have recently increased significantly. Hou et al. (2018) proposed a stochastic volatility model with correlated jumps. The empirical results indicate that the pricing mechanism underscores the importance of jumps in the cryptocurrency derivative markets. The theoretical framework is considered in the next section.

## 4.3 Theoretical framework

In this chapter, the GARCH option pricing model outlined in Section 2.2.2 is applied to BTC and CRIX. BTC and CRIX are both expressed in USD, therefore the United States three-month Treasury bill rate is used as a proxy for the risk-free rate, consistent with Hao and Zhang (2013). Furthermore, we assume that innovations are normally distributed, this is appropriate based on the findings by Chu et al. (2017).

In this study, two driving GARCH processes are considered, the GARCH(1,1) and the GJR-GARCH(1,1). According to Hansen and Lunde (2005), the GARCH(1,1) is highly robust and it is challenging to find a different GARCH model that produces consistent outperformance. Therefore, the GARCH(1,1) model is used as a benchmark in this chapter. Furthermore, Peng et al. (2018) compared different univariate GARCH models when applied to exchange rate and cryptocurrency volatility forecasting. Their results indicate that the GJR-GARCH(1,1) is the best performing model. Therefore, the asymmetric GJR-GARCH(1,1) model is considered in this chapter.

The pricing performance of the GARCH option pricing model is tested by comparing prices obtained using the GARCH option pricing model to BTC market option prices and the Heston stochastic volatility model (based on the work by Madan et al., 2019). The application of the Heston stochastic volatility model is an existing method for pricing BTC derivatives. According to Glasserman (2013), the risk-neutral asset price and volatility dynamics in the Heston framework are given by,

$$dS_t = rS_t dt + \sqrt{\Upsilon_t} S_t dW_t^{(1)},$$

$$d\Upsilon_t = \kappa(\varpi - \Upsilon_t)dt + \bar{\sigma}\sqrt{\Upsilon_t} dW_t^{(2)},$$

$$dW_t^{(1)} dW_t^{(2)} = \rho dt,$$

where $\kappa$ is the variance mean reversion speed, $\varpi$ is the long-run mean of the variance, $\bar{\sigma}$ is the volatility of the variance, $W_t^{(1)}$ and $W_t^{(2)}$ are standard Brownian motions, and $\rho$ is the correlation between the variance and the asset price. A closed-form solution does exist for European put and call options, therefore the model is generally calibrated to market option prices (or implied volatility). The data and estimation of GARCH model parameters are discussed in the next section.

## 4.4 Data and estimation

In this chapter, the GARCH option pricing model is applied to BTC and CRIX. The GARCH models are calibrated to historical data (see Section 2.2.4 for more detail). The BTC and US Treasury bill historical data were obtained from the Thomson Reuters Datastream databank. The CRIX historical dataset was obtained from `thecrix.de`. The weighting scheme of the CRIX is outlined in Trimborn and Härdle (2018). Daily data from the 1-Jan-2016 to 3-Jan-2020 for all variables were used for the estimation of parameters.

The descriptive statistics of BTC and CRIX log-returns are reported in Table 4.1 below:

Table 4.1: Descriptive statistics: log-returns

| | BTC | CRIX |
|---|---|---|
| Mean | 0.0027 | 0.0029 |
| Median | 0.0026 | 0.0032 |
| Maximum | 0.2384 | 0.2203 |
| Minimum | -0.2514 | -0.2533 |
| Standard Deviation | 0.046 | 0.0461 |
| Skewness | 0.0046 | -0.3903 |
| Kurtosis | 7.1336 | 7.3798 |
| Jarque-Bera | 743.2889 | 860.9537 |
| Observations | 1044 | 1044 |

The results indicate that the means of the log-returns for both BTC and CRIX are close to zero. Moreover, both series indicate evidence of fat tails, this is consistent with the stylised facts of financial returns (Cont, 2001). The Jarque-Bera test statistics indicate that both series are not normally distributed. Finally, when the two series are compared, the means and standard deviations are similar, this is in line with expectations because the weighting of BTC is high when calculating CRIX (Trimborn and Härdle, 2018).

## 4.5 Empirical results

In this section, the implied volatility surfaces of BTC and CRIX are considered. The importance of asymmetry is illustrated by comparing the implied volatility obtained from the symmetric model to the asymmetric model. Furthermore, the pricing performance of the GARCH option pricing is tested by comparing BTC option prices obtained from the GARCH option pricing model to market option prices, and prices obtained using the Heston stochastic volatility model.

The GARCH(1,1) and GJR-GARCH(1,1) implied volatility of BTC are plotted in Figure 4.1.

Figure 4.1: BTC volatility surfaces

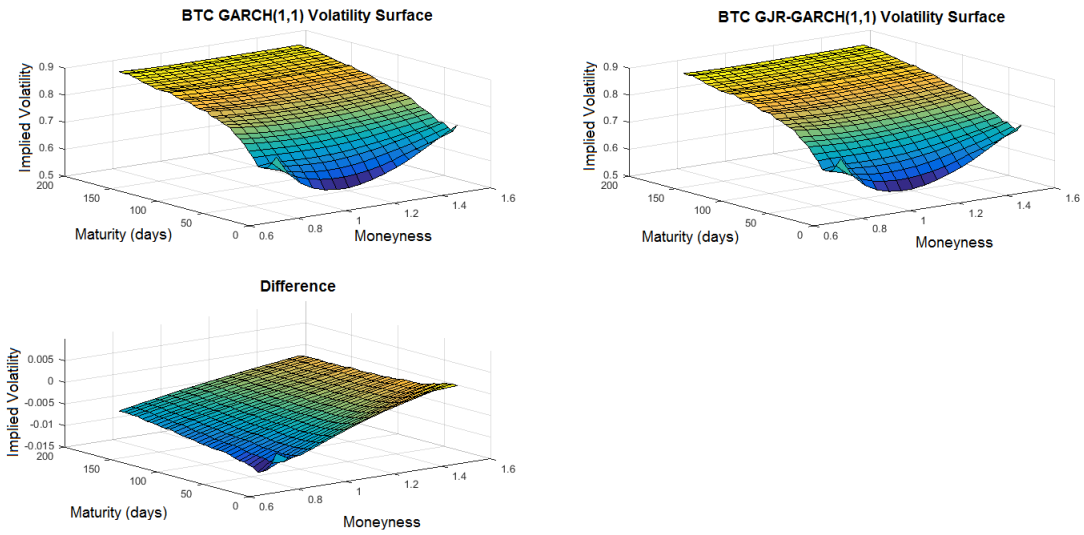


It is clear from Figure 4.1 above that the GARCH(1,1) and GJR-GARCH(1,1) option pricing models produce a volatility surface that is consistent with what is generally observed in the market. The difference between the two volatility surfaces (GJR-GARCH(1,1) volatility−GARCH(1,1) volatility) remains small across different levels of moneyness and maturity. This suggests that asymmetric effects are not important when modelling BTC volatility. This is in line with findings by Dyhrberg (2016) and Conrad et al. (2018).

Figure 4.2 illustrates the GARCH(1,1) and GJR-GARCH(1,1) implied volatility surfaces, and the difference between the two surfaces.

Figure 4.2: BTC volatility surfaces

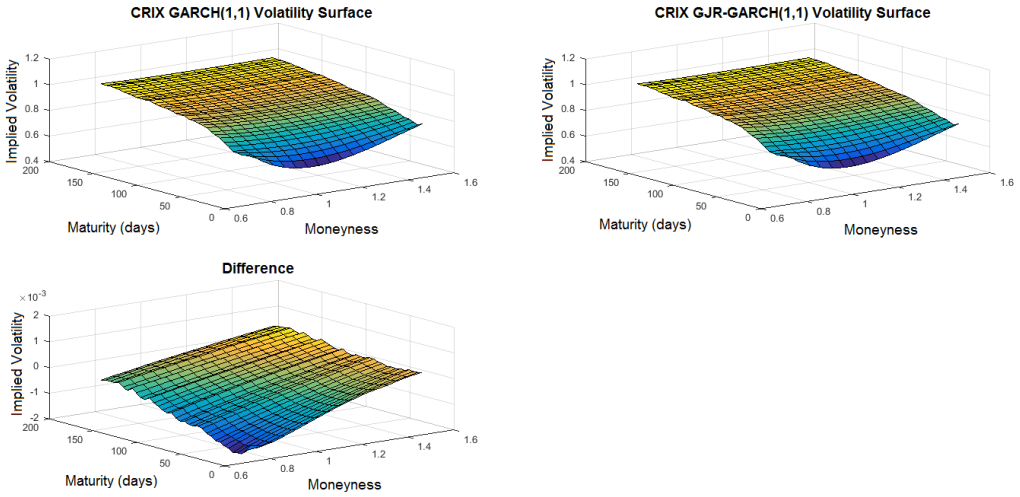


Very small differences are observed when the two surfaces are compared. This implies that CRIX volatility reacts similarly to positive and negative shocks. This is in line with the BTC volatility surface; as mentioned previously, this is consistent with expectations.

The pricing performance of the GARCH option pricing model applied to cryptocurrencies is tested by comparing the model prices to market prices of three-month BTC vanilla call options. The market option prices (value date 29 June 2018) were obtained from Madan et al. (2019). As shown above, asymmetry is not significant when pricing cryptocurrency options, therefore the pricing performance of the GARCH(1,1) model is considered. For this analysis, the GARCH(1,1) model is calibrated to log-returns from the 1st of January 2016 to the 27th June 2018. The market and model prices are plotted in Figure 4.3.

Figure 4.3: BTC option prices

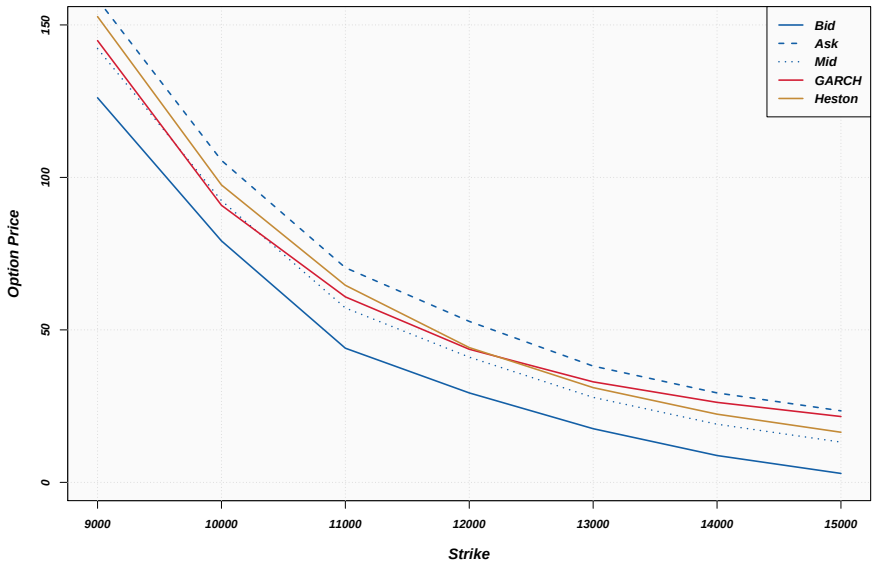


As shown in Figure 4.3 above, the GARCH(1,1) option pricing model provides realistic price discovery within the bid-ask prices suggested by the market, and when compared with the prices obtained from the Heston model. It is also important to note that the Heston model is calibrated to market option prices, while the GARCH model parameters are calibrated to historical returns data.

## 4.6 Summary

In this chapter, two different GARCH processes were applied to BTC and CRIX. The first model is symmetric and assumes that positive and negative shocks lead to the same effect on volatility. The second model takes asymmetric effects into account. By comparing the volatility surfaces implied by the two models, it gives an indication of the importance of asymmetric effects when pricing options on BTC or CRIX. Furthermore, the pricing performance of the GARCH option pricing model applied to BTC was also considered.

The results indicate that asymmetric effects are not significant when pricing options on BTC and CRIX, the differences obtained from the two surfaces are insignificant in each case. In addition, the prices obtained from the GARCH option pricing model are consistent with market BTC option prices (within the bid-ask spread). Hence, the models can also be used to inform trading decisions, to determine whether option prices are consistent with what is implied by the historical data. However, it is unclear whether historical data and GARCH option pricing models can be used to construct a BTC volatility index, which is the focus of Chapter 5.

# Chapter 5

# GARCH Generated Volatility Indices of Bitcoin and CRIX

## 5.1 Introduction

Previous chapters have shown that GARCH models can be used for price discovery in the absence of an established derivatives market. The focus of this chapter[1] is a volatility index in the absence of an established derivatives market.

As mentioned previously, cryptocurrencies have recently gained a lot of attention from finance researchers and practitioners. Currently, there is not a cryptocurrency volatility index. Furthermore, cryptocurrencies do not have a well-established derivatives market. In a recent paper, Alexander and Imeraj (2019) addressed this problem by comparing two methods to construct a BTC volatility index. The first is based on the standard geometric formula for the sum of squared log price increments; this is consistent with the CBOE VIX methodology. The second (arithmetic) approach represents a fair value for the average sum of squared log price increments.

According to Bouri et al. (2017), short horizon investment in BTC can serve as a hedge against global equity market uncertainty (form of electronic gold). Hence, the need for a BTC volatility index with different time horizons. In this chapter, the GARCH(1,1) option pricing model applied in Chapter 4 is used to estimate the volatility indices of BTC and CRIX. The CRIX implied volatility index will give a more holistic view of cryptocurrency volatility (30, 60, and 90-day). The estimation of a volatility index for CRIX in the absence of a derivatives market was considered by Kolesnikova (2018), this was based on an exponentially weighted moving average approach.

The theoretical framework applied in order to estimate a GARCH volatility index is considered in Sections 2.2.2 and 2.2.3. The rest of this chapter is structured as follows, Section 5.2 reviews the recent and relevant literature. This is followed by the empirical results. Finally, the main findings are summarised.

[1]This chapter is based on a paper (Venter and Maré , 2020a) published in the *Journal of Risk and Financial Management* .

## 5.2 Literature review

Studies based on cryptocurrency volatility indices are limited, this is because there is not a well-established cryptocurrency derivatives market. Volatility indices are used based on implied volatility obtained from the option market (*e.g.,* the CBOE VIX). Alexander and Imeraj (2019) constructed a BTC volatility index by making use of the VIX methodology (geometric variance swap), BTC option data was obtained from the Deribit exchange. In addition, Alexander (2008) note that BTC prices tend to jump, therefore the fair value of geometric variance swaps are underestimated using this method. Hence, the method based on arithmetic variance swaps was also employed. Alexander (2008) recommend the use of the arithmetic index for horizons of one month or more. However, the volatility index based on arithmetic or geometric (VIX methodology) variance swaps is dependent on an established derivatives market, this is not the case for all cryptocurrencies and therefore a different approach is required.

In a recent study, Kim et al. (2019) construct a cryptocurrency volatility index based on the CRIX. The purpose of the index is to offer a forecast for the mean annualised volatility of the next month. Due to the shortcomings of the cryptocurrency derivatives market, Kim et al. (2019) make use of a proxy for implied volatility, therefore rolling volatility is used, this is based on historical volatility of the underlying. To get forward looking estimates (for the next 30 days) of rolling volatility, Kim et al. (2019) made use of GARCH family models, the Heterogeneous Auto-Regressive model, and a neural network-based Long short-term memory cell. The performance of the different models was compared based on the mean squared error and the mean absolute error. Their empirical results show that the Heterogeneous Auto-Regressive model is the best performing model when forecasting rolling volatility of the CRIX. However, rolling volatility is based on historical volatility and is therefore not risk-neutral. Hence, the GARCH option pricing model is used in this study in order to estimate the implied volatility index (risk-neutral) in the absence of a well-established derivatives market.

The important studies required for the theory applied in this chapter are summarised in the table below:

| **Study** | **Topic** |
|---|---|
| Hansen and Lunde (2005) | GARCH(1,1) model |
| Duan (1995) | GARCH option pricing |
| Meddahi and Renault (2004) | SR-SARV processes |
| Hao and Zhang (2013) | GARCH-implied volatility index |
| Trimborn and Härdle (2018) | The CRIX |
| Chu et al. (2017) | GARCH Modelling of cryptocurrencies |
| Hafner (2020) | GARCH Modelling of cryptocurrencies and CRIX |

The empirical results are considered in the next section.

## 5.3 Empirical results

The GARCH(1,1) calibrated parameters are reported in Table 5.1.

Table 5.1: GARCH(1,1) calibrated parameters

| | BTC | CRIX |
|---|---|---|
| $\alpha_0$ | 0.0001 | 0.0001 |
| $\alpha_1$ | 0.1035 | 0.1504 |
| $\beta_1$ | 0.8650 | 0.8203 |
| $\lambda$ | 0.0744 | 0.0880 |
| AIC | -6.9982 | -6.9909 |

By making use of a similar approach to Alexander and Imeraj (2019), the 30-day, 60-day, and 90-day volatility indices are shown. The BTC and CRIX GARCH volatility indices shown are in Figures 5.1 and 5.2 below:

Figure 5.1: BTC GARCH(1,1) volatility indices

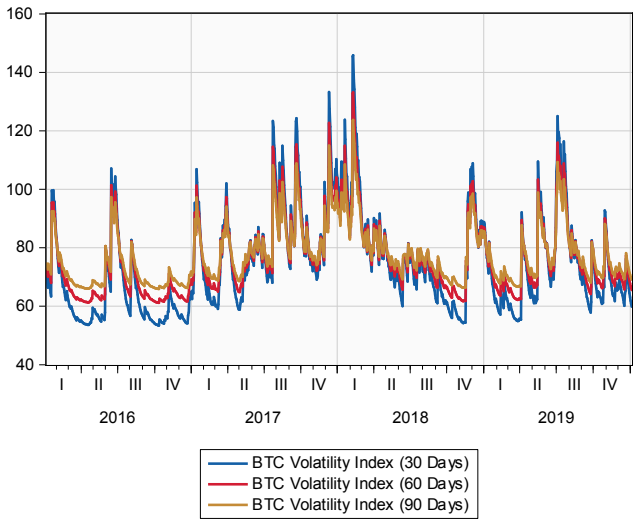

Figure 5.2: CRIX GARCH(1,1) volatility indices

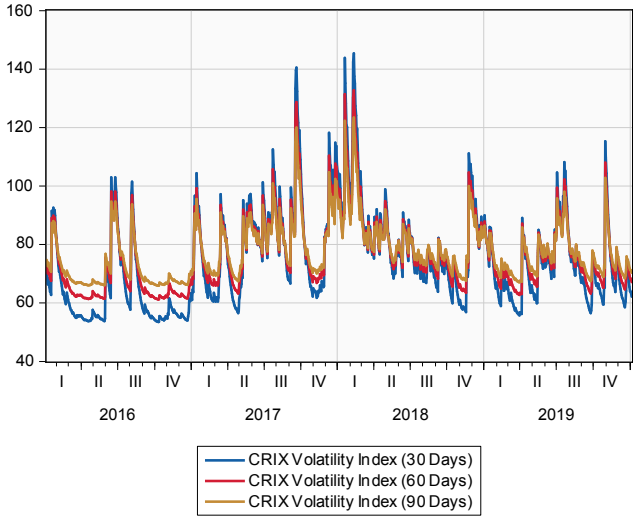


It is evident from the above that GARCH volatility indices tend to increase after positive and negative shocks. This is consistent with findings by Dyhrberg (2016) and Conrad et al. (2018). To illustrate how the term structure varies over time, the differences in volatility indices (left axis) and underlying assets (right axis) are plotted in Figures 5.3 and 5.4 below:

Figure 5.3: BTC GARCH(1,1) term structure

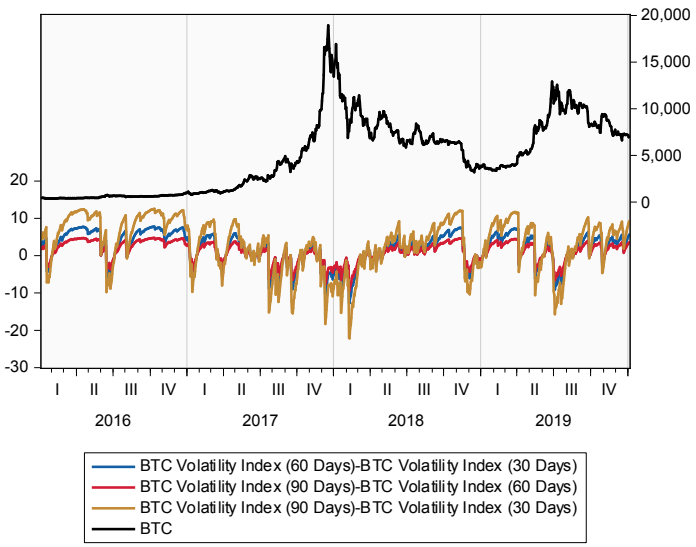

Figure 5.4: CRIX GARCH(1,1) term structure

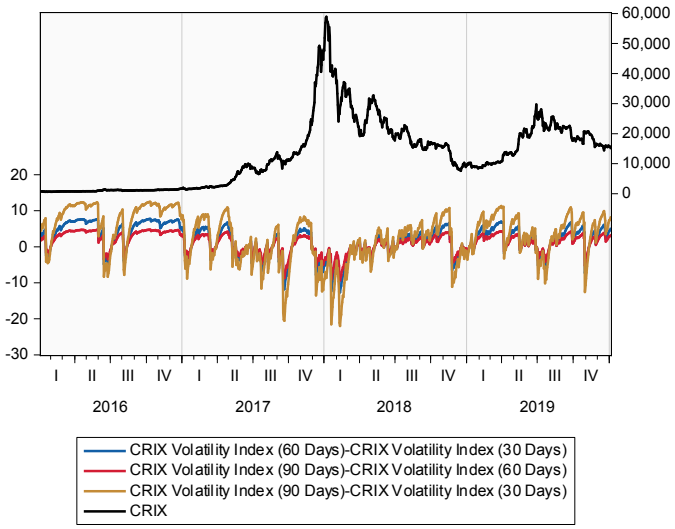


When the term structure of volatility is considered, the 30-day volatility index for both BTC and CRIX seem to be the lowest in most cases. This is consistent with expectations, because there is more uncertainty over a longer period of time. However, when large jumps occur in the underlying asset, the short term volatility index tends to increase to higher levels when compared to the 60-day and 90-day volatility indices (this is due to the fact that the volatility index is calculated as the expected arithmetic average of the variance in the $n$ subperiods of the following 30, 60, or 90 calendar days). The 30-day GARCH volatility indices of BTC and CRIX are compared in Figure 5.5 below:

Figure 5.5: 30-Day GARCH(1,1) volatility indices

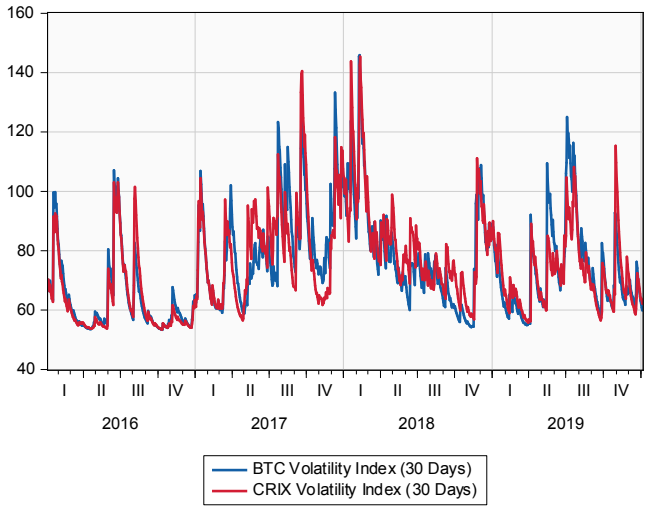

Figure 5.5 indicates that the 30-day GARCH volatility index for BTC is similar when compared to the 30-day CRIX GARCH volatility index.

## 5.4 Summary

In this chapter, the GARCH option pricing model is applied to BTC and CRIX to estimate a GARCH volatility index. Volatility indices are usually estimated using a model-free approach. This approach has previously been applied to BTC (Alexander and Imeraj, 2019). In this study, we rely on the symmetric GARCH volatility index. This is appropriate because previous findings (including the empirical results in Chapter 4) indicate that BTC volatility reacts similarly to positive and negative shocks.

Similar GARCH volatility indices are obtained when BTC and CRIX are compared. This is consistent with expectations due to BTC being highly weighted when calculating CRIX (Trimborn and Härdle, 2018). The term structure of volatilities are consistent with expectations, with 30-day volatility being lower when compared to longer maturities. In addition, short term volatility tends to increase to higher levels when compared to 60-day and 90-day volatility when large jumps occur in the underlying asset.

As per previous studies (Antonopoulos, 2014, Leong et al., 2020 Leong and Sung, 2018, Böhme et al., 2015), BTC, as a digital currency, has huge potential in applications and advantages, such as lower fees, fraud protection, simpler international payments, etc. The findings of this chapter, hopefully, would contribute to the development of future BTC research. This chapter concludes the work on crypto volatility indices. The next chapter considers the pricing of BTC futures options (univariate and multivariate) in a GARCH setting.

# Chapter 6

# Univariate and Multivariate GARCH Models Applied to Bitcoin Futures Option Pricing

## 6.1 Introduction

The focus of previous chapters has been the use of univariate GARCH models applied to vanilla option pricing and volatility indices. The focus of this chapter[1] is BTC futures option pricing. We consider both the univariate and multivariate (futures spread options) case. Abraham (2020) explains that a valuation model for BTC futures options will provide insight into a central-bank free currency.

As shown in previous chapters, modelling the historical returns of an asset as a univariate GARCH process is often used as a basis for price discovery in illiquid derivative markets. The model by Heston and Nandi (2000) is often used because it has a convenient closed-form solution. However, this is usually applied to spot price dynamics. This model was extended to futures options on commodities by Li (2019a). The Chicago Mercantile Exchange (CME) was the first established exchange to launch BTC futures options in the first quarter of 2020 (Bharadwaj, 2021). Therefore, BTC futures options are actively traded, and model prices can be compared to market prices to give an indication of pricing performance.

An important factor to consider is the ability to model joint dynamics for the pricing of multivariate derivatives, when pricing derivatives on a new asset class. According to Alexander and Heck (2020), crypto-asset futures are exposed to significant basis risk. Therefore, spread options on BTC futures are ideal for hedging basis risk. Spread options on BTC futures do not actively trade. In this study, we consider a modelling approach for price discovery in the BTC futures spread option market. The approach is based on work by Rombouts and Stentoft (2011), who derived the risk-neutral dynamics of the spot price

[1]This chapter is based on a paper (Venter and Maré, 2021b) that appeared in the *Journal of Risk and Financial Management*.

processes for a general class of multivariate heteroskedasticity models. In this study, the model by Rombouts and Stentoft (2011) is extended to multivariate futures options.

The rest of this chapter is structured as follows: Section 6.2 reviews the recent and relevant literature, Section 6.3 focuses on the theoretical framework (both univariate and mulitvariate options on BTC futures), Section 6.4 presents the empirical results, and finally, Section 6.5 summarises the main findings.

## 6.2 Literature review

Research focusing on GARCH models applied to BTC (and other crypto-assets) and BTC derivative pricing is well-documented in the literature. In a recent study, Fassas et al. (2020) made use of a vector error correction model to investigate the price discovery process in the BTC market. Their empirical results indicate that volume traded in the futures market is more important than the volume traded in the decentralised spot market when incorporating new information about the value BTC. In addition, Fassas et al. (2020) consider the volatility transmission between the BTC spot and futures market, by using multivariate GARCH models (BEKK and dynamic-conditional-correlation). There is evidence of cross market effects when the variability of BTC spot and futures returns are considered.

It is important to consider a reasonable forecast of BTC returns when trading BTC derivatives. In a study focusing on the use of information on the US-China trade war to forecast BTC returns, Plakandaras et al. (2021) made use of ordinary least squares regression, least absolute shrinkage and selection operator techniques, and support vector regression. The authors also controlled for explanatory variables that include: financial indices (including the volatility index), exchange rates, commodity prices, political uncertainty indices, and BTC characteristics. Their empirical results indicate that BTC returns are not affected by trade related uncertainties.

In a recent paper, Shahzad et al. (2019) made use of the bivariate cross-quantilogram to determine whether BTC exhibits safe haven properties (during extreme market conditions) for equity investments. The authors extend the work by Baur and Lucey (2010) to incorporate weak and strong safe haven assets. Furthermore, the safe haven properties of BTC were also compared to that of Gold and the general commodity index. Shahzad et al. (2019) conclude that BTC, gold, and the general commodity index can be considered (at best) a weak safe haven asset in some cases.

Fang et al. (2019) made use of the GARCH-MIDAS model to investigate how the long-run volatility of BTC, global equities, bonds, and commodities evolves with global economic policy uncertainty. Their empirical results indicate that global economic policy uncertainty is significant for all variables, except bonds. Furthermore, Fang et al. (2019) also considered the impact of global economic policy uncertainty on the correlation between BTC and global equities, commodities, and bonds. Based on the empirical results, the authors argue that BTC can act as a hedge under specific economic uncertainty conditions.

In a study highlighting the role of BTC futures, Chen and So (2020) focused on the relationship between BTC spot and futures prices, with the focus on hedging. Chen and

So (2020) tested the hedge performance of the naive method, ordinary least squares, and a dynamic hedge based on a bivariate BEKK-GJR-GARCH model. The results show that the hedge based on the bivariate GARCH model is the most reliable. Furthermore, Chen and So (2020) also show that the structure of BTC volatility is significantly different after the introduction of BTC futures.

In a recent study, Venter et al. (2020) applied symmetric and asymmetric GARCH option pricing models to BTC and CRIX (Chapter 4 of this thesis). The BTC option prices obtained from the model were compared to market option prices, which shows that the GARCH option pricing model produces reasonable price discovery. Furthermore, the implied volatility surfaces generated using symmetric and asymmetric GARCH models were compared. This comparison indicates that there is not a significant difference, implying that the symmetric model is a better choice as it is more efficient.

Jalan et al. (2020) focused on the pricing and risk of BTC options. Jalan et al. (2020) compared the option prices obtained from classical option pricing models, *i.e.,* the Black-Scholes-Merton model and the Heston-Nandi model. Furthermore, Jalan et al. (2020) also compared the risk (the Greeks) of BTC options to those of traditional commodity options. Jalan et al. (2020) conclude that the classical models produce prices that are slightly different when compared to the market. Their empirical results also indicate that BTC deltas are more stable over time when compared to traditional commodities. This implies that investors in BTC options are protected from undue BTC price changes.

In another recent study, Siu and Elliot (2021) made use of the self-exciting threshold autoregressive model (to incorporate regime switching) in conjunction with GARCH (Heston-Nandi) to model BTC return dynamics, for the pricing of BTC options. According to Siu and Elliot (2021), conditional heteroskedasticity has a significant impact on BTC option prices. However, the impact of self-exciting threshold autoregressive terms seems to be marginal.

Limited research has focused on the GARCH option pricing model applied to futures options. Li (2019a) extended the Heston-Nandi model to futures options. The overall purpose was the pricing of crude oil futures options. Li (2019a) concludes that option-implied filtering is superior when compared to futures based filtering when pricing crude oil futures options. Li (2019b) also applied the model to natural gas futures. However, this approach has not been applied to cryptocurrencies.

The application of GARCH models to multivariate option pricing is also well-documented in the literature. Duan and Pliska (2004) developed an option valuation theory for cointegrated assets, the model was used for the pricing of spread options with equity underlying assets. In a recent study, Mahringer and Prokopczuk (2015) applied the model by Duan and Pliska (2004) to the pricing of crack spread options (futures returns were modelled). Mahringer and Prokopczuk (2015) compared this to univariate modelling of the crack spread. Their empirical results show that the univariate approach is superior for the pricing of crack spread options.

Rombouts and Stentoft (2011) derived the risk-neutral dynamics (of the spot price processes) for a general class of multivariate heteroskedasticity models. In addition, a feasible way to price multivariate options is also provided. Rombouts and Stentoft (2011)

applied the models to options on equity indices. Their empirical results indicate that correlation risk and non-Gaussian features are important factors to consider when pricing multivariate options. In this chapter, the framework by Rombouts and Stentoft (2011) is extended to futures options, and applied to BTC futures spread options. The theoretical framework is considered in the next section.

## 6.3 Theoretical framework

In this study, we test the pricing performance of the Heston-Nandi futures option pricing model when applied to BTC. Furthermore, we extend the work by Rombouts and Stentoft (2011) to multivariate futures options to price spread options on BTC futures. The section is divided into three subsections. The first part focuses on the Heston-Nandi futures option pricing model, the second considers the multivariate GARCH option pricing framwork. Finally, the focus of the third subsection is the constant conditional correlation (CCC) and dynamic conditional correlation (DCC) GARCH (multivariate) models.

### 6.3.1 Heston-Nandi futures option pricing model

The model by Heston and Nandi (2000) is widely used in the literature for the pricing of vanilla options. This model was extended to futures options by Li (2019a), who applied the model to crude oil futures. The futures dynamics under the real-world measure $P$ are given by (Li, 2019b):

$$\ln\left(\frac{F_{t,T}}{F_{t-1,T}}\right) = \left(\lambda - \frac{1}{2}\right) h_t + \sqrt{h_t} z_t,$$

where $F_{t,T}$ is the futures price at time $t$ with expiry $T$, and $z_t$ is a standard normal random variable under $P$. The conditional variance takes the following form:

$$h_t = \alpha_0 + \alpha_1 (z_{t-1} - \delta_1 \sqrt{h_t})^2 + \beta_1 h_{t-1}. \tag{6.1}$$

In this chapter, the parameters $\lambda$, $\alpha_0$, $\alpha_1$, $\delta_1$, and $\beta_1$ are calibrated to historical BTC futures returns (under the real-world measure) using maximum likelihood estimation. When estimating the symmetric Heston-Nandi model, the asymmetry parameter $\delta_1$ takes a value of zero.

For the pricing of futures options, the risk-neutral dynamics are required. According to Li (2019a), the risk-neutral futures price process in the Heston-Nandi model is given by,

$$\ln\left(\frac{F_{t,T}}{F_{t-1,T}}\right) = -\frac{1}{2} h_t + \sqrt{h_t} z_t^*, \tag{6.2}$$

where $z_t^* = z_t + \lambda\sqrt{h_t}$ . The risk-neutral conditional variance takes the following form,

$$h_t = \alpha_0 + \alpha_1 (z_{t-1}^* - \delta_1^* \sqrt{h_t})^2,$$

where $\delta_1^* = \delta_1 + \lambda$. Given the risk-neutral dynamics, a closed-form formula for a European call option on a futures contract can be obtained, see Li (2019a) for more detail. The parameters are estimated using maximum likelihood estimation; the log-likelihood function is given by (Wang et al., 2017):

$$\ln L_{HN} = -\frac{N}{2}\ln(2\pi) - \frac{1}{2}\sum_{t=1}^{N}\left(\ln h_t + \left[\frac{F_{t,T}}{F_{t-1,T}} - \lambda h_t\right]^2 / h_t\right),$$

where again, $N$ is the estimation sample size. The multivariate GARCH futures option pricing model is outlined in the next section.

### 6.3.2 Multivariate GARCH futures option pricing model

We assume the following futures return dynamics $\ln\left(\frac{F_{j,t,T_j}}{F_{j,t-1,T_j}}\right) = R_{j,t,T_j}$ under the real-world measure $P$:

$$R_{j,t,T_j} = \mu_{j,T_j} - f(-c_j) + E_{j,t,T_j} \text{ for } j = 1, ..., n, \tag{6.3}$$

where $F_{j,t,T_j}$ is the futures price of asset $j$ with expiry $T_j$ at time $t$; $\mu_{j,T_j}$ is the conditional mean of asset $j$; $f(\cdot)$ denotes the cumulant generating function; $c_j$ is a vector of zeros except for position $j$, which takes a value of one. Furthermore, we assume a multivariate heteroskedastic process, therefore,

$$E_t = H_t Z_t,$$

where $Z_t$ is identically and independently distributed with mean zero and covariance matrix equal to the identity matrix under the real-world measure $P$. In addition, $H_t$ is an $n \times n$ matrix of full rank, more specifically,

$$\Sigma_t = H_t H_t',$$

where $\Sigma_t$ is the conditional covariance matrix, driven by a multivariate GARCH process.

In order to obtain the risk-neutral dynamics ($Q$ measure) required for pricing, we use the following Radon-Nikodym derivative,

$$\frac{dQ}{dP}\bigg|\mathcal{F}_t = \exp\left\{-\sum_{i=1}^{t}\left(\nu_i' E_i + f(\nu_i)\right)\right\}, \tag{6.4}$$

where $\nu_i$ is an $N$ dimensional vector sequence. Rombouts and Stentoft (2011) prove that Equation 6.4 is in fact a Radon-Nikodym derivative. Furthermore, it can also be shown (using the tower property) that,

$$\begin{aligned}\mathbb{E}_t^P\left[\frac{dQ}{dP}\right] &= \mathbb{E}^P\left[\exp\left\{(\nu_1' E_1 + f(\nu_1))\right\}\right] \\ &= \exp\left\{-f(\nu_1)\right\}\exp\left\{f(\nu_1)\right\} \\ &= 1,\end{aligned}$$

as required.

**Proposition 1: Risk-neutral measure**

The risk-neutral measure $Q$ defined by the Radon-Nikodym derivative in Equation 6.4 is an equivalent martingale if and, only if,

$$f(\nu_t - c_j) - f(\nu_t) - f(-c_j) + \mu_{j,T_j} = 0, \tag{6.5}$$

for $j = 1, ..., n$.

*Proof.* Clark (2014) explains that under the $T_j$-forward measure, the futures price process is driftless. However, when assuming constant interest rates, the risk-neutral ($Q$) and $T_j$-forward measures are equivalent. Therefore,

$$\mathbb{E}_t^Q \left[ \frac{F_{j,t,T_j}}{F_{j,t-1,T_j}} \right] = 1.$$

Hence, by making use of the Radon-Nikodym derivative,

$$\begin{aligned}
\mathbb{E}_t^Q \left[ \frac{F_{j,t,T_j}}{F_{j,t-1,T_j}} \right] &= \mathbb{E}_t^P \left[ \left( \frac{\frac{dQ}{dP}|\mathcal{F}_{t-1}}{\frac{dQ}{dP}|\mathcal{F}_{t-1}} \right) \frac{F_{j,t,T_j}}{F_{j,t-1,T_j}} \right] \\
&= \mathbb{E}_t^P \left[ \exp\left\{ \nu_t' E_t - f(\nu_t) \right\} \exp\left\{ \mu_{j,T_j} - f(-c_j) + E_{j,t,T_j} \right\} \right] \\
&= \exp\left\{ -f(\nu_t) + \mu_{j,T_j} - f(-c_j) \right\} \mathbb{E}_t^P \left[ \exp\left\{ (c_j - \nu_t)' E_{j,t,T_j} \right\} \right] \\
&= \exp\left\{ -f(\nu_t) + \mu_{j,T_j} - f(-c_j) + f(\nu_t - c_j) \right\}.
\end{aligned}$$

Using the driftless property of the futures price under the risk-neutral measure, it follows that

$$f(\nu_t - c_j) - f(\nu_t) - f(-c_j) + \mu_{j,T_j} = 0,$$

which completes the proof. □

To derive the risk-neutral dynamics, the following lemma from Rombouts and Stentoft (2011) is required:

**Lemma 5: Conditional moment generating function**

Under the risk-neutral measure, the conditional moment generating function takes the following form,

$$\mathbb{E}^Q \left[ \exp\left\{ -u' E_t \right\} \right] = \exp\left\{ f(\nu_t + u) - f(\nu_t) \right\}.$$

*Proof.* See Rombouts and Stentoft (2011). □

Using the lemma above, the following expression for the risk-neutral cumulant generating function is obtained

$$f^*(u) = f(\nu_t + u) - f(\nu_t). \tag{6.6}$$

Hence, for any choice of $\nu_t$, the risk-neutral dynamics can be obtained by substituting Equation 6.6 and 6.5 into the mean Equation 6.3. The risk-neutral futures log-returns are given by:

$$R^*_{j,t,T_j} = f^*(-c_j) + E^*_{j,t,T_j},$$

$*$ denotes that the variables are considered under the risk-neutral measure.

In this chapter, we assume a multivariate Gaussian distribution. Rombouts and Stentoft (2011) show that the conditional cumulant generating function is given by:

$$f(u) = \frac{1}{2}u'\Sigma_t u, \tag{6.7}$$

where $u$ is an arbitrary vector, if the multivariate Gaussian distribution is assumed. By substituting Equation 6.7 into Equation 6.5, it is easily shown that $\nu_t$ takes the following form:

$$\nu_t = \Sigma_t^{-1}\mu_t.$$

In addition, the risk-neutral cumulant generating function is given by:

$$\begin{aligned} f^*(u) &= f(\nu_t u) - f(\nu_t) \\ &= \frac{1}{2}(\nu_t + u)'\Sigma_t(\nu_t + u) - \frac{1}{2}\nu_t'\Sigma_t\nu_t \\ &= u'\Sigma_t\nu_t + \frac{1}{2}u'\Sigma_t u. \end{aligned}$$

We assume the following mean model,

$$\mu_t = diag\Sigma_t\lambda,$$

where $diag\Sigma_t$ is a diagonal matrix of conditional variances, and $\lambda$ is the unit risk premium. This suggests that

$$f^*(u) = u'diag\Sigma_t\lambda + \frac{1}{2}u'\Sigma_t u.$$

This implies that the risk-neutral dynamics are given by:

$$\begin{aligned} R^*_{j,t,T_j} &= f^*(-c_j) + \epsilon^*_{j,T_j} \\ &= (-c_j)'diag\Sigma_t\lambda + \frac{1}{2}c_j'\Sigma_t c_j + \epsilon^*_{j,T_j}. \end{aligned}$$

The multivariate GARCH models are outlined in the next subsection.

### 6.3.3 Multivariate GARCH models

According to Francq and Zakoian (2019), the CCC-GARCH model is formulated as follows:

$$\Sigma_t = D_t \Lambda D_t,$$

where $\Lambda$ is the constant correlation matrix of $\epsilon_{j,T_j}$ (estimated using historical data). The diagonal matrix $D_t$ takes the following form

$$D_t = \begin{pmatrix} \sqrt{h_{1,t}} & 0 & \cdots & 0 \\ 0 & \ddots & & \\ \vdots & & \ddots & \\ 0 & & & \sqrt{h_{N,t}} \end{pmatrix}.$$

The conditional variance of each asset is assumed to be consistent with Equation 6.1.

An obvious shortcoming of the CCC-GARCH model is the assumption of constant correlation. To address this problem, Engle (2002) extended the model to incorporate dynamic conditional correlation (DCC). The DCC-GARCH model is formulated as follows:

$$\Sigma_t = D_t \Lambda_t D_t,$$

where

$$\Lambda_t = diag(\Psi_t)^{-\frac{1}{2}} \Psi_t diag(\Psi_t)^{-\frac{1}{2}}.$$

$\Psi_t$ is modelled using an autoregressive process:

$$\Psi_t = (1 - \theta_1 - \theta_2)\bar{\Psi} + \theta_1 v_{t-1} v'_{t-1} + \theta_2 \Psi_{t-1},$$

where $v_t = \epsilon_{j,T_j} / \sqrt{h_{j,t}}$, $\bar{\Psi}$ is the unconditional covariance matrix of $\epsilon_{j,T_j}$, and to ensure stationarity and positive definiteness, $\theta_1 + \theta_2 < 1$ and $\theta_1,\ \theta_2 > 0$. The log-likelihood function (up to a constant) of both the CCC-GARCH and DCC-GARCH models is given by:

$$\ln L_M = -\frac{1}{2} \sum_{t=1}^{N} \ln |\Sigma_t| - \frac{1}{2} \sum_{t=1}^{N} \epsilon'_t \Sigma_t^{-1} \epsilon_t.$$

In this study, we consider futures prices on BTC with different expiry dates. Therefore, highly correlated asset price processes are expected (same underlying). Given the volatility process, risk-neutral sample paths of BTC futures prices can be simulated. The price of a BTC futures spread option at time $t$, that expires at time $T$, is given by,

$$V_t = DF(t,T) \times \mathbb{E}^Q \left[ \max\{F_{1,T,T_1} - F_{2,T,T_2} - s_K\}, 0 \right],$$

where $T_1, T_2 \geq T$, $T_1 \neq T_2$, and $s_K$ is the spread. It is clear from the above that when $s_K = 0$, it is an exchange option. The empirical results are considered in the next section.

## 6.4 Empirical results

In this section, the empirical results are presented and discussed. In this study, daily data[2] from 30-Oct-2020 to 1-Apr-2021 were used. The expiry dates of the BTC futures prices are as follows: 30-Apr-2021, 28-May-2021, and 25-Jun-21. The BTC futures prices and returns are plotted in Figures 6.1 and 6.2 below.

Figure 6.1: BTC futures


Figure 6.2: BTC futures returns

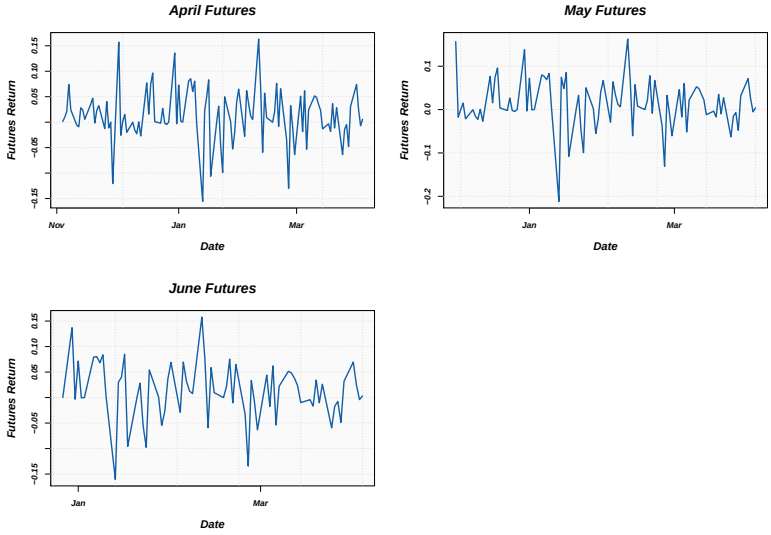


It is clear from the above that BTC futures prices are trended. Furthermore, the returns

[2]The dataset was obtained from the Thomson Reuters Datastream databank.

show signs of volatility clustering, which is consistent with the typical stylised facts of financial returns (McNeil et al., 2015).

The descriptive statistics of the BTC futures returns are reported in Table 6.1 below.

Table 6.1: Descriptive statistics: BTC futures returns

| | April | May | June |
|---|---|---|---|
| Mean | 0.0132 | 0.0139 | 0.0126 |
| Median | 0.0057 | 0.0038 | 0.0112 |
| Maximum | 0.1631 | 0.1626 | 0.1578 |
| Minimum | -0.1557 | -0.2118 | -0.1605 |
| Std. Dev. | 0.0517 | 0.0572 | 0.0563 |
| Skewness | -0.2318 | -0.5091 | -0.4326 |
| Kurtosis | 4.6279 | 5.3923 | 3.9755 |
| Jarque-Bera | 13.0122 | 25.0679 | 4.9587 |
| Probability | 0.0015 | 0.0000 | 0.0838 |
| Observations | 109 | 89 | 70 |

The descriptive statistics indicate that the conditional expectation of the returns is close to zero, the returns are not normally distributed, and the returns also show signs of leptokurtosis. This is consistent with the stylised facts of financial returns (McNeil et al., 2015).

The estimated parameters (maximum likelihood) and information criteria of the symmetric and asymmetric Heston-Nandi model applied to BTC futures returns are reported in Tables 6.2 and 6.3 below.

Table 6.2: Symmetric Heston-Nandi parameters

| | April | May | June |
|---|---|---|---|
| $\lambda$ | 5.2100 | 4.2970 | 4.0490 |
| $\alpha_0$ | 0.0024 | 0.0030 | 0.0028 |
| $\alpha_1$ | 2.0E-04 | 3.5E-10 | 3.2E-11 |
| $\beta_1$ | 2.3E-07 | 0.0685 | 0.0930 |
| AIC | -4.1841 | -3.7271 | -3.2558 |

Table 6.3: Asymmetric Heston-Nandi parameters

| | April | May | June |
|---|---|---|---|
| $\lambda$ | 5.0020 | 4.2970 | 4.0490 |
| $\alpha_0$ | 0.0023 | 0.0030 | 0.0028 |
| $\alpha_1$ | 2.3E-04 | 3.5E-10 | 3.5E-11 |
| $\beta_1$ | 3.4E-08 | 0.0671 | 0.0927 |
| $\delta_1$ | 16.1600 | 0.3934 | 0.0986 |
| AIC | -2.1870 | -1.7271 | -1.2558 |

The AIC indicates that the symmetric time-varying volatility model is a better fitting model. This is consistent with previous findings in the literature (see, *e.g.,* Venter and Maré , 2020a, Conrad et al., 2018, Dyhrberg, 2016). In addition to the AIC, a likelihood ratio test is also used to compare the estimated symmetric and asymmetric models. The test statistic of the likelihood ratio test for each expiry is reported in Table 6.4 below:

Table 6.4: Likelihood ratio test (Heston-Nandi)

| Expiry | Test Statistic |
|---|---|
| April | 1.2856 |
| May | 2.8E-08 |
| June | -2.1E-08 |

We do not reject the null hypothesis for each expiry (Held and Sabanés Bové, 2014), this is also in favor of the symmetric Heston-Nandi model.

The futures option prices of the two models and market prices[3] (scaled by the relevant futures price) are plotted in Figure 6.3 below. Furthermore, the pricing performance metrics of the two models applied to different futures are outlined in Tables 6.5 to 6.7.

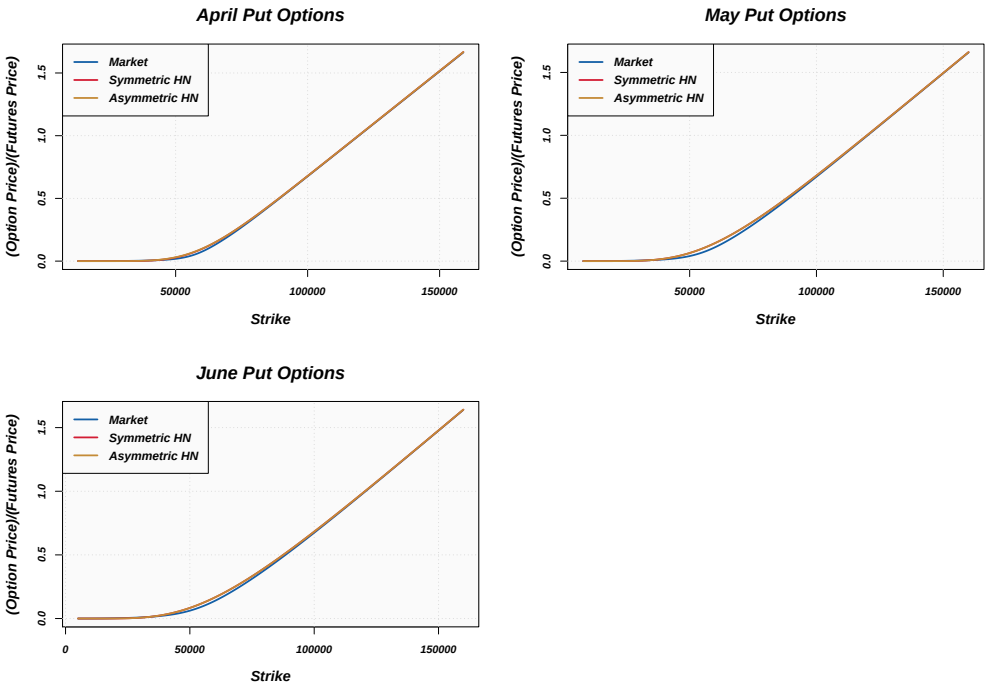


Figure 6.3: BTC futures option prices

[3]The market prices were obtained from CME Group.

Table 6.5: April performance metrics

| | Symmetric Heston-Nandi | Asymmetric Heston-Nandi |
|---|---|---|
| RMSE | 669.6865 | 724.2534 |
| MAE | 496.0976 | 533.5693 |

Table 6.6: May performance metrics

| | Symmetric Heston-Nandi | Asymmetric Heston-Nandi |
|---|---|---|
| RMSE | 1302.6712 | 1302.6727 |
| MAE | 1092.2221 | 1092.2235 |

Table 6.7: June performance metrics

| | Symmetric Heston-Nandi | Asymmetric Heston-Nandi |
|---|---|---|
| RMSE | 1149.2917 | 1149.2875 |
| MAE | 1018.2780 | 1018.2741 |

It is clear that similar European put futures option prices are obtained when the different models are compared. The models produce reasonable prices when compared to market prices. The RMSE and MAE of the symmetric Heston-Nandi model are slightly lower when compared to the asymmetric Heston-Nandi model.

The performance metrics of the two models are similar. Therefore, to determine whether the predictive accuracy of the two models are the same, the test by Diebold and Mariano (1995) is applied. The test statistic for each expiry is reported in Table 6.8 below:

Table 6.8: Diebold-Mariano test

| Expiry | Test Statistic |
|---|---|
| April | -2.5072* |
| May | -3.3034* |
| June | 4.0599 |

In the table above, * denotes significance at a 1% level. The null hypothesis of the test is that the symmetric and asymmetric Heston-Nandi model have the same accuracy, and the alternative hypothesis is that the symmetric model outperforms the asymmetric model (this is consistent with previous findings in the literature, and previous chapters). The Diebold-Mariano test indicates that the symmetric model outperforms the asymmetric model for options that expire in April and May, but the predictive accuracy of the models is the same for options that expire in June.

Based on the pricing performance of univariate options, the symmetric Heston-Nandi GARCH process is used for the pricing of short-dated spread options on BTC futures. For

the CCC-GARCH model, no additional parameters need to be estimated. The additional parameters of the DCC-GARCH model are reported in Table 6.9 below:

Table 6.9: DCC-GARCH estimated parameters

| | Estimated parameter |
|---|---|
| $\theta_1$ | 1.4E-09 |
| $\theta_2$ | 0.5657 |

The CCC-GARCH and DCC-GARCH models are compared using a likelihood ratio test. The value of the test statistic is -3.8E-07, which is insignificant. Hence, we do not reject the null hypothesis, which is in favour of the CCC-GARCH model. Therefore, the CCC-GARCH model is used for the pricing of BTC futures spread options.

As mentioned previously, BTC futures are highly correlated. To illustrate this concept, risk-neutral sample paths are illustrated in Figure 6.4 below.

Figure 6.4: BTC futures sample paths

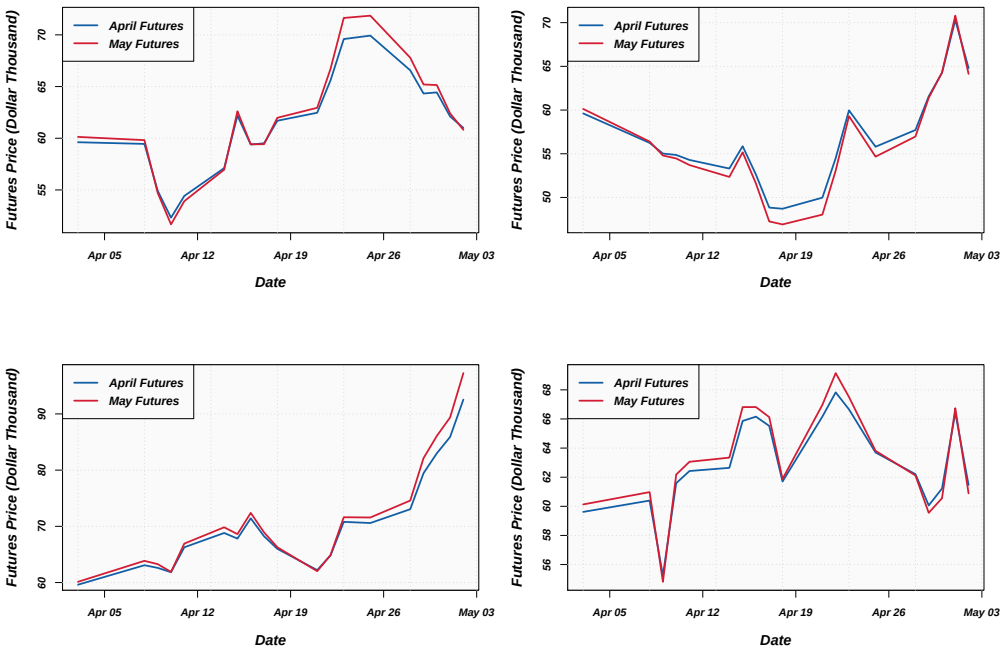


The sample paths are consistent with expectations. CCC-GARCH spread option prices (scaled by the April futures prices) are plotted in Figure 6.5 below. The spread option is based on the difference between the April and May futures prices, with an expiry date of 18-Apr-21.

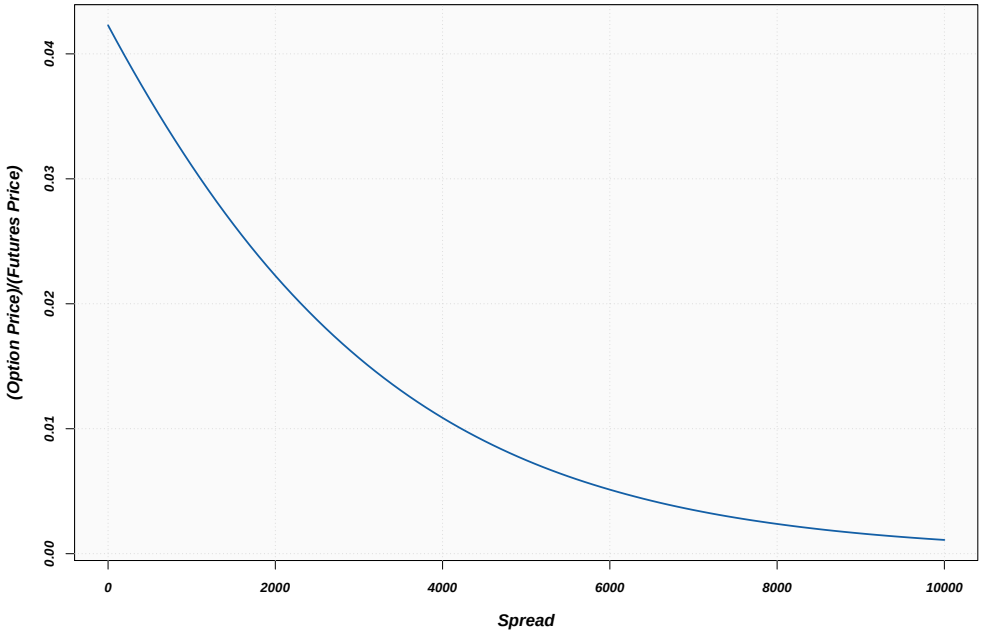


Figure 6.5: BTC futures spread option prices

Spread options on BTC futures do not actively trade and, therefore the model prices can not be compared to market prices.

## 6.5 Summary

BTC futures options were launched in the first quarter of 2020. GARCH modelling of BTC returns and BTC option pricing is well-documented in the literature. However, the pricing of BTC futures options in a GARCH framework has not been considered. In addition, a methodology for price discovery of multivariate options on BTC futures has not been developed.

In this chapter, BTC futures options were priced using the Heston-Nandi futures option pricing model (Li, 2019a). The empirical results show that the symmetric Heston-Nandi model is a better fitting model, this is consistent with previous studies that focused on BTC spot return dynamics. The pricing performance metrics show that the Heston-Nandi model produces reasonable BTC option prices, and that the symmetric Heston-Nandi model also produces more accurate option prices when compared to market prices for two out of the three expiry dates considered.

In addition to the pricing of univariate BTC futures options, the work by Rombouts and Stentoft (2011) was also extended to the pricing of multivariate futures options. The model was applied to BTC futures spread options. The model produces reasonable spread

option prices. However, spread options on BTC futures do not actively trade. Therefore, the model prices cannot be compared to market prices.

The empirical results show that the symmetric Heston-Nandi model is more accurate in most cases. This implies that the symmetric model is a better choice when pricing exotic options (univariate) and other illiquid derivatives written on BTC futures. Furthermore, the multivariate GARCH analysis showed that the CCC-GARCH model is more appropriate (based on historical data) when pricing multivariate BTC futures options. Hence, the symmetric Heston-Nandi model and CCC-GARCH model can serve as a basis for pricing and risk measurement (quantifying market risk and capital calculations) of BTC futures options.

This chapter concludes Part II on option pricing and volatility indices in the cryptocurrency market. Thus far we have shown that volatility indices can be used to improve the accuracy of GARCH option pricing models and that volatility indices can be constructed in illiquid markets. However, options on volatility indices were not considered. The pricing and hedging of options written on volatility indices is the focus of Part III.

# Part III

# Options on Volatility Indices

# Chapter 7

# Price Discovery in the Volatility Index Option Market: A Univariate GARCH Approach

## 7.1 Introduction

Previous chapters have focused on price discovery, the use of volatility indices when modelling different underlying assets, and constructing an implied volatility index in the absence of an established derivatives market. In this chapter,[1] we consider the case where a volatility index is the underlying asset. The use of volatility indices to identify risk regimes and to hedge volatility-related risks has become very popular in recent years. According to Rhoads (2011), the VIX derivatives (futures and options) market has recently experienced significant increases in trading volume since inception. Rhoads (2011) explains that this is due to the inverse relationship between market implied volatility and prices in the equity market, where both VIX options and futures can be used as a hedge against decreases in the equity market.

Market makers of volatility derivatives are faced with the problem of price discovery in the absence of a well-established volatility derivatives market. According to Wang et al. (2017), research focused on VIX is well-documented in the literature, however, not many studies have focused on the pricing of VIX derivatives in the GARCH framework. The focus of this chapter is the GARCH option pricing model applied to price discovery in volatility index option markets.

In a study, Huang et al. (2019) considered different option pricing models for price discovery in the Taiwanese VIX options market. The models include: standard Black-Scholes, square-root, log-normal Ornstein-Uhlenbeck, and the GARCH option pricing models. In the GARCH option pricing framework, Huang et al. (2019) model the spot dynamics of the Taiwanese VIX with only the symmetric GARCH model considered. Furthermore, the Taiwanese VIX options do not actively trade, therefore the prices obtained from the dif-

[1] This chapter is based on a publication (Venter and Maré, 2021a) in *Finance Research Letters*.

ferent models could not be compared to market option prices to get an idea of the pricing performance.

According to Wang et al. (2011), the standard Black model applied to VIX option pricing performs best. The standard Black model is based on the futures price dynamic, which is modelled as a driftless geometric Brownian motion. However, this model requires market implied volatility, which relies on the presence of an established derivatives market. A different approach is to model the risk-neutral dynamics of VIX futures using a univariate GARCH model, which previous studies have not considered. Previous studies have focused on the dynamics of the underlying index, *i.e.,* S&P500, (see *e.g.,* Wang et al., 2017), or the volatility index spot dynamics (*e.g.,* Huang et al., 2019).

The purpose of this chapter is to determine whether the GARCH option pricing model can be used for price discovery in volatility index options markets in the absence of a well-established volatility index options market (absence of market implied volatility). The approach by Huang et al. (2019) is extended to model the VIX futures price dynamics. In addition, the approach is also extended to different GARCH models. Finally, we also consider different error distributions (Huang et al., 2019 consider the Gaussian distribution only). The models are applied to CBOE VIX options (calibrated to futures returns only) to compare model prices to (well-established) market option prices. This will give an indication of whether the model produces reasonable price discovery.

The rest of this chapter is structured as follows: Section 7.2 reviews the recent relevant literature, Section 7.3 outlines the theoretical framework implemented in this study, Sections 7.4 and 7.5 focus on the preliminary data analysis and empirical results, respectively; finally the main findings are summarised in Section 7.7.

## 7.2 Literature review

Research focusing on VIX is well-documented in the literature. However, according to Wang et al. (2017), not many studies have focused on the pricing of VIX derivatives in the GARCH framework. Wang et al. (2017) made use of the Heston-Nandi (Heston and Nandi, 2000) model to estimate VIX futures prices. Five different log-likelihood functions were considered for the estimation of the Heston-Nandi model. The functions were based on returns, model-implied VIX, and VIX futures prices. Two joint likelihood functions were considered, the first based on returns and model-implied VIX, the other based on VIX futures and model-implied VIX. Their empirical results indicate that the estimation based on VIX futures provides the smallest pricing error, however, this leads to distorting of the model-implied VIX. Therefore, Wang et al. (2017) conclude that estimating the model based on VIX futures and implied VIX is the best approach. This provides similar pricing performance without distortion of the model-implied VIX.

In a similar study, Zhu and Lian (2012) derived a closed-form solution for VIX futures using a stochastic volatility model. Jumps were included in both the asset price and volatility processes. The pricing performance was tested by comparing the model-implied futures prices to market futures prices published by the CBOE. Based on the empirical analysis, Zhu and Lian (2012) conclude that the Heston stochastic volatility model is a

good candidate for pricing VIX futures. Furthermore, including jumps in the asset price process improves the pricing performance. Finally, including jumps in the volatility process does not lead to a significant improvement in the pricing performance of the model.

More recently, Huang et al. (2019b) made use of realised volatility for the pricing of VIX futures. Huang et al. (2019b) made use of the heterogeneous autoregressive model with a Gamma innovation and more flexible leverage components (suggested by Majewski et al., 2015) to model-implied volatility (in the risk-neutral measure). The model was calibrated using the maximum likelihood method based on a joint-likelihood function (returns and futures), and a likelihood function based on futures only. The model outputs were also compared to the Heston-Nandi approach by Wang et al. (2017). Huang et al. (2019) conclude that the heterogeneous autoregressive model is superior to the Heston-Nandi model when pricing performance is considered, especially during high volatility periods.

Lou et al. (2019) provide a unified theoretical framework for the pricing of VIX derivatives, including futures and options written on VIX and the short term VIX (VXST, 9 day VIX). Lou et al. (2019) make use of a two-factor model to model the returns of the S&P500 under the risk-neutral measure and the instantaneous VIX. Their empirical results show that the model is capable of capturing various shapes of the VIX term structure and term structures of average at-the-money implied volatility and its skew.

Psychoyios et al. (2010) made use of a jump diffusion model for the pricing of VIX futures and options. Psychoyios et al. (2010) show that a mean-reverting logarithmic process with jumps is capable of capturing the stylised facts of VIX dynamics, which include: rapid mean-reversion when the VIX is at high levels, level effects of volatility (as the level of implied volatility increases the volatility of implied volatility increases proportionally), and large upward movements during times of market stress. Finally, Psychoyios et al. (2010) conclude that incorrectly omitting jumps in a VIX derivative pricing model can lead to considerable problems for pricing and hedging VIX derivatives.

In a study focused on VIX option pricing, Wang et al. (2011) tested the pricing performance of VIX option pricing models. Wang et al. (2011) considered the standard Black model by Whaley (2007), the mean reversion approach by Grünbichler and Longstaff (1996), the model-free approach (Carr and Lee, 2007), and finally the stochastic models derived by Lin and Chang (2009). Wang et al. (2011) conclude that no model performs well for all types of moneyness. However, Wang et al. (2011) argue that the standard Black model applied to VIX options performs the best. This model is based on the futures price dynamic, which is modelled as a driftless Brownian Motion.

In a recent study, Jing et al. (2020) developed a general valuation framework for VIX options that incorporates asymmetric jumps and a stochastic skew. The pricing performance was tested by comparing the model-implied prices to market option prices. Their empirical results show that multi-factor stochastic volatility models are superior to single-factor stochastic volatility models, especially for out-of-the-money options. Furthermore, allowing for downward jumps could improve the pricing performance of the model.

In a recent study, Cao et al. (2020) made use of affine GARCH models based on Gaussian and Inverse Gaussian distributions to derive semi-closed-form solutions for the Price of VIX options and target volatility options. The models are applied to the S&P500,

where VIX options are priced by modelling the GARCH model implied VIX. The models were calibrated to historical returns and market quotes on VIX and S&P500 Index options. Cao et al. (2020) conclude that the inclusion of a skewed distribution for modelling the asset returns improves the pricing performance.

Huang et al. (2019) made use of different models for price discovery in the Taiwanese VIX option market. Huang et al. (2019) considered the following models: the Black-Scholes model (Black and Scholes, 1973), the square-root model (Grünbichler and Longstaff, 1996), the log-normal Ornstein-Uhlenbeck model (Detemple and Osakwe, 2000), and the GARCH option pricing model (Duan, 1995). Huang et al. (2019) conclude that the GARCH option pricing model produces the highest option prices, which is followed by Black-Scholes, square-root, and finally the log-normal Ornstein-Uhlenbeck model.

Taiwanese VIX options are not actively traded yet; therefore the pricing performance could not be tested. In addition, the models were also estimated under the physical measure. Huang et al. (2019) calibrated the GARCH option pricing model to the spot return of the Taiwanese VIX (the spot price was modelled as a driftless process); therefore a unit risk premium was included. Furthermore, only the symmetric GARCH model was considered. In this study, we extend the work by Huang et al. (2019) to asymmetric models. Furthermore, the GARCH models are calibrated to the futures return (consistent with Li, 2019a, who applied the Heston-Nandi model to commodity futures returns). Finally, the models are applied to the VIX, which is actively traded. Hence, the pricing performance of the GARCH option pricing model applied to volatility indices can be tested by comparing model-implied prices to market option prices. The most important studies required for the theory applied in this chapter are summarised in the table below.

| **Study** | **Topic** |
|---|---|
| Duan (1995) | GARCH option pricing |
| Hao and Zhang (2013) | GARCH option pricing (additional models) |
| Li (2019a) | GARCH option pricing applied to Futures |
| Huang et al. (2019) | GARCH option pricing applied to VIX |

The theoretical framework is considered in the next section.

## 7.3 Theoretical framework

In this section, the theory applied in this study is outlined. The aim of the empirical analysis is to determine whether the GARCH option pricing model provides reasonable price discovery in the VIX option market when compared to market prices. By making use of a similar approach to Li (2019a), the futures price dynamics are modelled.

In this study, the VIX futures price process is assumed to be consistent with Equation 6.2. We consider the GARCH(1,1), GJR-GARCH(1,1), and AGARCH(1,1) models (Equations 2.2 to 2.4) for the conditional variance. With regard to the distribution of $\xi_t$, this can clearly be generalised. However, in this study we consider the Gaussian distribu-

tion as a benchmark. In addition, the skewed Student-$t$ distribution (Azzalini and Salehi, 2020) is also considered to capture the effect of skewness and excess kurtosis often found in financial returns (McNeil et al., 2015).

As mentioned previously, the price of a contingent claim (a European put option in this case) is the risk-neutral expectation of the discounted payoff (Wilmott, 2007). Liu et al. (2015) explain that VIX is defined under the risk-neutral measure only. Therefore, the risk-neutral dynamics can be calibrated to the futures return series. Hence, given the calibrated parameters, different realisations of the VIX level at expiry can be simulated. The preliminary data analysis is considered in the next section.

## 7.4 Data analysis

In this section, the statistical properties of the VIX futures returns are considered. The futures price data was obtained from the CBOE. The following delivery dates are included in the analysis: 19-Aug-2020, 16-Sep-2020, 21-Oct-2020, and 18-Nov-2020. This allows us to price VIX options across a range of different strike prices and expiry dates.

The futures prices for the different delivery dates are plotted in Figure 7.1 below.

Figure 7.1: Futures price

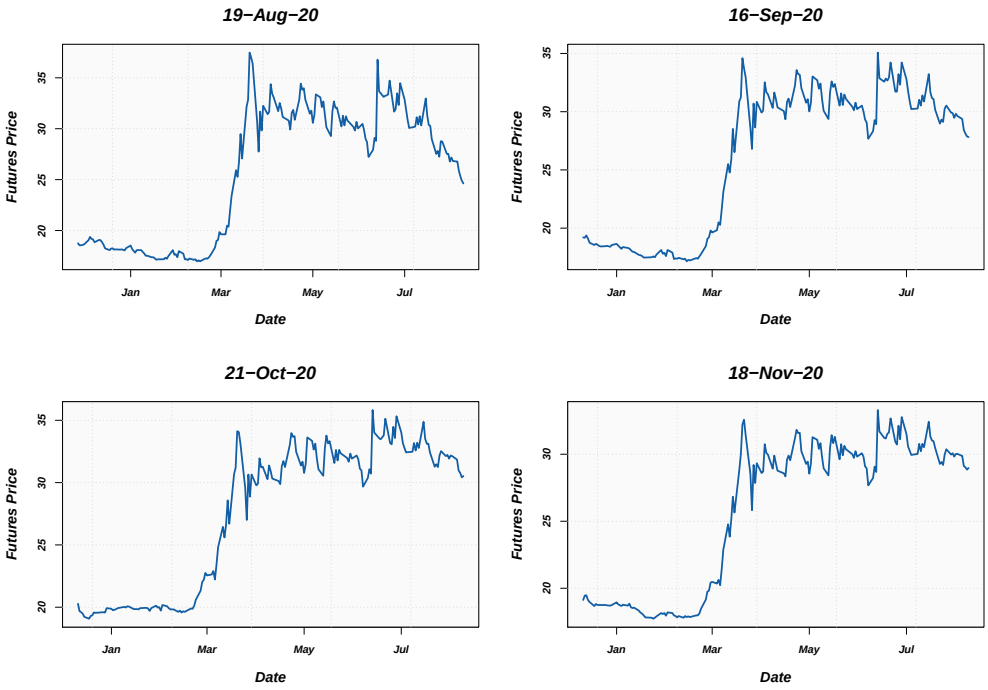


The futures prices seem to be trended over time. However, the different GARCH models considered in this study are calibrated to futures returns. The futures returns are plotted

in Figure 7.2 below.

Figure 7.2: Futures return

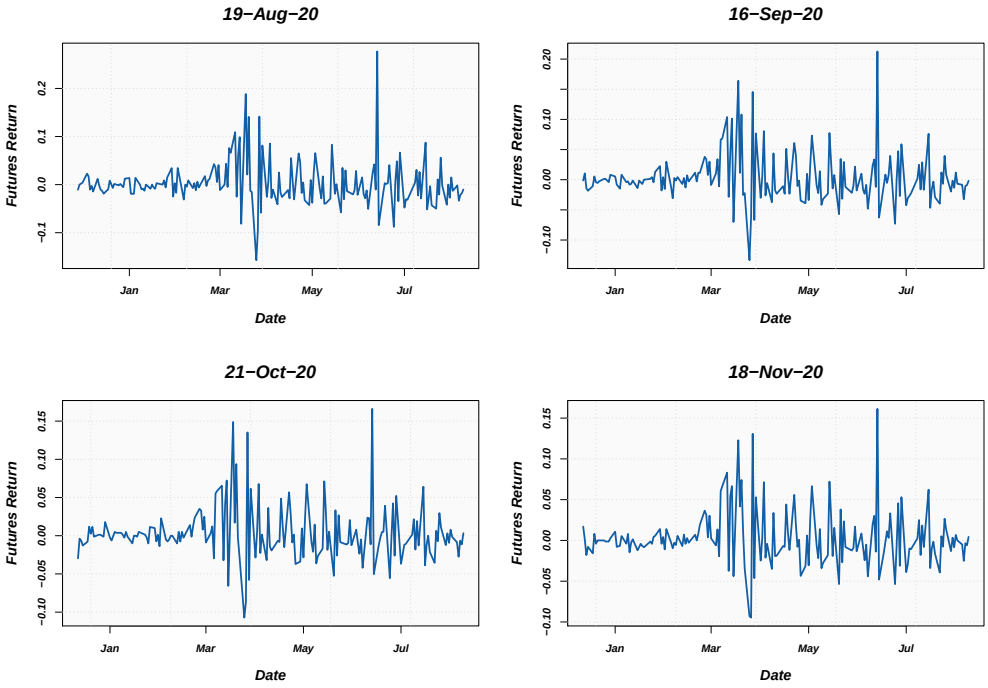


The returns seem to show signs of volatility clustering and also have a conditional expectation of close to zero, which is consistent with the stylised facts of financial returns (McNeil et al., 2015). The descriptive statistics are reported in Table 7.1 below.

Table 7.1: Descriptive statistic: futures return

| Delivery | 19-Aug-2020 | 16-Sep-2020 | 21-Oct-2020 | 18-Nov-2020 |
|---|---|---|---|---|
| Mean | 0.0015 | 0.0022 | 0.0025 | 0.0025 |
| Median | -0.0031 | -0.0032 | -0.0013 | -0.0027 |
| Maximum | 0.2444 | 0.1928 | 0.1536 | 0.1495 |
| Minimum | -0.171 | -0.1432 | -0.1134 | -0.0994 |
| Std. Dev. | 0.0446 | 0.0399 | 0.0343 | 0.0332 |
| Skewness | 1.2516 | 1.1756 | 1.0331 | 0.9865 |
| Kurtosis | 9.7118 | 7.8522 | 7.392 | 6.6765 |
| Jarque-Bera | 376.3021 | 202.2948 | 163.9283 | 121.1384 |

The descriptive statistics indicate that the mean of the futures return for each delivery is close to zero. Furthermore, the Jarque-Bera test statistic shows that the returns series

are not normally distributed. The kurtosis indicates that the returns are fat tailed, which is also consistent with the stylised facts of financial returns (McNeil et al., 2015). Finally, the skewness statistic indicates that the futures return series are positively skewed. The empirical results are considered in the next section.

## 7.5 Results

In this section, the calibrated parameters and information criteria of the fitted parameters are reported. Furthermore, the pricing performance of the three GARCH option pricing models are compared. The calibrated parameters and information criteria of the different models considered in this study are reported in Tables 7.2 to 7.7 below. The parameters $\omega$ and $\nu$ denote the skewness and shape parameters of the skewed Student-$t$ distribution.

Table 7.2: GARCH(1,1) parameters (Gaussian distribution)

| | 19-Aug-2020 | 16-Sep-2020 | 21-Oct-2020 | 18-Nov-2020 |
|---|---|---|---|---|
| $\alpha_0$ | 7E-05 | 4E-05 | 2E-05 | 2E-05 |
| $\alpha_1$ | 0.3425 | 0.3248 | 0.2787 | 0.2952 |
| $\beta_1$ | 0.6565 | 0.6742 | 0.7203 | 0.7038 |
| AIC | -3.6492 | -3.9075 | -4.2903 | -4.3791 |
| SIC | -3.5952 | -3.8515 | -4.2343 | -4.323 |

Table 7.3: GJR-GARCH(1,1) parameters (Gaussian distribution)

| | 19-Aug-2020 | 16-Sep-2020 | 21-Oct-2020 | 18-Nov-2020 |
|---|---|---|---|---|
| $\alpha_0$ | 6E-05 | 4E-05 | 2E-05 | 2E-05 |
| $\alpha_1$ | 0.4952 | 0.4024 | 0.1941 | 0.2961 |
| $\beta_1$ | 0.6433 | 0.6681 | 0.7068 | 0.7039 |
| $\gamma$ | -0.2791 | -0.143 | 0.1963 | -0.0019 |
| AIC | -3.6515 | -3.8988 | -4.2937 | -4.3671 |
| SIC | -3.5795 | -3.8241 | -4.219 | -4.2924 |

Table 7.4: AGARCH(1,1) parameters (Gaussian distribution)

| | 19-Aug-2020 | 16-Sep-2020 | 21-Oct-2020 | 18-Nov-2020 |
|---|---|---|---|---|
| $\alpha_0$ | 7E-05 | 4E-05 | 2E-05 | 1E-05 |
| $\alpha_1$ | 0.3341 | 0.2988 | 0.279 | 0.2705 |
| $\beta_1$ | 0.6317 | 0.674 | 0.72 | 0.7183 |
| $\gamma$ | -0.3152 | -0.2964 | 0.0061 | -0.1937 |
| AIC | -3.668 | -3.9154 | -4.2783 | -4.3729 |
| SIC | -3.5959 | -3.8407 | -4.2036 | -4.2982 |

Table 7.5: GARCH(1,1) parameters (Skewed Student-$t$ distribution)

| | 19-Aug-2020 | 16-Sep-2020 | 21-Oct-2020 | 18-Nov-2020 |
|---|---|---|---|---|
| $\alpha_0$ | 2E-05 | 2E-05 | 1E-05 | 1E-05 |
| $\alpha_1$ | 0.2883 | 0.2827 | 0.2818 | 0.2797 |
| $\beta_1$ | 0.7107 | 0.7163 | 0.7172 | 0.7193 |
| $\omega$ | 1.6041 | 1.4228 | 1.2655 | 1.3181 |
| $\nu$ | 5.6587 | 4.1556 | 4.4321 | 4.2372 |
| AIC | **-4.077** | -4.2557 | **-4.5600** | **-4.6238** |
| SIC | **-3.987** | -4.1623 | **-4.4666** | **-4.5305** |

Table 7.6: GJR-GARCH(1,1) Parameters (Skewed Student-$t$ distribution)

| | 19-Aug-2020 | 16-Sep-2020 | 21-Oct-2020 | 18-Nov-2020 |
|---|---|---|---|---|
| $\alpha_0$ | 2E-05 | 2E-05 | 1E-05 | 1E-05 |
| $\alpha_1$ | 0.3824 | 0.4601 | 0.2898 | 0.3592 |
| $\beta_1$ | 0.7267 | 0.7595 | 0.7204 | 0.7423 |
| $\gamma$ | -0.1903 | -0.3779 | -0.0204 | -0.1821 |
| $\omega$ | 1.6542 | 1.4289 | 1.2662 | 1.3197 |
| $\nu$ | 5.1822 | 3.2286 | 4.3588 | 3.7506 |
| AIC | -4.0761 | **-4.2628** | -4.5481 | -4.618 |
| SIC | -3.968 | **-4.1507** | -4.4361 | -4.506 |

Table 7.7: AGARCH(1,1) Parameters (Skewed Student-$t$ distribution)

| | 19-Aug-2020 | 16-Sep-2020 | 21-Oct-2020 | 18-Nov-2020 |
|---|---|---|---|---|
| $\alpha_0$ | 2E-05 | 2E-05 | 1E-05 | 1E-05 |
| $\alpha_1$ | 0.2688 | 0.2006 | 0.2671 | 0.2215 |
| $\beta_1$ | 0.7236 | 0.7358 | 0.7286 | 0.7363 |
| $\gamma$ | -0.1567 | -0.5583 | -0.1107 | -0.4317 |
| $\omega$ | 1.6005 | 1.4267 | 1.2703 | 1.3292 |
| $\nu$ | 5.6304 | 3.7395 | 4.3302 | 3.9219 |
| AIC | -4.0696 | -4.2589 | -4.5489 | -4.623 |
| SIC | -3.9615 | -4.1469 | -4.4369 | -4.511 |

The bold values in the tables above indicate the minimum value of the AIC or SIC of the relevant futures price. This indicates the best fitting model based on the historical data. The AIC and SIC indicate that the GARCH(1,1) model with a skewed Student-$t$ error distribution is the best fitting model for all of the futures return series except the 16-Sep-2020 delivery, the GJR-GARCH(1,1) model with a skewed Student-$t$ error distribution is the best fitting model in this case.

The estimated GARCH option pricing models were used to estimate VIX European

put option prices, which were compared to market option prices[2]. The pricing performance based on the RMSE and MAE of the three GARCH models are reported in Tables 7.8 and 7.9 below.

Table 7.8: Pricing performance (Gaussian distribution)

| | RMSE | MAE |
|---|---|---|
| GARCH(1,1) | 2.0201 | 1.7851 |
| GJR-GARCH(1,1) | 1.8723 | 1.6199 |
| AGARCH(1,1) | 2.1503 | 1.9003 |

Table 7.9: Pricing performance (Skewed Student-$t$ distribution)

| | RMSE | MAE |
|---|---|---|
| GARCH(1,1) | **1.0977** | **0.8866** |
| GJR-GARCH(1,1) | 1.9863 | 1.4408 |
| AGARCH(1,1) | 1.4750 | 1.1073 |

The bold values indicate the minimum value of the MAE and RMSE. The MAE and RMSE both indicate that GARCH(1,1) model with a skewed Student-t error distribution is the best performing model. To illustrate the pricing performance, the market option prices for each maturity date are plotted in addition to the model prices in Figure 7.3 below.

Figure 7.3: Put option prices

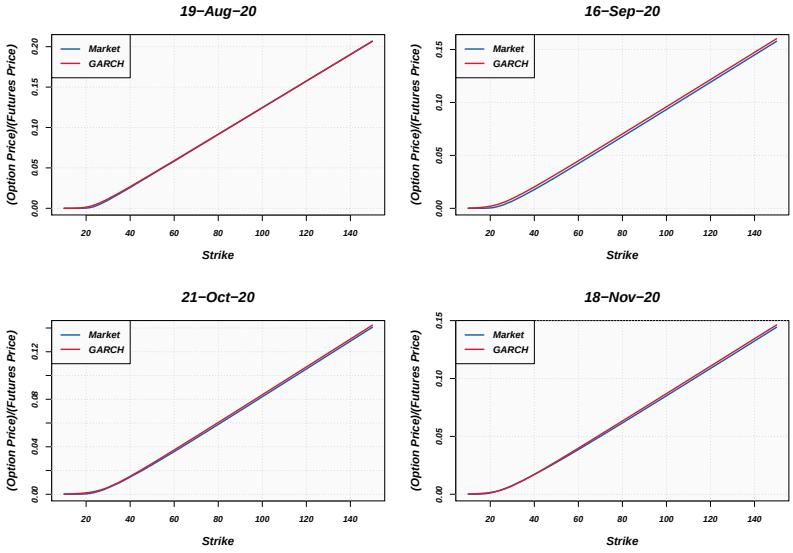


[2]Market VIX option prices were obtained from the Thomson Reuters Datastream databank.

The empirical results are discussed in the next section.

## 7.6 Discussion

The preliminary data analysis shows that the VIX futures return series are consistent with the stylised facts (Cont, 2001) of financial returns (mean of close to zero and leptokurtosis). It is also important to note that the return series are positively skewed, thus, the use of the skewed Student-$t$ distribution (in addition to the Gaussian distribution) used to model the error distribution is justified in this case. Furthermore, Alexander (2008) explains that non-Gaussian error distributions usually outperform the Gaussian distribution when modelling financial returns using GARCH models.

When the GARCH parameters and information criteria are considered, it is clear that the skewed Student-$t$ error distribution assumption produces a better fitting model (for the three GARCH processes considered). This is consistent with expectations given the excess kurtosis and positive skewness. Overall, the GARCH(1,1) model with a skewed Student-t error distribution is the best fitting model, which is aligned with the argument by Hansen and Lunde (2005), that it is difficult to find a GARCH model that consistently outperforms a GARCH(1,1) model. The negative asymmetry parameters ($\gamma$) indicate that the rise in volatility is greater after a positive shock. This implies that VIX futures behave more like a commodity.

The pricing performance metrics show that the GARCH(1,1) model with skewed Student-$t$ errors produces the most accurate VIX put option prices. This is consistent with expectations as it is aligned with the information criteria. The plot of the VIX option market and model prices (Figure 7.3) show that the GARCH option pricing model produces reasonable VIX option prices. Therefore, the GARCH option pricing model can be used in the absence of a well-established volatility index option market. The summary is outlined in the next section.

## 7.7 Summary

In this chapter, the GARCH option pricing model is applied to VIX futures returns to determine whether the model can be used for price discovery in the absence of a well-established volatility index option market. Huang et al. (2019) applied the GARCH option pricing model to the Taiwanese VIX spot return, the spot price was modelled as a driftless process, and the variance process included a unit risk premium. Furthermore, Huang et al. (2019) focused on the symmetric GARCH(1,1) model with normally distributed errors. In this chapter, we extend the work of Huang et al. (2019) by calibrating the GARCH models to the historical futures returns (consistent with Li, 2019a). Furthermore, the symmetric GARCH(1,1) was used in addition to the asymmetric GJR-GARCH(1,1) and AGARCH(1,1) models. Finally, both Gaussian and skewed Student-$t$ error distributions were considered. The models were applied to VIX, which has an established options market, in order to determine the accuracy of the model-implied prices.

The empirical results indicate that the GARCH(1,1) model, with skewed Student-$t$ errors, provides the best fitting model (in most cases) based on the information criteria. Furthermore, when the pricing performance is considered, the GARCH(1,1) model with skewed Student-$t$ errors is also the best performing model (consistent with the argument by Hansen and Lunde, 2005). Reasonable price discovery is obtained when using the GARCH option pricing model calibrated to VIX futures returns.

The empirical results suggest that it is appropriate to use the GARCH option pricing model for price discovery in the absence of a well-established volatility index options market. However, it is important to make use of error distributions that incorporate skewness and kurtosis to accurately model the risk-neutral dynamics. An important factor that was not considered is the hedge performance of the GARCH option pricing model applied to VIX futures options, which is the focus of the next chapter.

# Chapter 8

# Hedging VIX Futures Options: An Application of the Heston-Nandi Model

## 8.1 Introduction

Volatility indices and volatility index derivatives have become popular risk management tools in recent years. The focus of this chapter[1] is the hedging of CBOE VIX futures options, using VIX futures. The pricing of VIX options (considered in Chapter 7) is well-documented in the literature. However, not many studies focus on the hedging of VIX options.

As discussed in Section 7.2, in a study focused on the pricing of VIX options Wang et al. (2011) showed that the standard Black (1976) model is the most reliable when it comes to pricing VIX options. Therefore, the Black (1976) model is used as a benchmark in this study. According to Lassance and Vrins (2018), the ability of a model to describe the underlying dynamics is an important factor to consider when using models for hedging.

As mentioned previously, conventional wisdom among financial modelling researchers is that the assumption of constant volatility is not always a realistic assumption. Therefore, the hedge performance of the model by Heston and Nandi (2000) applied to VIX futures options is also considered. The rest of this chapter is structured as follows: Section 8.2 outlines the recent and relevant literature, the theory applied in this chapter is outlined in Section 8.3, the empirical results are shown in Section 8.4, and the main findings are summarised in Section 8.5.

[1] A previous version of this chapter was presented at the 2021 Student Simposium in Natural Sciences (North-West University).

## 8.2 Literature review

Research focused on the pricing of volatility index futures is well-documented in the literature (see *e.g.,* Zhang and Zhu, 2006, Zhu and Lian, 2012, Huang et al., 2019b, Wang et al., 2017). Similarly, the pricing of volatility index options is also well-documented. Wang et al. (2011) considered four different VIX option pricing models. The pricing performance metrics are based on the difference between the market price and the theoretical model price. Their empirical results indicate that the standard Black (1976) model performs best when applied to VIX options. In this chapter, the Black (1976) model is applied to the hedging of VIX options.

In a recent paper, Venter and Maré (2021a) (Chapter 7 is based on this paper) applied different univariate GARCH models to historical VIX futures returns for the pricing of VIX options. The authors considered symmetric and asymmetric GARCH models, different error distribution (Gaussian and distributions that capture skewness and kurtosis) assumptions were also considered. The authors conclude that the symmetric GARCH model with skewed Student-$t$ errors is the best performing model.

Lassance and Vrins (2018) considered the mismatch between the pricing and hedging performance of option pricing models when applied to equity options. Lassance and Vrins (2018) considered the pricing and hedging performance of: Black-Scholes, practitioner Black-Scholes, and the Heston-Nandi model applied to the S&P500 Index, and Apple options. The authors explain that a model's hedge performance is dependent on the underlying asset price dynamics. The main conclusion is that Black-Scholes and practitioner Black-Scholes largely outperform the Heston-Nandi model when it comes to hedge performance.

Kuen Siu et al. (2014) considered the hedge performance of the GARCH option pricing model when applied to the hedging of crude oil derivatives. Their analysis focused on hedging strategies based on Delta and Delta-Gamma. The hedge performance different models were compared based on value-at-risk and expected shortfall. Their empirical results indicate that the GARCH option pricing model with shifted gamma innovations outperform the GARCH option pricing model with normal innovations, and the Black-Scholes model.

Not many studies have focused on the hedging of VIX options. In a recent study, Fukasawa et al. (2021) applied three different models (Black-Scholes, CIR, and rough stochastic volatility) to the hedging of VIX options using a forward variance swap. The hedge performance of the different models was based on the stability of the P&L. Their empirical results indicate that the rough stochastic volatility model is the most reliable hedging model.

## 8.3 Theoretical framework

In this chapter, using a similar approach to Lassance and Vrins (2018), the futures option pricing models derived by Black (1976) and Li (2019a) are applied to the hedging of VIX futures options. The risk-neutral asset price process in the Black (1976) model is given

by,

$$dF_{t,T} = \sigma F_{t,T} dW_t,$$

where $\sigma$ is the implied volatility (assumed to be constant), and $W_t$ is a standard Brownian motion under the risk-neutral measure $Q$. The problems associated with the assumption of constant volatility (for the pricing and hedging of derivatives) are well-documented in the literature. Therefore, a stochastic volatility model is also considered.

As mentioned previously, the model by Heston and Nandi (2000) was extended by Li (2019a) to futures options. The Heston and Nandi (2000) model is usually calibrated to spot price dynamics under the real-world measure (as it is applied in Chapter 6). However, in this chapter the model is calibrated to futures option prices. Therefore, only the risk-neutral asset price dynamics are required. The risk-neutral futures price process is consistent with Equation 6.2. For the estimation of parameters, the root-mean squared error of the model price relative to the market price (similar to Christoffersen and Jacobs, 2004). The following function is minimised:

$$RMSE_t = \sqrt{\frac{1}{N_{Mkt}} \sum_{i=1}^{N} \left( C_{i,t}^{Mkt} - C_{i,t}^{HN} \right)^2},$$

where $N_{Mkt}$ is the number of market options used for calibration at at time $t$, $C_{i,t}^{Mkt}$ is the market price of the $i$th option at time $t$, and $C_{i,t}^{HN}$ is the corresponding Heston-Nandi price. The models are calibrated on a daily basis, using an approach that is consistent with Alexander and Nogueira (2004) the hedged portfolio is rebalanced on a daily basis (using the daily closing price).

In our analysis, we assume that we have written a range of call options (different strike prices) on VIX futures. The delta ($\Delta_t$ - hedge ratio) of either the Black (1976) or the Heston-Nandi futures model (Li, 2019a) are computed numerically (central difference). At each point in time $t$, the hedged portfolio consists of a short call option, $\Delta_t$ VIX futures, and an amount of cash either borrowed or invested at the risk-free rate (Maré, 2009). We consider delta hedging only (consistent with Lassance and Vrins, 2018). The superior hedge model will produce the most stable profit and loss (P&L) distribution (average standard deviation across different strikes considered). The empirical results are outlined in the next section.

## 8.4 Empirical results

This section focuses on the hedge performance of the Black and Heston-Nandi futures option pricing models applied to the hedging of VIX futures options. The futures options were hedged from 22-Oct-2020 up to 21-Apr-2021 (the futures option expiry date). The following strike prices were considered: 15, 16,..., 30. The VIX futures price and returns are plotted in Figures 8.1 and 8.2 below:

Figure 8.1: VIX futures price

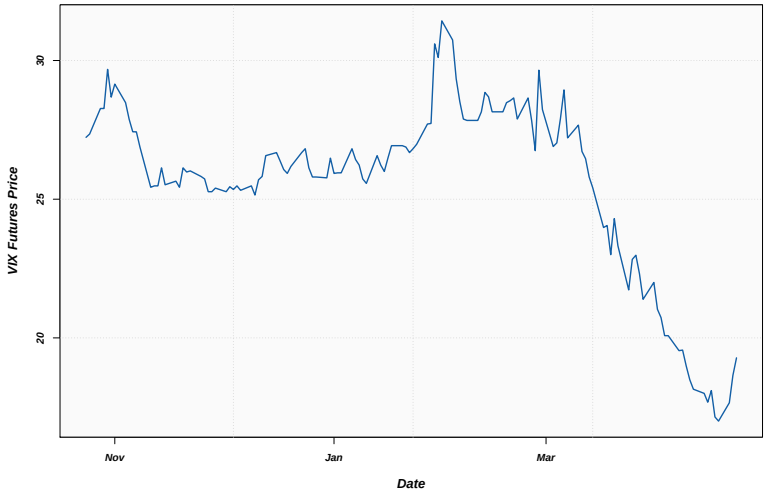


Figure 8.2: VIX futures return

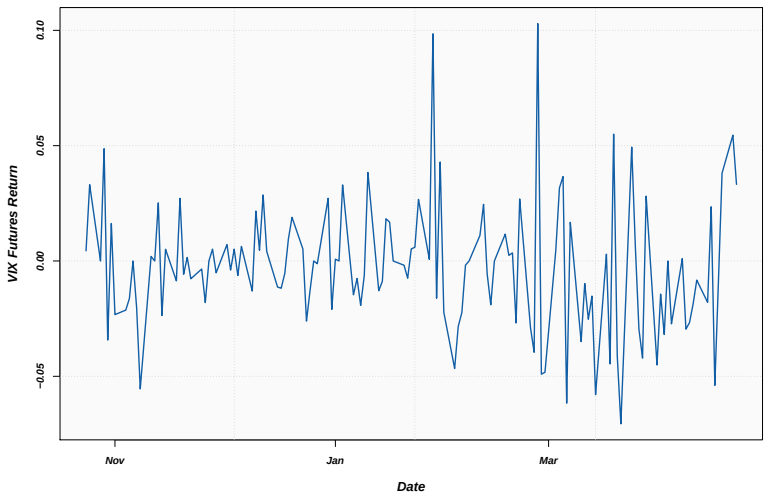


The futures returns do seem to indicate signs of volatility clustering. Therefore, the use of the Heston-Nandi model is appropriate. However, in this study the Heston-Nandi model is not calibrated to futures returns, it is calibrated to option prices. The time series of VIX option prices (strike = \$23) is plotted in Figure 8.3 below:

Figure 8.3: VIX option price (strike = 23)

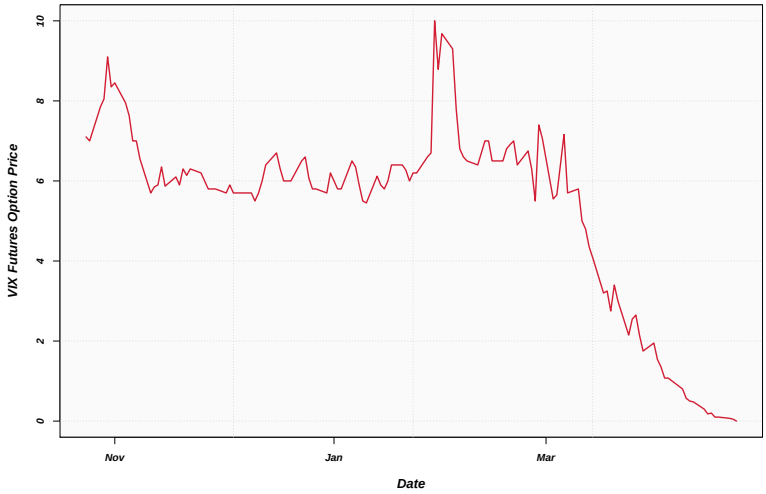


Daily rebalancing is assumed in this study (consistent with Alexander and Nogueira, 2004). Hence, the Heston-Nandi futures model is calibrated to VIX options (multiple strikes) on each day included in the sample period.

As explained in the previous section, the superior hedging model will produce a more stable P&L distribution. The average (across the different strike prices considered) P&L standard deviations are reported in Table 8.1 below (average Dollar standard deviation):

Table 8.1: Hedge performance

| Model | Standard Deviation |
|---|---|
| Heston-Nandi | 0.7333 |
| Black 76 | 0.7963 |

It is clear from the above that the Heston-Nandi model produces a more stable P&L distribution on average. This implies that the non-Gaussian dynamics of VIX futures returns are better explained by the Heston-Nandi model as apposed to the Black model (Lassance and Vrins, 2018).

## 8.5 Summary

The focus of this chapter is the hedging of VIX futures options. The standard Black (1976) model was used as a benchmark. Furthermore, to take leptokurtosis and the stochastic nature of volatility into account, the model by Heston and Nandi (2000) was also considered. The models were compared based on the standard deviation of the P&L generated by the hedged portfolio. Empirical results indicate that the Heston-Nandi model

is more reliable when applied to the hedging of VIX futures options. The Heston-Nandi model better explains the dynamics (leptokurtosis and volatility clustering often found in financial time series) of VIX futures.

This chapter concludes part III on the pricing and hedging of options on volatility indices using the GARCH option pricing model. The focus of part IV is the application of the GARCH option pricing model to more modern derivative pricing frameworks that take additional factors into account that were not considered prior to the GFC.

# Part IV

# GARCH Option Pricing After the GFC

# Chapter 9

# Collateralised Option Pricing in a South African Context: A Univariate GARCH Approach

## 9.1 Introduction

Parts I to III have focused on the pricing of derivatives and volatility indices in illiquid markets. The focus of Part IV is GARCH option pricing in a more modern framework. The GFC of 2008 was a turning point for financial markets, especially for financial modelling and risk management of contingent claims. As discussed, these claims, such as financial options, were typically valued in the Black-Scholes-Merton framework (Black and Scholes, 1973). Common modelling assumptions within this modelling paradigm are the existence of constant unique risk-free interest rate, constant volatility, normally distributed asset returns, and no transaction costs (Black and Scholes, 1973). Previously, the pricing of derivative instruments was not as complicated as it is today.

An important factor that needs to be considered after the GFC is the effect of funding, which, in essence, imposes constraints on the balance sheet of the financial intermediating entity. This has forced financial modelling researchers and practitioners to develop a new pricing framework. Piterbarg (2010) extended the Black-Scholes framework by relaxing the assumption of a unique risk-free rate. The purpose of the model derived by Piterbarg (2010) is the pricing of derivatives in the presence of collateral. Three different rates are required when pricing derivatives in this framework: the repurchase agreement rate, the collateral rate, and the funding rate.

In this chapter, the GARCH option pricing model (in the presence of collateral) derived by Labuschagne and Von Boetticher (2017) is extended to two different models, namely the symmetric GARCH(1,1) model and the non-linear AGARCH model. This is done to illustrate the effect of asymmetry when pricing collateralised options (vanilla and exotic) in the GARCH option pricing framework. The purpose of our analysis is to demonstrate pricing effects of contingent claims in the presence of balance sheet constraints, and use a stochastic volatility model to relax volatility assumptions. The remainder of this chap-

ter is structured as follows: Section 9.2 focuses on recent and relevant literature. The methodology is considered in Section 9.3, Section 9.4 reports the empirical results, and the main findings are summarised in Section 9.5.

## 9.2 Literature review

In a recent study, Oberholzer and Venter (2019) made use of the Heston-Nandi model to approximate option price surfaces for the CIVETS (Columbia, Indonesia, Vietnam, Egypt, Turkey and South Africa) countries' equity indices. Their empirical results indicate that the option price surfaces obtained from the model are consistent with those usually found in the market. However, the options considered do not incorporate collateral agreements. Furthermore, only vanilla options were considered.

Christoffersen et al. (2013) compared a wide range of different GARCH models for option valuation market traded option prices. Their results showed that market option-based objective functions and models that allow for a standard leverage effect produce the most parsimonious GARCH option pricing model. However, the estimation of these models were done in the Black-Scholes framework which does not account for collateral. As mentioned previously, collateral agreements have become very important after the GFC. Therefore, a more modern pricing framework (Piterbarg, 2010) is considered in this chapter.

In a similar study, Hsieh and Ritchken (2005) compared the Heston-Nandi model to the AGARCH option pricing model by Duan (1995). The accuracy of the models was tested by comparing the model option prices to actual market option prices on the S&P500 index. Their results indicated that the AGARCH model is superior to the Heston-Nandi model, and should be considered by traders and risk managers. Similar to Christoffersen et al. (2013), this study was performed before the GFC. Hence, collateral was not considered.

In a recent paper, Levendis and Venter (2019) made use of local volatility in the Piterbarg framework to price collateralised Asian options. Local volatility assumes that volatility is a deterministic function of the spot price and time. Levendis and Venter (2019) explain that no closed-form solution exists for an arithmetic Asian option in the Piterbarg framework. Therefore, Monte Carlo simulation was used. Their empirical results indicate that the presence of collateral has a greater effect on in-the-money options (*i.e.,* more expensive). The calibration of local volatility requires an implied volatility surface which is not always available in emerging markets (GARCH models can be calibrated to historical data). Assuming that volatility is a deterministic function of the spot price and time is a better assumption than constant volatility. However, this does not capture the stochastic nature of volatility. Therefore, GARCH models are applied in this study.

Labuschagne and Von Boetticher (2017) extended the GARCH option pricing model by Duan (1995) to incorporate collateral in the Piterbarg (2010) framework. The GJR-GARCH and exponential GARCH models were considered. Their empirical results showed that both the GJR-GARCH and exponential GARCH models produce the characteristic volatility skew that can be observed in the markets. However, no comparison was made with a symmetric model. Furthermore, exotic options were not considered.

## 9.3 Methodology

In this chapter, the GARCH option pricing model is used to price collateralised options on the Top40. We use closing spot levels of the Top40 from 1 January 2010 to 31 October 2019 to fit the parameters. The remainder of this section is divided into two subsections, the first focuses on the Piterbarg (2010) framework and the second focuses on the GARCH option pricing model.

### 9.3.1 The Piterbarg framework

As mentioned previously, the Piterbarg (2010) model extends the Black-Scholes framework to incorporate three different interest rates: the collateral rate ($r_C$), the repurchase agreement rate ($r_R$), and the funding rate ($r_F$.) In general, the following inequality holds,

$$r_C \leq r_R \leq r_F.$$

The prices of fully collateralised ($V_{FC}$) and zero collateral ($V_{ZC}$) European call options in the Piterbarg framework are given by,

$$\begin{aligned} V_t^{(FC)} &= \exp\{-r_C(T-t)\}\left(S_t \exp\{r_R(T-t)\}\Phi(d_1) - K\Phi(d_2)\right) \\ V_t^{(ZC)} &= \exp\{-r_F(T-t)\}\left(S_t \exp\{r_R(T-t)\}\Phi(d_1) - K\Phi(d_2)\right), \end{aligned}$$

respectively. In addition, $d_1$ and $d_2$ are given by,

$$\begin{aligned} d_1 &= \frac{\ln\left(\frac{S_t}{K}\right) + (r_R + \frac{1}{2}\sigma^2)(T-t)}{\sigma\sqrt{(T-t)}} \\ d_2 &= d_1 - \sigma\sqrt{(T-t)}. \end{aligned}$$

The framework is discussed more formally in Section 10.3.2. The GARCH option pricing model is considered in the next subsection.

### 9.3.2 GARCH option pricing

Labuschagne and Von Boetticher (2017) make the following assumption regarding the dynamics of the underlying asset under the real-world measure $P$,

$$\ln\left(\frac{S_t}{S_{t-1}}\right) = r_R + \lambda\sqrt{h_t} - \frac{1}{2}h_t + \epsilon_t, \tag{9.1}$$

where $\epsilon_t \sim \mathcal{N}(0, h_t)$, $h_t$ is some GARCH process, and $\lambda$ is the unit risk premium. In this chapter, the conditional variance is assumed to be driven by a GARCH(1,1) and an AGARCH(1,1) process, respectively. The real-world and risk-neutral conditional variance processes are outlined in Section 2.2.2. Labuschagne and Von Boetticher (2017) show that the dynamics of the underlying asset under the risk-neutral measure ($Q_{r_R}$) are given by,

$$\ln\left(\frac{S_t}{S_{t-1}}\right) = r_R - \frac{1}{2}h_t + \xi_t, \tag{9.2}$$

where $\xi_t \sim \mathcal{N}(0, h_t)$ under the $Q_{r_R}$ measure.

In this study, the GARCH model parameters are estimated using the maximum likelihood method based on historical returns data (implied volatility is not required). Furthermore, Monte Carlo simulation (50000 simulations) is used to approximate option price surfaces. Hence, different realisations of Equation 9.2 are simulated to obtain the expectation of the discounted payoff of an option.

Both vanilla and exotic (Asian and lookback) options are considered in this study. As mentioned previously, the payoff of a (vanilla) European call option is given by,

$$\max\{S_T - K, 0\}.$$

The payoff of an Asian call option is given by,

$$\max\left\{\frac{1}{N_{Avg}}\sum_{i=1}^{N_{Avg}} S_i - K, 0\right\},$$

where $N_{Avg}$ is the number of averaging periods. In this study, daily averaging throughout the life of the option is assumed. The payoff of a (fixed) lookback call option is,

$$\max\{S_{\max} - K, 0\},$$

where $S_{\max}$ is the maximum underlying asset price achieved during the life of the option. The empirical results are reported in the next section.

## 9.4 Empirical results

This section focuses on the approximated GARCH option price surfaces, which illustrate the effect of collateral and asymmetry. The GARCH option price surfaces are plotted and compared. Both vanilla options and exotic options are considered. For the estimation of parameters, $r_R$ is assumed to be consistent with the 91 day Treasury bill rate (6.67%). In addition, we assume that $r_C = r_R - 1\%$, and $r_F = r_R + 1\%$. The GARCH model parameters are reported in Table 9.1 below:

Table 9.1: GARCH model parameters

| | GARCH(1,1) | AGARCH(1,1) |
|---|---|---|
| $\alpha_0$ | 2.17E-06 | 2.12E-06 |
| $\alpha_1$ | 0.0714 | 0.0472 |
| $\beta_1$ | 0.9086 | 0.828 |
| $\lambda$ | 0.0465 | 0.0009 |
| $\gamma$ | | 1.523 |
| AIC | -6.4385 | -6.4866 |
| SIC | -6.4293 | -6.4775 |

The GARCH model parameters in the table above are used to approximate the option price surfaces that follow. The asymmetry term ($\gamma$) of the AGARCH(1,1) model is positive. This is usually the case when applying the AGARCH model to equity returns (Alexander, 2008).

In this study, both vanilla and exotic call option price surfaces are considered. The GARCH(1,1) (vanilla) European call option price surfaces are plotted in Figure 9.1 below. Both the full collateral and zero collateral surfaces are plotted. In addition, the differences between the zero and full collateral surfaces are also plotted to show the effect of collateral. All price surfaces and differences are expressed as a percentage of the initial spot price.

Figure 9.1: GARCH(1,1) European call option price surfaces

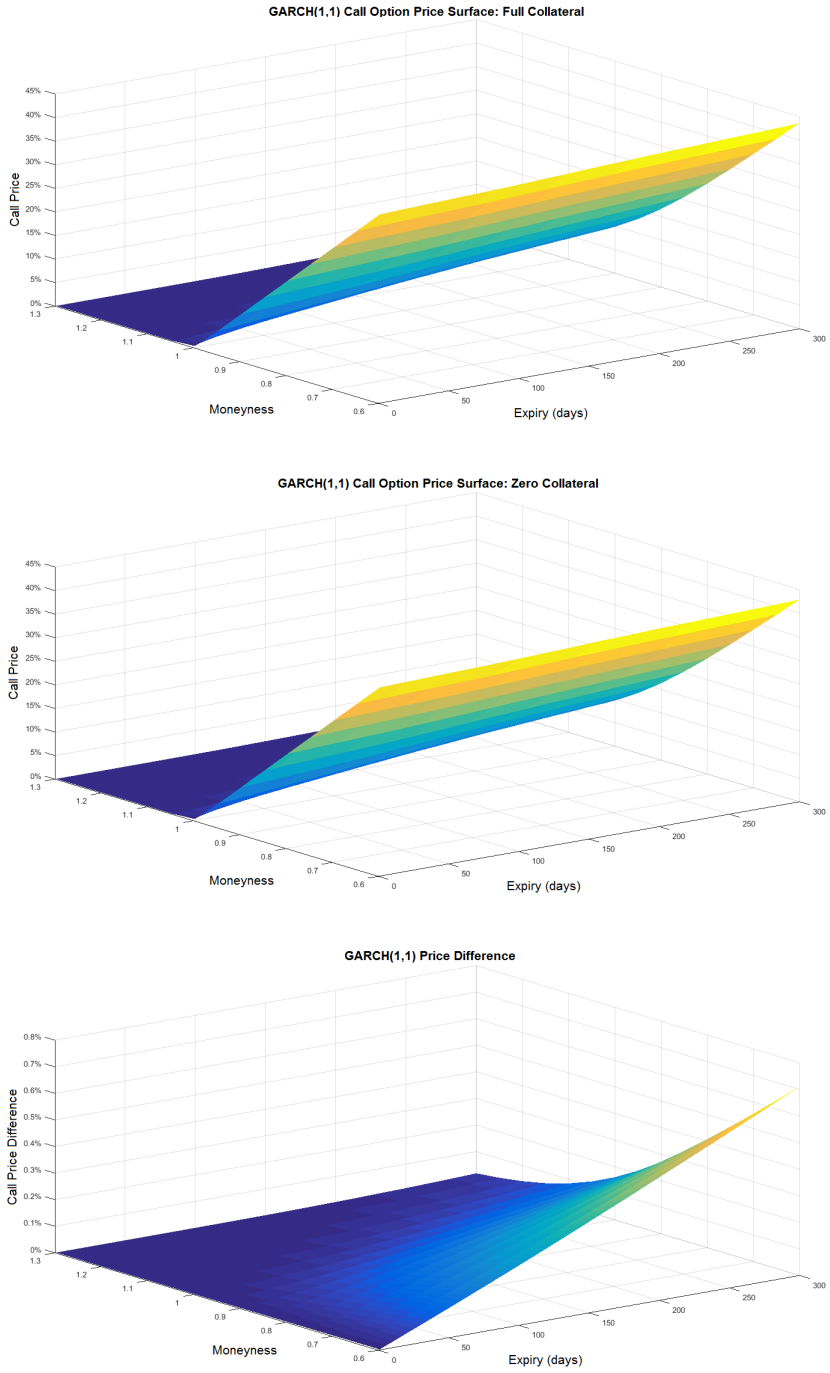

Similar option price surfaces were obtained when using the AGARCH(1,1) model. The difference in the full collateral and zero collateral surfaces increases as the option price increases. The call option is more in the money and over longer expiries. This is consistent with Levendis and Venter (2019).

The difference between the GARCH(1,1) and AGARCH(1,1) surfaces are plotted in Figure 9.2 below to illustrate the effect of asymmetry. Similar results were obtained for full collateral and zero collateral, therefore only the difference between the full collateral surfaces is considered.

Figure 9.2: European option price differences

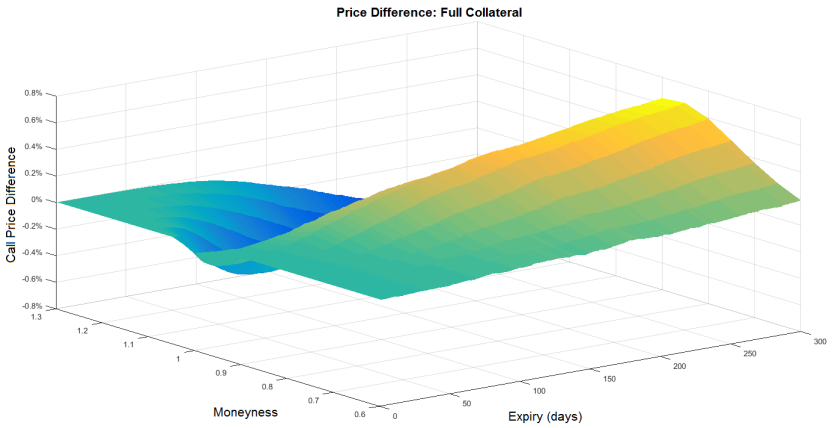


Small differences are obtained when the GARCH(1,1) and AGARCH(1,1) option prices are compared. However, the difference in prices tends to increase as the time to expiry increases. This is consistent with expectations because the probability of negative shocks is greater over a longer period of time (more uncertainty).

Collateral has a similar effect on the Asian call option price surface. However, to illustrate the effect of asymmetry on Asian options, the difference between the AGARCH(1,1) Asian call option price surface and the GARCH(1,1) full collateral Asian call option price surface is plotted in Figure 9.3 below.

Figure 9.3: Asian option price differences

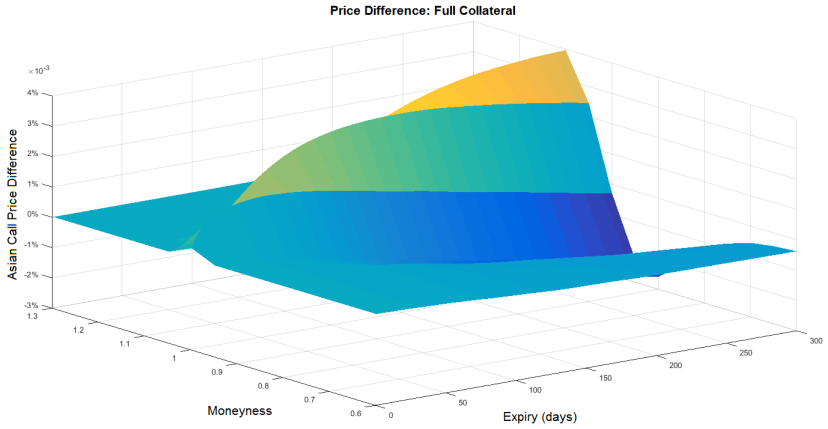


The difference between the AGARCH(1,1) and GARCH(1,1) Asian call option price surfaces in Figure 9.3 illustrates that asymmetry is not as significant when pricing Asian options in the collateralised GARCH option pricing framework. This is consistent with expectations, because the averaging feature of Asian options reduces the volatility inherent in the options (see *e.g.,* Jeon et al., 2016). This also explains why Asian options are generally cheaper than European options.

The difference between the full and zero collateral price of the lookback call option price surface is illustrated in Figure 9.4 below.

Figure 9.4: Effect of collateral (lookback option)

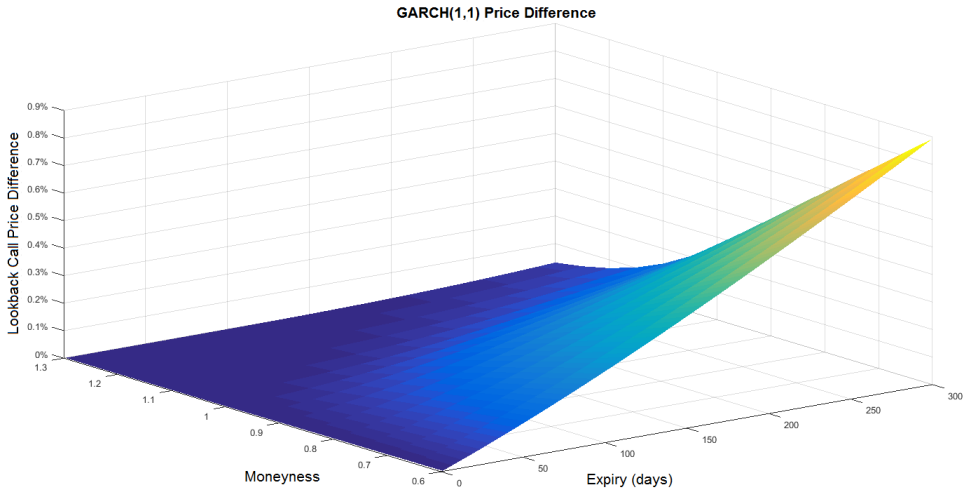

Collateral clearly has a greater impact on the lookback option (when compared to the vanilla option price difference). This is intuitive, as the price of a lookback call option is always greater than, or equal to, the price of a vanilla call option (greater option price implies greater collateral). The difference between the AGARCH(1,1) and GARCH(1,1) price surfaces of fully collateralised lookback options is plotted in Figure 9.5 below:

Figure 9.5: Lookback option price differences

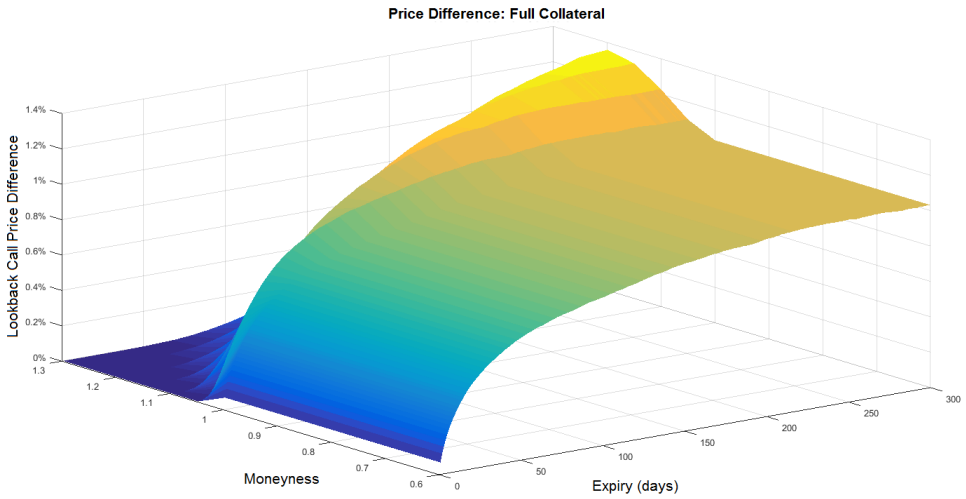


Asymmetry clearly also has a greater effect on the price of a lookback option.

The empirical results show that asymmetry and collateral have different effects on exotic and vanilla options. As the option price increases, the amount of collateral increases. When dealing with an Asian option (generally cheaper than a vanialla option), less collateral is required. Furthermore, asymmetry is also less significant. Therefore, it will be less computationally expensive to price Asian options using a symmetric model. When it comes to lookback options, both asymmetry and collateral are more significant when compared to the vanilla option. Hence, it is important to use a model that accounts for asymmetry when pricing lookback options.

## 9.5 Summary

In this chapter, the work by Labuschagne and Von Boetticher (2017) is extended to two different models, the symmetric GARCH(1,1) and the asymmetric AGARCH(1,1) model to price European options on the Top40 in the presence of collateral. Full collateral and zero collateral option price surfaces were approximated using the GARCH(1,1) and AGARCH(1,1) option pricing models.

The difference between the full collateral and zero collateral surfaces indicates that the

effect of collateral increases as the option price increases, this is consistent with previous findings in the literature. The difference between the GARCH(1,1) and AGARCH(1,1) surfaces indicated that asymmetry has a greater effect on the option price as the expiry increases. This is in line with expectations as there is greater probability for negative shocks as the time to expiry increases.

In order to illustrate the effect of collateral and asymmetry on options with exotic features, a similar analysis was performed using Asian and lookback option price surfaces. Collateral has a similar effect on the Asian option price surface. Furthermore the difference between the collateralised GARCH(1,1) and AGARCH(1,1) Asian option price surfaces indicates that asymmetry is not as important when pricing collateralised Asian options on the Top40. Hence, it will be more efficient to price collateralised Asian options using the GARCH(1,1) model. However, this is not the case for lookback options on the Top40. It is important to take asymmetry into account when pricing lookback options.

Interest rates in South Africa are fairly high, which implies greater differences between collateral and funding rates. Lower spreads are expected in developed markets with lower interest rates. Therefore, an important area for future research is the comparison of collateralised option pricing in other developed and emerging markets. Other areas for future research include different error distribution assumptions that incorporate skewness and kurtosis. In addition, the hedging performance of the GARCH option pricing models should be tested when applied to collateralised options. Furthermore, the application of the collateralised GARCH option pricing model should also be applied to single stocks in the South African market. Finally, the hedging performance of the collateralised GARCH option pricing model should also be tested when applied in a South African equity context.

As mentioned in the introduction, pricing after the GFC is more complicated than before. Additional factors such as collateral and credit risk need to be considered. An obvious shortcoming of this chapter is that although collateral is accounted for in the GARCH option pricing model by Labuschagne and Von Boetticher (2017), counterparty credit risk is not. Pricing of options in the presence of collateral and counterparty credit risk is considered in the next chapter.

# Chapter 10

# Pricing Collateralised Options in the Presence of Counterparty Credit Risk: An Extension of the Extended Heston-Nandi Model

## 10.1 Introduction

The pricing model (based on work by Labuschagne and Von Boetticher, 2017) applied in Chapter 9 extends the model by Duan (1995) (Black-Scholes framework) to incorporate collateral (Piterbarg framework). However, as mentioned previously, this model does not have a closed-form solution, and therefore option prices are computed numerically. As discussed, the model by Heston and Nandi (2000) is convenient because it has a closed-form solution. However the Heston-Nandi model relies on the assumption of a unique risk-free rate. Von Boetticher (2017) extended the model by Heston and Nandi (2000) to the Piterbarg (2010) framework to adress this problem.

An additional assumption required from the Black-Scholes framework is no counterparty credit risk. As a solution to this problematic assumption, Wang (2017) extended the model by Heston and Nandi (2000) to incorporate counterparty credit risk for vanilla options. This has also been extended to exotic options by Wang (2020). However, this model also assumes the existence of a risk-free rate.

In this chapter,[1] the work by Von Boetticher (2017) is extended to the pricing of collateralised options using the Heston-Nandi model in the Piterbarg framework, in the presence of counterparty credit risk. The rest of this paper is structured as follows: Section 10.2 considers the recent and relevant literature, Section 10.3 focuses on the theoretical framework and derivation of the pricing model, Section 10.4 focuses on the empirical results of a numerical example, finally in Section 10.5 the main findings are summarised.

[1] A previous version of this chapter appears as a publication (Venter and Maré, 2022) in *South African Statistical Journal*.

## 10.2 Literature review

Research focusing on the pricing of derivatives using GARCH models to model volatility is well-documented in the literature. Duan (1995) initially considered a risk-neutral pricing framework based on GARCH volatility modelling. This allowed for the pricing of derivatives with time-varying volatility in the Black and Scholes (1973) framework. A shortcoming of the model by Duan (1995) (based on a non-linear asymmetric GARCH model) is that it does not have a closed-form solution, and therefore numerical methods are required.

Heston and Nandi (2000) extended the work by Duan (1995) and derived a closed-form solution for vanilla options when volatility is modelled using a GARCH process. This model addresses the assumption of constant volatility in the Black-Scholes framework. However, it still requires the assumption of a unique risk-free rate and no credit risk; these are not necessarily realistic assumptions.

The GFC of 2008 has changed the way in which derivative instrument trades are conducted. An important factor that needs to be considered in modern pricing frameworks is the presence of collateral (Hunzinger et al., 2014). Piterbarg (2010) extended the Black-Scholes framework to the pricing of derivatives in the presence of collateral. This framework allows for three different interest rates; the discount rate is dependent on the amount of collateral that is posted. Von Boetticher (2017) extended the work by Piterbarg (2010) to incorporate the Heston-Nandi methodology to address the constant volatility assumption.

The Heston-Nandi model in the Black-Scholes framework requires the assumption of no counterparty credit risk. The GFC of 2008 has clearly shown that counterparty credit risk is an important factor to consider when pricing derivative instruments. To address this problem, Wang (2017) extended the Heston-Nandi model to incorporate counterparty credit risk. This model allows for correlation between the conditional variance of the underlying asset and the default intensity process.

Wang (2017) shows numerically that vanilla options are cheaper in the presence of counterparty credit risk. Intuitively, this makes sense because the option holder suffers losses if the counterpary defaults. This model was later extended to the pricing of executive stock options (Wang, 2018) and Asian options (Wang, 2020). However, this model still relies on a unique risk-free rate (single-curve framework), and does not take collateral into account. Therefore, this chapter contributes to the existing literature by extending the Heston-Nandi model to the pricing of derivatives in the presence of collateral and counterparty credit risk.

## 10.3 Theoretical framework

In this section, the theory applied in this paper is outlined. This section is divided into four subsections. The first focuses on the Heston-Nandi model (in the Black-Scholes framework). The second subsection briefly discusses the Piterbarg framework (Black-Scholes with collateral). Thereafter, the Heston-Nandi model with collateral is briefly

outlined. Finally, the Heston-Nandi model with collateral and counterparty credit risk is considered.

### 10.3.1 Heston-Nandi model

The main assumption of the model derived by Heston and Nandi (2000) is that the asset price dynamics under the real-world measure, $P$, are given by,

$$\ln\left(\frac{S_t}{S_{t-1}}\right) = r + \lambda h_t + \sqrt{h_t} z_t.$$

The real-world and risk-neutral conditional variance processes are outlined in Section 6.3.1. The conditional generating function of the asset price under the measure $P$ is given by,

$$f_{BS}(t,\phi) = \mathbb{E}_t^P\left[S_T^\phi\right].$$

The conditional generating function is dependent on the parameters and state variables, however, this is suppressed for notational convenience.

Heston and Nandi (2000) show that the asset price dynamics under the risk-neutral measure $Q$ in the Black-Scholes framework are given by,

$$\ln\left(\frac{S_t}{S_{t-1}}\right) = r - \frac{1}{2}h_t + \sqrt{h_t} z_t^*.$$

The risk-neutral generating function (ensures that the risk-neutral expected price at time $T > t$ is $S_t e^{r(T-t)}$) takes the following log-linear form,

$$f_{BS}^*(t,\phi) = S_t^\phi \exp\left\{A_{BS}(t,\phi) + B_{BS}(t,\phi) h_{t+1}\right\},$$

where,

$$A_{BS}(t,\phi) = \phi r + A_{BS}(t+1,\phi) + \alpha_0 B_{BS}(t+1,\phi) - \frac{1}{2}\ln\left(1 - 2\alpha_1 B_{BS}(t+1,\phi)\right) \quad (10.1)$$

$$B_{BS}(t,\phi) = \beta_1 B_{BS}(t+1,\phi) - \frac{1}{2}\delta_1^2 + \phi(\lambda + \delta_1) + \frac{(\phi - \delta_1)^2}{2\left(1 - 2\left(\alpha_1 B_{BS}(t+1,\phi)\right)\right)}. \quad (10.2)$$

These coefficients can be calculated recursively using the terminal conditions,

$$A_{BS}(T,\phi) = B_{BS}(T,\phi) = 0.$$

Heston and Nandi (2000) explain that the generating function of the spot price is the moment generating function of the logarithm of the spot price. Hence, $f_{BS}^*(t, i\phi)$ is the characteristic function of the logarithm of the spot price (where $i = \sqrt{-1}$). Using the risk-neutral dynamics, it is possible to derive a closed-form formula for a European call option. The Heston-Nandi price of a European call option is stated in Theorem 3 below:

**Theorem 3: Heston-Nandi call option in the Black-Scholes framework**

The price of a European call option at time $t$, is given by,

$$V_t = \frac{1}{2}S_t + \frac{e^{-r(T-t)}}{\pi}\int_0^\infty \text{Re}\left[\frac{K^{-i\phi}f^*_{BS}(t, i\phi+1)}{i\phi}d\phi\right] - Ke^{-r(T-t)}\left(\frac{1}{2} + \frac{1}{\pi}\int_0^\infty \text{Re}\left[\frac{K^{-i\phi}f^*_{BS}(t, i\phi)}{i\phi}d\phi\right]\right), \tag{10.3}$$

where Re$[\cdot]$ denotes the real portion of a complex number.

*Proof.* See Heston and Nandi (2000). □

### 10.3.2 The Piterbarg framework

An important assumption required for the Heston-Nandi model in the Black-Scholes framework is the existence of a unique risk-free rate. As mentioned previously, the purpose of the model derived by Piterbarg (2010) is the pricing of derivatives in the presence of collateral. The Piterbarg framework is an extension of the Black-Scholes framework, which relaxes the assumption of a unique risk-free rate.

It is assumed that collateral is posted in the form of cash. The funding rate is associated with the most risk (unsecured lending), and finally a repurchase agreement (collateralised loan) is less risky than unsecured lending; however, there is more risk associated with the underlying asset than there is with cash.

Piterbarg (2010) assumes the following asset price dynamics under the real-world measure, $P$,

$$dS_t = \mu S_t dt + \sigma S_t dW_t,$$

where again, $W_t$ is a standard Brownian Motion under $P$. In the Piterbarg framework, pricing is done under the $Q_{r_R}$ measure. As mentioned in Section 9.3.1, the Piterbarg framework incorporates three different interest rates: the collateral rate ($r_C$), the repurchase agreement rate ($r_R$), and the funding rate ($r_F$.) Hence, the dynamics under the risk-neutral measure $Q_{r_R}$ are given by,

$$dS_t = r_R S_t dt + \sigma S_t d\tilde{W}_t,$$

where $\tilde{W}_t$ is a standard Brownian Motion under $Q_{r_R}$. Using a replicating portfolio argument and an application of the Feynman-Kac theorem (see Shreve, 2004), it is possible to derive an expression for the price of a call option in the Piterbarg framework (essentially a derivation of the Black-Scholes model with different interest rates); this is given in Theorem 4 below:

**Theorem 4: Piterbarg call option**

The price of a European call option at time $t$ is given by

$$\begin{aligned} V_t =& \mathbb{E}_t^{Q_{r_R}} \left[ e^{-\int_t^T r_C(u)du} (S_T - K)^+ \right] \\ & - \mathbb{E}_t^{Q_{r_R}} \left[ \int_t^T e^{-\int_t^T r_C(u)du} (r_F(s) - r_C(s))(V(s) - \gamma_C(s))ds \right], \end{aligned}$$

where $\gamma_C$ denotes the collateral account.

*Proof.* See Piterbarg (2010). □

It is clear from the above that the price of a fully collateralised call option is given by,

$$V_t^{(FC)} = \mathbb{E}_t^{Q_{r_R}} \left[ e^{-\int_t^T r_C(u)du} (S_T - K)^+ \right], \tag{10.4}$$

and the price of a zero collateral call option is given by,

$$V_t^{(ZC)} = \mathbb{E}_t^{Q_{r_R}} \left[ e^{-\int_t^T r_F(u)du} (S_T - K)^+ \right].$$

The extended Heston-Nandi model (with collateral) is considered in the next subsection.

### 10.3.3 Heston-Nandi model with collateral

The Heston-Nandi model in the Black-Scholes framework relies on the existence of a unique risk-free rate. Therefore, Von Boetticher (2017) extended the model by Heston and Nandi (2000) to price collateralised options; this was done in the Piterbarg framework. Von Boetticher (2017) shows that the Heston-Nandi asset price dynamics under measure $Q_{r_R}$ take the following form,

$$\ln\left(\frac{S_t}{S_{t-1}}\right) = r_R - \frac{1}{2}h_t + \sqrt{h_t} z_t^*, \tag{10.5}$$

the conditional variance $h_t$ is the same as as in the Black-Scholes framework. Furthermore, the log-linear form of the risk-neutral generating function is given by,

$$f_P^*(t, \phi) = S_t^\phi \exp\left\{ A_P(t, \phi) + B_P(t, \phi) h_{t+1} \right\},$$

where,

$$\begin{aligned} A_P(t, \phi) &= \phi r_R + A_P(t+1, \phi) + \alpha_0 B_P(t+1, \phi) - \frac{1}{2}\ln\left(1 - 2\alpha_1 B_P(t+1, \phi)\right) \\ B_P(t, \phi) &= \beta_1 B_P(t+1, \phi) - \frac{1}{2}\delta_1^2 + \phi(\lambda + \delta_1) + \frac{(\phi - \delta_1)^2}{2\left(1 - 2\left(\alpha_1 B_P(t+1, \phi)\right)\right)}. \end{aligned}$$

Clearly, $A_P(t,\phi)$ and $B_P(t,\phi)$ are the same as Equations 10.1 and 10.2 respectively, the only difference is that the risk-free rate $r$ is replaced by the repurchase agreement rate $r_R$. Using the boundary conditions,

$$A_P(T,\phi) = B_P(T,\phi) = 0,$$

$A_P(t,\phi)$ and $B_P(t,\phi)$ are calculated recursively.

The Heston-Nandi price of a European call option in the Piterbarg framework is given in Theorem 5 below:

**Theorem 5: Heston-Nandi call option in the Piterbarg framework**

The Heston-Nandi price of a fully collateralised call option at time $t$ is given by,

$$V_t^{(FC)} = \frac{1}{2}\left(S(t)e^{\int_t^T (r_R(u)-r_C(u))du} - Ke^{\int_t^T r_C(u)du}\right) + \frac{K}{\pi}\tilde{\psi}(r_C),$$

where the function

$$\tilde{\psi}(r_C) = e^{-\int_t^T r_C(s)ds}\frac{e^{\int_t^T r_R(s)ds}}{K}\int_0^\infty \text{Re}\left[\frac{K^{-i\phi}f_P^*(t,i\phi+1)}{i\phi}\right]d\phi - e^{-\int_t^T r_C(s)ds}\int_0^\infty \text{Re}\left[\frac{K^{-i\phi}f_P^*(t,i\phi)}{i\phi}\right]d\phi,$$

and $f_P^*(t,\phi)$ ensures that $\mathbb{E}_t^{Q_{r_R}}[S_T] = S_t e^{r_R(T-t)}$. The price of a zero collateral call option is,

$$V_t^{(ZC)} = \frac{1}{2}\left(S(t)e^{\int_t^T (r_R(u)-r_F(u))du} - Ke^{\int_t^T r_F(u)du}\right) + \frac{K}{\pi}\tilde{\psi}(r_F).$$

*Proof.* See Von Boetticher (2017) Section 3.2. □

It is clear from the above that if $r_C = r_R = r_F = r$, the Heston-Nandi price of a call option in the Black-Scholes framework (Equation 10.3) is obtained. The use of the above model addresses the unreasonable assumption of a unique risk-free rate. However, it does not take the effect of counterparty credit risk into account; this is the focus of the next subsection.

### 10.3.4 Heston-Nandi model with collateral and counterparty credit risk

The focus of this subsection is the derivation of the Heston-Nandi price of a default risky European call option (in the presence of collateral), in the Piterbarg framework. The overall objective is to extend the model derived by Von Boetticher (2017) to incorporate counterparty credit risk by making use of an approach similar to Wang (2017).

The asset price dynamics under measure $Q_{r_R}$, are consistent with Equation 10.5. The random default time $\tilde{\tau}$ is modelled as the first jump time of a Cox process with intensity $\kappa_t$ (Wang, 2017). The following $Q_{r_R}$ dynamics are assumed for the default intensity,

$$\kappa_t = w + b\kappa_{t-1} + az_{t-1}^{(\kappa)}.$$

The mean arrival rate of default in $(t, t+1]$ is given by

$$Q_{r_R}(\tilde{\tau} > t+1|\mathcal{F}_t) = \mathbb{E}^{Q_{r_R}}\left[e^{-\kappa_t}\right] = e^{-\kappa_{t+1}}.$$

We also assume that $z_t^*$ and $z_t^{(\kappa)}$ have correlation coefficient $\rho$.

Wang (2017) explains that when pricing a default risky call option, two parts need to be considered. The first part is if no default event during the life of the trade, in this case the payoff, is equal to the payoff of a vanilla call option (full collateral or zero collateral in this case). The second part considers that a default event occurs during the life of the trade, in this case only a portion of the option value can be recovered.

By making use of Equation 10.4 and the argument above, the price of a default risky European call option, which is fully collateralised, is formulated as follows (assuming constant interest rates),

$$\begin{aligned}
\tilde{V}_t^{(FC)} &= e^{r_C(T-t)}\mathbb{E}_t^{Q_{r_R}}\left[\left(1_{\{\tilde{\tau}>T\}}\right)(S_T-K)^+\right] + \\
&\qquad \mathbb{E}_t^{Q_{r_R}}\left[\left(1_{\{t\le\tilde{\tau}\le T\}}\right)\theta e^{r_C(\tilde{\tau}-t)}\mathbb{E}_{\tilde{\tau}^{Q_{r_R}}}\left[e^{r_C(T-\tilde{\tau})}(S_T-K)^+\right]\right] \\
&= e^{r_C(T-t)}\mathbb{E}_t^{Q_{r_R}}\left[\left(1_{\{\tilde{\tau}>T\}}\right)(S_T-K)^+\right] + \theta e^{r_C(T-t)}\mathbb{E}_t^{Q_{r_R}}\left[\left(1_{\{t\le\tilde{\tau}\le T\}}\right)(S_T-K)^+\right] \\
&= e^{r_C(T-t)}\mathbb{E}_t^{Q_{r_R}}\left[\left(1_{\{\tilde{\tau}>T\}}\right)(S_T-K)^+ + \theta\left(1_{\{t\le\tilde{\tau}\le T\}}\right)(S_T-K)^+\right],
\end{aligned}$$

where $\theta$ is the recovery rate, and $1_{\{\tilde{\tau}>T\}}$ is an indicator function that takes a value of one if a default event occurs after the expiry of the option ($\tilde{\tau} > T$) and zero otherwise. The value of a zero collateral option is expressed as,

$$\tilde{V}_t^{(ZC)} = e^{r_F(T-t)}\mathbb{E}_t^{Q_{r_R}}\left[\left(1_{\{\tilde{\tau}>T\}}\right)(S_T-K)^+ + \theta\left(1_{\{t\le\tilde{\tau}\le T\}}\right)(S_T-K)^+\right].$$

It is important to note that $1_{\{t\le\tilde{\tau}\le T\}} = 1 - 1_{\{\tilde{\tau}>T\}}$. Hence, the fully collateralised price can be simplified as follows,

$$\begin{aligned}
\tilde{V}_t^{(FC)} &= e^{r_C(T-t)}\mathbb{E}_t^{Q_{r_R}}\left[\left(1_{\{\tilde{\tau}>T\}}\right)(S_T-K)^+ + \theta\left(1_{\{t\le\tilde{\tau}\le T\}}\right)(S_T-K)^+\right] \\
&= (1-\theta)e^{r_C(T-t)}\mathbb{E}_t^{Q_{r_R}}\left[\left(1_{\{\tilde{\tau}>T\}}\right)(S_T-K)^+\right] + \theta e^{r_C(T-t)}\mathbb{E}_t^{Q_{r_R}}\left[(S_T-K)^+\right] \\
&= (1-\theta)e^{r_C(T-t)}(I_1 - KI_2) + \theta e^{r_C(T-t)}(I_3 - KI_4),
\end{aligned}$$

where

$$I_1 = \mathbb{E}_t^{Q_{r_R}}\left[S_T\left(1_{\{\tilde{\tau}>T, S_T\ge K\}}\right)\right], \tag{10.6}$$

$$I_2 = \mathbb{E}_t^{Q_{r_R}}\left[\left(1_{\{\tilde{\tau}>T, S_T\ge K\}}\right)\right], \tag{10.7}$$

$$I_3 = \mathbb{E}_t^{Q_{r_R}}\left[S_T\left(1_{\{S_T\ge K\}}\right)\right], \tag{10.8}$$

$$I_4 = \mathbb{E}_t^{Q_{r_R}}\left[\left(1_{\{S_T\ge K\}}\right)\right]. \tag{10.9}$$

$I_2$ is the probability of the counterparty surviving up to time, $T$, and the option expiring in the money ($I_1$ scales this value by the expected value of the underlying price at expiry). $I_4$ is the probability of the option expiring in the money (default risk is not taken into account), $I_4$ scales this value by the expected value of the underlying price at expiry. The zero collateral price of a default risky call option takes a similar form,

$$\tilde{V}_t^{(ZC)} = (1-\theta)e^{r_F(T-t)}(I_1 - KI_2) + \theta e^{r_F(T-t)}(I_3 - KI_4).$$

Deriving closed-form expressions for Equations 10.6 to 10.9 will allow for the derivation of a closed-form expression for the Heston-Nandi price of an option in the Piterbarg framework in the presence of counterparty credit risk. Wang (2017) derived an expression for the characteristic function under the $Q$ measure. Under the $Q_{r_R}$ measure the derivation is the same, the only difference is the drift of the underlying asset is equal to $r_R$. In this case, the risk-neutral generating (log-linear) function is given by,

$$f^*_{PD}(t,\phi_1,\phi_2) = \exp\left\{\phi_1 x_t + \phi_2 \sum_{s=1}^{t}\kappa_s + A_{PD}(t,\phi_1,\phi_2)\right\} \times \exp\left\{B^{(1)}_{PD}(t,\phi_1,\phi_2)h_{t+1} + B^{(2)}_{PD}(t,\phi_1,\phi_2)\kappa_{t+1}\right\},$$

where $x_T = \ln S_T$, and

$$\begin{aligned} A_{PD}(t,\phi_1,\phi_2) &= \phi_1 r_R + A_{PD}(t+1,\phi_1,\phi_2) + \alpha_0 B^{(1)}_{PD}(t+1,\phi_1,\phi_2) \\ &\quad + wB^{(2)}_{PD}(t+1,\phi_1,\phi_2) - \frac{1}{2}\ln\left(1 - 2aB^{(2)}_{PD}(t+1,\phi_1,\phi_2)(1-\rho^2\right) \\ &\quad - \frac{1}{2}\ln\left(1 - 2\left(\alpha_1 B^{(1)}_{PD}(t+1,\phi_1,\phi_2) + \frac{aB^{(2)}_{PD}(t+1,\phi_1,\phi_2)\rho^2}{1-2aB^{(2)}_{PD}(t+1,\phi_1,\phi_2)(1-\rho^2)}\right)\right), \end{aligned}$$

$$\begin{aligned} B^{(1)}_{PD}(t,\phi_1,\phi_2) &= \beta_1 B^{(1)}_{PD}(t+1,\phi_1,\phi_2) - \frac{1}{2}\phi_1 + \alpha_1(\delta_1+\lambda)^2 + B^{(1)}_{PD}(t+1,\phi_1,\phi_2) \\ &\quad + \frac{(\phi_1 - 2\alpha_1(\delta_1+\lambda)B^{(1)}_{PD}(t+1,\phi_1,\phi_2))^2}{2\left(1 - 2\left(\alpha_1 B^{(1)}_{PD}(t+1,\phi_1,\phi_2) + \frac{aB^{(2)}_{PD}(t+1,\phi_1,\phi_2)\rho^2}{1-2aB^{(2)}_{PD}(t+1,\phi_1,\phi_2)(1-\rho^2)}\right)\right)}, \end{aligned}$$

$$B^{(2)}_{PD}(t,\phi_1,\phi_2) = bB^{(1)}_{PD}(t+1,\phi_1,\phi_2) + \phi_2,$$

with boundary conditions,

$$A_{PD}(T,\phi_1,\phi_2) = B^{(1)}_{PD}(T,\phi_1,\phi_2) = B^{(2)}_{PD}(T,\phi_1,\phi_2) = 0.$$

Given the boundary conditions, $A_{PD}(t,\phi_1,\phi_2)$, $B^{(1)}_{PD}(t,\phi_1,\phi_2)$ and $B^{(2)}_{PD}(t,\phi_1,\phi_2)$ are calculated recursively. The closed-form expression is reported in Theorem 6 below:

**Theorem 6: Heston-Nandi credit risky call option in the Piterbarg framework**

In the presence of counterparty credit risk, the price of a fully collateralised European call option is given by,

$$\begin{aligned}\tilde{V}_t^{(FC)} &= e^{r_C(T-t)}(1-\theta)\times \\ &\left(\Pi_1(t,T) + \frac{1}{2}f^*_{PD}(t,1,-1) - K\Pi_2(t,T) - \frac{1}{2}Kf^*_{PD}(t,0,-1)\right) + \\ &e^{r_C(T-t)}\theta\left(\Pi_3(t,T) + \frac{1}{2}f^*_{PD}(t,1,0) - K\Pi_4(t,T) - \frac{1}{2}K\right),\end{aligned}$$

where $f^*_{PD}(\cdot)$ is the risk-neutral characteristic function, and

$$\begin{aligned}\Pi_1(t,T) &= \frac{1}{\pi}\int_0^{-\infty} \mathrm{Re}\left[\frac{e^{i\phi_1 \ln K} f^*_{PD}(t, i\phi_1+1, -1)}{i\phi_1}\right] d\phi_1, \\ \Pi_2(t,T) &= \frac{1}{\pi}\int_0^{-\infty} \mathrm{Re}\left[\frac{e^{i\phi_1 \ln K} f^*_{PD}(t, i\phi_1, -1)}{i\phi_1}\right] d\phi_1, \\ \Pi_3(t,T) &= \frac{1}{\pi}\int_0^{-\infty} \mathrm{Re}\left[\frac{e^{i\phi_1 \ln K} f^*_{PD}(t, i\phi_1+1, 0)}{i\phi_1}\right] d\phi_1, \\ \Pi_4(t,T) &= \frac{1}{\pi}\int_0^{-\infty} \mathrm{Re}\left[\frac{e^{i\phi_1 \ln K} f^*_{PD}(t, i\phi_1, 0)}{i\phi_1}\right] d\phi_1.\end{aligned}$$

Similarly, the zero collateral price in the presence of counterparty credit risk is

$$\begin{aligned}\tilde{V}_t^{(ZC)} &= e^{r_F(T-t)}(1-\theta)\times \\ &\left(\Pi_1(t,T) + \frac{1}{2}f^*_{PD}(t,T,1,-1) - K\Pi_2(t,T) - \frac{1}{2}Kf^*_{PD}(t,T,0,-1)\right) + \\ &e^{r_C(T-t)}\theta\left(\Pi_3(t,T) + \frac{1}{2}f^*_{PD}(t,T,1,0) - K\Pi_4(t,T) - \frac{1}{2}K\right).\end{aligned}$$

*Proof.* See Appendix A □

## 10.4 Empirical results

In this study, the Heston-Nandi option pricing model in the Piterbarg framework is applied to the pricing of three-year S&P500 index call options in the presence of counterparty credit risk. Daily data from 4-Jan-2010 to 31-Jan-2021 were obtained from the Thomson-

Reuters Datastream databank. The Heston-Nandi parameters are calibrated to historical returns in the Black-Scholes framework ($r_C = r_R = r_F = r$) using the maximum likelihood method. Furthermore, for the default intensity, parameters consistent with a Ba rating for corporate bonds are assumed (consistent with Wang, 2020). According to Hull (2018), the average cumulative issuer-weighted default rate (based on 1970 to 2009) of a Ba rated bond with a three-year term is 4.492%. The risk-free rate is assumed to be equal to the three-year US treasury yield.

The parameters are outlined in Tables 10.1 and 10.2 below:

Table 10.1: Underlying process parameters

| Parameter | Value |
|---|---|
| $\lambda$ | 4.6429 |
| $\alpha_0$ | 0 |
| $\alpha_1$ | 5.28E-06 |
| $\beta_1$ | 0.7557 |
| $\delta_1$ | 183.7511 |

Table 10.2: Default intensity parameters

| Parameter | Value |
|---|---|
| $w$ | 1.54E-07 |
| $a$ | 2.60E-11 |
| $b$ | 0.9770 |

For illustrative purposes, $\rho = 0.5$. The three-year US treasury yield on 31-Jan-2020 is $r = 1.3\%$. We assume that $r_R = r$, $r_C = 1\%$ (collateralised and therefore less risky, which implies a lower rate), and $r_F = 1.6\%$ (higher rate because there is no collateral). The call option prices (relative to the spot price) assuming no default risk in a single-curve framework (Heston and Nandi, 2000), full collateral options, and zero collateral (Von Boetticher, 2017) options are plotted below (Figure 10.1). In addition, the default risky (Wang, 2017, for the single-curve case) prices are also included. Moneyness is defined as the spot price over the strike price.

Figure 10.1: S&P500 index option prices

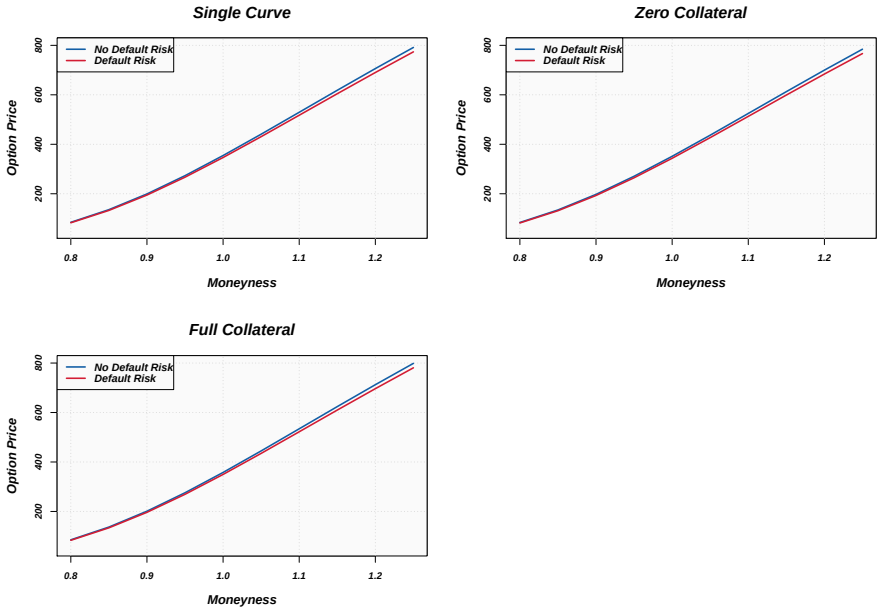


It is clear from the above that default risky options are cheaper than options that are not default risky. This is consistent with expectations (if a default occurs, the payoff is less than that of a vanilla option). Furthermore, fully collateralised options are more expensive (less risk) when compared to zero collateral options. To illustrate the effect of correlation, at-the-money (ATM) option prices assuming different correlation values are illustrated in Figure 10.2 below.

Figure 10.2: Effect of correlation

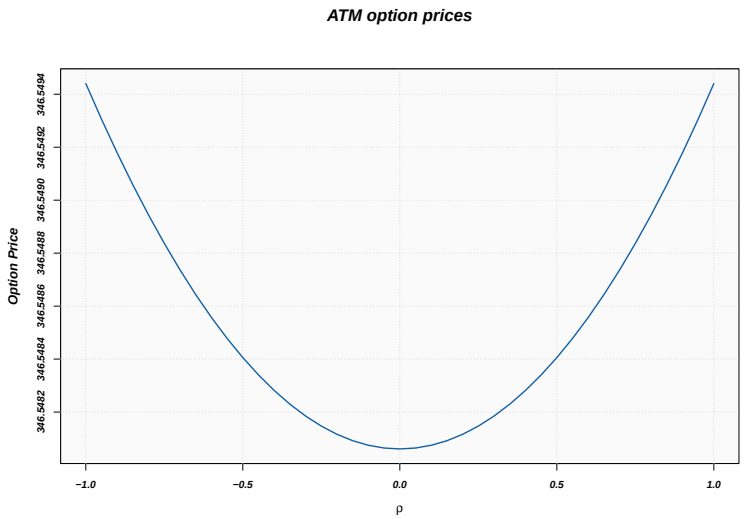

It is clear from the above that the correlation between the underlying volatility process and default intensity does not have a significant impact on ATM option prices using the parameters outlined above.

## 10.5 Summary

In this chapter, a closed-form expression for the Heston-Nandi price of a collateralised European call option in the presence of counterparty credit risk was derived. This is an extension of the work by Von Boetticher (2017), who derived an expression for the Heston-Nandi price of a collateralised European call option in the absence of counterparty credit risk in the Piterbarg framework. Using an approach similar to Wang (2017), the work by Von Boetticher (2017) is extended to incorporate counterparty credit risk.

As a numerical example, the model was applied to three-year S&P500 index options. The underlying process parameters were calibrated in a single-curve framework, assuming no default risk. The assumed default risk parameters are consistent with a Ba rated corporate bond. The prices obtained are consistent with expectations, default risky bonds are cheaper than options with no counterparty credit risk, and fully collateralised options are more expensive when compared to zero collateral options. The effect of correlation is tested by plotting the default risky ATM option price for different levels of correlation. The results indicate that correlation has an insignificant impact when pricing using the calibrated parameters.

# Chapter 11

# Conclusion

When it comes to the modelling of financial assets, a reliable estimate of the asset's volatility (synonymous with the risk associated with the asset) is required. A reliable estimate of volatility is not always available, especially in illiquid markets or for assets that do not have a well-established derivatives market. This problem serves as a basis for the various analyses performed in this thesis.

The GFC has changed financial markets permanently and therefore additional factors need to be considered. The extension of simpler models to account for additional factors is also an important contribution. As outlined in Chapter 1, the following research questions were considered:

1. *Can volatility indices be used to obtain more accurate GARCH option pricing models when applied to the South African market, and can this be extended to different asset classes?*

2. *Does the GARCH option pricing model produce reasonable price discovery when applied to a new asset class, can it be used to construct a reasonable volatility index, and can the model be used for the pricing of multivariate options?*

3. *Which GARCH model and error distributional assumption is most reliable when pricing volatility index options, and does GARCH outperform classical methods when applied to hedging volatility index options?*

4. *What is the effect of collateral and asymmetry on vanilla and exotic options in a GARCH option pricing framework, and can the GARCH option pricing framework be extended to account for collateral and counterparty credit risk?*

Chapter 2 contributes to the literature by extending the analysis by Hao and Zhang (2013) to the South African market to determine which GARCH model is the most appropriate when modelling the SAVI. The information criteria showed that asymmetry is an important factor to consider when modelling Top40 returns; this is consistent with previous findings in the literature. In most cases, the joint likelihood function based on historical returns and historical SAVI produced the most reliable results. This is consistent

with the argument by Christoffersen et al. (2013), the joint likelihood based on historical returns and option prices (SAVI in this case) ensures that the asset is consistent with historical dynamics, and also the market's expectation of the future.

Chapter 2 also contributes to the literature by extending the work by Hao and Zhang (2013) to the testing of the pricing performance of the models calibrated to the volatility index. Our empirical results indicated that the use of asymmetric GARCH option pricing models improves the model performance in the South African equity market. However, the improvement is marginal. The use of a symmetric model will be computationally more efficient. Chapter 2 adresses the first part of Research Question 1.

The novelty of Chapter 3 is that it extends the concept of a GARCH-implied volatility index to the FX market (to address the second part of Research Question 1). Furthermore, the FX variance risk premium is also considered. The analysis was applied to both a developed (United States) and an emerging market (South Africa). As expected, the ZAR is the more volatile of the two currencies. The joint likelihood function (based on returns and the historical volatility index) is the most reliable when modelling the GARCH-implied SAVI Dollar. However, the likelihood function based on the historical volatility index only is the most reliable for the Euro VIX. For both currencies, asymmetry is an important factor that needs to be considered. An obvious shortcoming of Chapters 2 and 3 is reliance on the normal distribution. An area for future research is the GARCH-implied SAVI and SAVI Dollar based on different GARCH models and error distributions that take skewness and kurtosis into account.

Cryptocurrencies are the focus of Part II. Reliable models for price discovery are essential when a new asset class (to address the first part of Research Question 2) is introduced (the absence of an established derivatives market). According to Chu et al. (2017), most studies focusing on cryptocurrencies focus on BTC only, and therefore both BTC and CRIX are considered to give a holistic view of the cryptocurrency market. The empirical analysis applied in Chapter 4 is a novel approach to cryptocurrency volatility modelling (based on option price surfaces). The results showed that asymmetry does not make a significant difference when pricing cryptocurrency options. This is consistent with previous findings in the literature.

In addition to price discovery in an illiquid market, the absence of a volatility index is an important problem when dealing with a new asset class (second part of Research Question 2). The novelty of Chapter 5 is that it is the first application of the GARCH option pricing model to the construction of a cryptocurrency volatility index. Different maturities are considered to get an indication of the term structure of volatility (based on the work by Alexander and Imeraj, 2019). The empirical results show that the term structure of volatilities are consistent with expectations, with 30-day volatility being lower when compared to longer maturities. Previous findings in the literature have shown that jumps are often found in crypto-asset prices. An important area for future research is a crypto volatility index based on a GARCH option pricing model that incorporates jumps.

Chapter 6 considered the pricing of BTC futures options using the Heston-Nandi (symmetric and asymmetric) futures model (based on the work by Li, 2019a) to get an indication of pricing performance. Chapter 6 also makes a theoretical contribution by deriving the

risk-neutral futures price processes for a general class of multivariate heteroskedasticity models. This is relevant in the current market environment, as crypto-asset futures are exposed to significant basis risk (Alexander and Heck, 2020). This is applied to BTC futures spread options. The empirical results showed that a symmetric model is a better fit when applied to BTC futures returns (consistent with the findings of previous chapters), and also produces more accurate option prices compared to market prices. BTC futures spread options do not actively trade and therefore the model prices obtained could not be compared to market prices. Chapter 6 addresses the third (and final) part of Research Question 2.

Part III of this thesis considers the case where the volatility index is the underlying asset. Volatility indices do not actively trade. However, futures on volatility indices often do trade. Chapters 7 and 8 model the VIX futures price in a GARCH framework for option pricing and hedging. The empirical results in Chapter 7 showed that the symmetric GARCH model with skewed Student-$t$ errors is the best performing model, and that the GARCH option pricing model provides reasonable price discovery when applied to the VIX. The novelty of Chapter 8 is that it is the first application of the Heston-Nandi futures model the to the hedging of VIX options (using VIX futures). The analysis is based on the work by Lassance and Vrins (2018). Empirical results indicate that the Heston-Nandi model is more reliable when applied to the hedging of VIX futures options. The Heston-Nandi model better explains the dynamics (leptokurtosis and volatility clustering often found in financial time series) of VIX futures. An important shortcoming of Part III is that it focuses on VIX futures and options markets, which is a liquid and well-established market. An area for future research is the GARCH option pricing model applied to the pricing and hedging of emerging market volatility index options. Chapters 7 and 8 address Research Question 3.

GARCH option pricing in a more modern derivatives pricing framework was considered in Part IV. The work by Labuschagne and Von Boetticher (2017) was extended to different GARCH processes and exotic options in Chapter 9 to illustrate the effect of collateral and asymmetry on options written on the Top40. Empirical results showed that when it comes to vanilla options, the effect of collateral increases as the option price increases, this is consistent with previous findings in the literature. Furthermore, asymmetry has a greater effect on the option price as the expiry increases. This is consistent with expectations as there is greater probability for negative shocks as the time to expiry increases. The effect of collateral is similar when exotic options are considered. Finally, asymmetry is important when pricing lookback options, but not as significant when pricing Asian options (a symmetric model should be used when computational efficiency is a concern). Chapter 9 addresses the first part of Research Question 4.

The focus of Chapter 10 is the second part of Research Question 4. Chapter 10 makes a theoretical contribution by extending the model by Heston and Nandi (2000) to include collateral (based on the work by Von Boetticher, 2017) and counterparty credit risk (based on the work by Wang, 2017). As a numerical example, the model is applied to S&P500 index options. The prices obtained were consistent with expectations. Furthermore, the results showed that correlation does not have a significant impact on ATM option prices.

Areas for future research include the application of the model to different underlying assets (*e.g.,* emerging markets), exotic options (*e.g.,* geometric Asian options), and different bond process assumptions (we assumed a Ba rated corporate bond).

# Bibliography

Abboud, H., 2017. H/Rindex: The Hashing Power and Robustness Index, Computational Power-weighted Benchmark for Global Blockchain and Crypto Market.

Abraham, R., 2020. The role of investor sentiment in the valuation of bitcoin and bitcoin derivatives. *International Journal of Financial Markets and Derivatives, 7(3),* pp. 203-223.

Agyarko, K., Buabeng, A. and Acquah, J., 2019. Modelling the Volatility of the Price of Bitcoin. *American Journal of Mathematics and Statistics, 9(4),* pp. 151-159.

Ahmad, M.H. and Ping, P.Y., 2014. Modelling Malaysian gold using symmetric and asymmetric GARCH models. *Applied Mathematical Sciences, 8(17),* pp. 817-822.

Alexander, C., 2008. *Market Risk Analysis, Practical Financial Econometrics (Vol. 2).* John Wiley & Sons.

Alexander, C. and Heck, D.F., 2020. Price discovery in Bitcoin: The impact of unregulated markets. *Journal of Financial Stability, 50,* 100776.

Alexander, C. and Imeraj, A., 2019, Introducing the BITIX: The Bitcoin Fear Gauge. *Available at SSRN 3383734.*

Alexander, C. Kapraun, J. and Korovilas, D. 2015. Trading and investing in volatility products. *Financial Markets, Institutions & Instruments, 24(4),* pp. 313-347.

Alexander, C. and Nogueira, L.M., 2004. Hedging with stochastic local volatility.

Antonopoulos, A.M., 2014. *Mastering Bitcoin: Unlocking Digital Cryptocurrencies.* O'Reilly Media, Inc.

Asteriou, D. and Hall, S.G., 2015. *Applied Econometrics.* Macmillan International Higher Education.

Azzalini, A. and Salehi, M., 2020. Some computational aspects of maximum likelihood estimation of the skew-t distribution. *In Computational and Methodological Statistics and Biostatistics (pp. 3-28).* Springer, Cham.

Bank for International Settlements, Triennial Central Bank Survey, Global foreign exchange market turnover in 2019.

Barnes, P., 2018. Crypto Currency and its Susceptibility to Speculative Bubbles, Manipulation, Scams and Fraud. *Journal of Advanced Studies in Finance, 9(2),* pp. 60-77.

Baruník, J. Kočenda, E. and Vácha, L. 2017. Asymmetric volatility connectedness on the forex market. *Journal of International Money and Finance, 77*, pp. 39-56.

Baur, D.G. and Dimpfl, T., 2018. Asymmetric volatility in cryptocurrencies. *Economics Letters,* 173, pp. 148-151.

Baur, D.G. and Lucey, B.M., 2010. Is gold a hedge or a safe haven? An analysis of stocks, bonds and gold. *Financial Review, 45(2),* pp. 217-229.

Bharadwaj, V., 2021. Growing Crypto Derivatives Market in India and the Government Regulations around it. *European Journal of Molecular & Clinical Medicine, 7(10),* pp. 3708-3715.

Bhat, A. and Arekar, K. 2016. Empirical performance of Black-Scholes and GARCH option pricing models during turbulent times: the Indian evidence. *International Journal of Economics and Finance, 8(3),* pp. 123-136.

Black, F., 1976. The pricing of commodity contracts. *Journal of Financial Economics, 3(1-2),* pp. 167-179.

Black, F. and Scholes, M., 1973. The pricing of options and corporate liabilities. *Journal of Political Economy, 81(3),* pp. 637-654.

Böhme, R., Christin, N., Edelman, B. and Moore, T., 2015. Bitcoin: Economics, technology, and governance. *Journal of Economic Perspectives, 29(2),* pp. 213-38.

Bollerslev, T., 1986, Generalized autoregressive conditional heteroskedasticity. *Journal of econometrics*, 31(3), pp. 307-327.

Bollerslev, T., Marrone, J., Xu, L. and Zhou, H., 2014. Stock return predictability and variance risk premia: statistical inference and international evidence. *Journal of Financial and Quantitative Analysis,* pp. 633-661.

Bouri, E., Gupta, R., Tiwari, A.K. and Roubaud, D., 2017, Does Bitcoin hedge global uncertainty? Evidence from wavelet-based quantile-in-quantile regressions. *Finance Research Letters, 23*, pp. 87-95.

Brooks, C., 2014, *Introductory Econometrics for Finance.* Cambridge university press.

Cao, H., Badescu, A., Cui, Z. and Jayaraman, S., 2020. Valuation of VIX and Target Volatility Options with Affine GARCH Models.

Carr, P. and Lee, R., 2007. Realized volatility and variance: Options via swaps. *Risk, 20(5),* pp. 76-83.

Carr, P. and Wu, L. 2009. Variance risk premiums. *The Review of Financial Studies, 22(3),* pp. 1311-1341.

Chen, S., Chen, C.Y.H., Härdle, W.K., Lee, T.M. and Ong, B., 2018. Econometric analysis of a cryptocurrency index for portfolio investment. *In Handbook of Blockchain, Digital Finance, and Inclusion,* 1 pp. 175-206. Academic Press.

Chen, Y. and So, L.C., 2020. New Insights from the Bitcoin Futures Market. *Modern Economy, 11(08),* pp. 1463.

Christoffersen, P. and Jacobs, K., 2004. Which GARCH model for option valuation? *Management science, 50(9),* pp. 1204-1221.

Christoffersen, P., Heston, S. and Jacobs, K., 2006. Option valuation with conditional skewness. *Journal of Econometrics, 131(1-2),* pp. 253-284.

Christoffersen, P., Jacobs, K. and Ornthanalai, C., 2013. GARCH option valuation: theory and evidence. *The Journal of Derivatives, 21(2),* pp. 8-41.

Chu, J., Chan, S., Nadarajah, S. and Osterrieder, J., (2017). GARCH modelling of cryptocurrencies. *Journal of Risk and Financial Management, 10(4),* p. 17.

Clark, I.J., 2014. *Commodity Option Pricing: A Practitioner's Guide.* John Wiley & Sons.

Conrad, C., Custovic, A. and Ghysels, E., (2018). Long-and short-term cryptocurrency volatility components: A GARCH-MIDAS analysis. *Journal of Risk and Financial Management,* 11(2), p. 23.

Cont, R., 2001. Empirical properties of asset returns: stylized facts and statistical issues. *Quantitative Finance,* pp. 223-236.

Danielsson, J., 2011 *Financial Risk Forecasting: The Theory and Practice of Forecasting Market Risk With Implementation in R and Matlab.* John Wiley & Sons.

Della Corte, P. Ramadorai, T. and Sarno, L. 2016. Volatility risk premia and exchange rate predictability. *Journal of Financial Economics, 120(1)*, pp. 21-40.

Detemple, J. and Osakwe, C., 2000. The valuation of volatility options. *Review of Finance, 4(1),* pp. 21-50.

Diebold, F.X., Mariano, R. 1995. Comparing predictive accuracy. *Journal of Business and Economic Statistics, 13,* pp. 253–265

Dimitriou, D. and Kenourgios, D. 2013. Financial crises and dynamic linkages among international currencies. *Journal of International Financial Markets, Institutions and Money, 26,* pp. 319-332.

Duan, J.C., 1995. The GARCH option pricing model. *Mathematical Finance, 5(1),* pp. 13-32.

Duan, J.C. and Pliska, S.R., 2004. Option valuation with co-integrated asset prices. *Journal of Economic Dynamics and Control, 28(4),* pp. 727-754.

Duan, J.C. and Wei, J.Z. 1997. Pricing Foreign Currency and Cross-Currency Options under GARCH. *The Journal of Derivatives, 7(1),* pp. 51-63.

Duncan, A.S. and Liu, G.D., 2009. Modelling South African currency crises as structural changes in the volatility of the rand. *South African Journal of Economics, 77(3),* pp. 363-379.

Dyhrberg, A.H., (2016). Bitcoin, gold and the dollar - A GARCH volatility analysis. *Economic Letters, 16,* pp. 85-92.

Elendner, H., Trimborn, S., Ong, B. and Lee, T.M., 2018. The cross-section of crypto-currencies as financial assets: Investing in crypto-currencies beyond bitcoin. In *Handbook of Blockchain, Digital Finance, and Inclusion, Volume 1 (pp. 145-173).* Academic Press.

Engle, R., 2002. Dynamic conditional correlation: A simple class of multivariate generalized autoregressive conditional heteroskedasticity models. *Journal of Business & Economic Statistics, 20(3),* pp. 339-350.

Fang, L., Bouri, E., Gupta, R. and Roubaud, D., 2019. Does global economic uncertainty matter for the volatility and hedging effectiveness of Bitcoin? *International Review of Financial Analysis, 61,* pp. 29-36.

Fassas, A.P. and Papadamou, S. 2018. Variance risk premium and equity returns. *Research in International Business and Finance, 46,* pp. 462-470.

Fassas, A.P., Papadamou, S. and Koulis, A., 2020. Price discovery in bitcoin futures. *Research in International Business and Finance, 52,* 101116.

Fernandes, M., Medeiros, M.C. and Scharth, M., 2014, Modeling and predicting the CBOE market volatility index. *Journal of Banking & Finance, 40,* pp. 1-10.

Flint, E. and Maré, E., 2017. Estimating option-implied distributions in illiquid markets and implementing the Ross recovery theorem. *South African Actuarial Journal, 17(1),* pp. 1-28.

Flint, E.J., Ochse, E.R. and Polakow, D.A., 2014. Estimating long-term volatility parameters for market-consistent models. *South African Actuarial Journal, 14(1),* pp. 19-72.

Francq, C. and Zakoian, J.M., 2019. *GARCH Models: Structure, Statistical Inference and Financial Applications.* John Wiley & Sons.

Fukasawa, M., Horvath, B. and Tankov, P., 2021. Hedging under rough volatility. *arXiv preprint arXiv:2105.04073.*

Glasserman, P., 2013. *Monte Carlo Methods in Financial Engineering.* Springer Science & Business Media.

Glosten, L.R., Jagannathan, R. and Runkle, D.E., 1993. On the relation between the expected value and the volatility of the nominal excess return on stocks. *The Journal of Finance, 48(5),* pp. 1779-1801.

Grünbichler, Andreas. and Longstaff, Francis A., 1996. Valuing futures and options on volatility. *Journal of Banking & Finance, 20(6),* pp. 985-1001.

Gyamerah, S.A., 2019. Modelling the volatility of Bitcoin returns using GARCH models. *Quantitative Finance and Economics, 3(4),* p.739.

Hafner, C.M., 2020. Testing for bubbles in cryptocurrencies with time-varying volatility. *Journal of Financial Econometrics, 18(2),* pp. 233-249.

Hansen, P.R. and Lunde, A., 2005. A forecast comparison of volatility models: does anything beat a GARCH (1, 1)? *Journal of Applied Econometrics, 20(7),* pp. 873-889.

Hao, J. and Zhang, J.E., 2013. GARCH option pricing models, the CBOE VIX, and variance risk premium. *Journal of Financial Econometrics, 11(3),* pp. 556-580.

Held, L. and Sabanés Bové, D., 2014. *Applied Statistical Inference.* Springer, Berlin Heidelberg.

Heston, S.L., 1993. A closed-form solution for options with stochastic volatility with applications to bond and currency options. *The Review of Financial Studies, 6(2),* pp. 327-343.

Heston, S.L. and Nandi, S., 2000. A closed-form GARCH option valuation model. *The Review of Financial Studies, 13(3),* pp. 585-625.

Hou, A.J., Wang, W., Chen, C.Y.H. and Härdle, W.K., (2018). Pricing cryptocurrency options: The case of bitcoin and CRIX. *Available at SSRN 3159130.*

Hsieh, K.C. and Ritchken, P., 2005. An empirical comparison of GARCH option pricing models. *Review of Derivatives Research, 8(3),* pp. 129-150.

Huang, Hung-Hsi., Lin, Shin-Hung. and Wang, Chiu-Ping., 2019. Reasonable evaluation of VIX options for the Taiwan stock index. *The North American Journal of Economics and Finance, 48,* pp. 111-130.

Huang, Zhou., Tong, Chen. and Wang, Tianyi., 2019. VIX term structure and VIX futures pricing with realized volatility. *Journal of Futures Markets, 39(1),* pp. 72-93.

Hull, J., 2017. *Risk Management and Financial Institutions,* 5th edition. John Wiley & Sons.

Hunzinger, C.B., Labuschagne, C.C. and von Boetticher, S.T., 2014. Volatility skews of indexes of BRICS securities exchanges. *Procedia Economics and Finance, 14,* pp. 263-272.

Huskaj, B. and Larsson, K., 2016. An empirical study of the dynamics of implied volatility indices: international evidence. *Quantitative Finance Letters, 4(1),* pp. 77-85.

Jalan, A., Matkovskyy, R. and Aziz, S., 2020. The Bitcoin options market: A first look at pricing and risk. *Applied Economics,* pp. 1-16.

Jeon, J., Yoon, J.H. and Kang, M., 2016. Valuing vulnerable geometric Asian options. *Computers & Mathematics with Applications, 71(2)*, pp. 676-691.

Jing, Bo., Li, Sheng-hong. and Tan, Xiao-yu, 2020. Pricing VIX options with stochastic skew and asymmetric jumps. *Applied Mathematics-A Journal of Chinese Universities, 35(1),* pp. 33-56.

Kanniainen, J. Lin, B. and Yang, H. 2014. Estimating and using GARCH models with VIX data for option valuation. *Journal of Banking & Finance, 43,* pp. 200-211.

Karkkainen, T., 2018. Price Discovery in the Bitcoin Futures and Cash Markets. *Available at SSRN 3243969.*

Kathiravan, C., Selvam, M., Maniam, B., Venkateswar, S., Gayathri, J. and Pavithran, A., 2019. Effect of Weather on Cryptocurrency Index: Evidences from Coinbase Index. *International Journal of Financial Research, 10(4).*

Katsiampa, P., (2017). Volatility estimation for Bitcoin: A comparison of GARCH models. *Economics Letters, 158,* pp. 3-6.

Kendall, M. and Stuart, A., 1977. *The Advanced Theory of Statistics. Vol. 1: Distribution Theory.* London: Griffin.

Kim, A., Trimborn, S. and Härdle, W.K., 2019. VCRIX-A Volatility Index for Crypto-Currencies. *Available at SSRN 3480348.*

Klein, T., Thu, H.P. and Walther, T., 2018. Bitcoin is not the New Gold–A comparison of volatility, correlation, and portfolio performance. *International Review of Financial Analysis, 59,* pp. 105-116.

Kolesnikova, A., 2018 CRIX-volatility index for crypto-currencies on the basis of CRIX, (Master's thesis, Humboldt-Universität zu Berlin).

Kotzé, A., Joseph, A. and Oosthuizen, R., 2009. The new South-African Volatility Index: New SAVI. *Available at SSRN 2198359.*

Kuen Siu, T., Nawar, R. and Ewald, C.O., 2014. Hedging crude oil derivatives in GARCH-type models. *Journal of Energy Markets, 7(1).*

Kurihara, Y. and Fukushima, A., (2018). How Does Price of Bitcoin Volatility Change? *International Research in Economics and Finance, 2(1),* p. 8.

Lassance, N. and Vrins, F., 2018. A comparison of pricing and hedging performances of equity derivatives models. *Applied Economics, 50(10),* pp. 1122-1137.

Li, Bingxin. 2019 Option-implied filtering: evidence from the GARCH option pricing model. *Review of Quantitative Finance and Accounting,* 1-21.

Li, B., 2019. Pricing dynamics of natural gas futures. *Energy Economics, 78,* pp. 91-108.

Lin, Yueh-Neng. and Chang, Chien-Hung., 2009. VIX option pricing. *Journal of Futures Markets: Futures, Options, and Other Derivative Products,* 29(6), pp. 523-543.

Liu, Q., Guo, S. and Qiao, G., 2015. VIX forecasting and variance risk premium: A new GARCH approach. *The North American Journal of Economics and Finance, 34,* pp. 314-322.

Leong, K. and Sung, A., 2018. FinTech (Financial Technology): what is it and how to use technologies to create business value in fintech way? *International Journal of Innovation, Management and Technology,* 9(2), pp. 74-78.

Leong K., Sung A. and Teissier C. (2020) *Financial Technology for Sustainable Development. In: Leal Filho W., Azul A., Brandli L., Özuyar P., Wall T. (eds) Partnerships for the Goals. Encyclopedia of the UN Sustainable Development Goals.* Springer, Cham

Labuschagne, C.C. and von Boetticher, S.T., 2017, January. The GJR-GARCH and EGARCH option pricing models which incorporate the Piterbarg methodology. *In 2017 International Conference on Economics, Finance and Statistics (ICEFS 2017).* Atlantis Press.

Levendis, A. and Venter, P., 2019. Implementation of local volatility in Piterbarg's framework. In *International Conference on Applied Economics* (pp. 507-521). Springer, Cham.

Luo, Xingguo., Zhang, Jin E. and Zhang, Wenjun., 2019. Instantaneous squared VIX and VIX derivatives. *Journal of Futures Markets, 39(10),* pp. 1193-1213.

Madan, D.B., Reyners, S. and Schoutens, W., (2019). Advanced model calibration on bitcoin options. *Digital Finance, 1(1-4),* pp. 117-137.

Mahringer, S. and Prokopczuk, M., 2015. An empirical model comparison for valuing crack spread options. *Energy Economics, 51,* pp. 177-187.

Majewski, Adam A., Bormetti, Giacomo. and Corsi, Fulvio., 2015. Smile from the past: A general option pricing framework with multiple volatility and leverage components. *Journal of Econometrics, 187(2),* pp. 521-531.

Maré, E., 2009. How does traditional option hedging perform in the South African equity market? *Investment Analysts Journal, 38(70),* pp. 27-31.

McAleer, M. and Hafner, C.M., 2014. A one line derivation of EGARCH. *Econometrics, 2(2),* pp. 92-97.

McNeil, A.J., Frey, R. and Embrechts, P., 2015. *Quantitative Risk Management: Concepts, Techniques and Tools (Revised Edition).* Princeton university press.

Meddahi, N. and Renault, E., 2004. Temporal aggregation of volatility models. *Journal of Econometrics, 119(2),* pp. 355-379.

Oberholzer, N. and Venter, P., 2015. Univariate GARCH models applied to the JSE/FTSE stock indices. *Procedia Economics and Finance, 24,* pp. 491-500.

Oberholzer, N. and Venter, P.J., 2019. Heston Nandi Option Pricing Model Applied to the CIVETS indices. *In International Conference on Applied Economics (pp. 593-603).* Springer, Cham.

Pagnottoni, P., (2020). Neural Network Models for Bitcoin Option Pricing. Front. *AI and Financial Technology, 2(5).*

Peng, Y., Albuquerque, P.H.M., de Sá, J.M.C., Padula, A.J.A. and Montenegro, M.R., 2018. The best of two worlds: Forecasting high frequency volatility for cryptocurrencies and traditional currencies with Support Vector Regression. *Expert Systems with Applications, 97,* pp. 177-192.

Piterbarg, V., 2010. Funding beyond discounting: collateral agreements and derivatives pricing. *Risk, 23(2),* p.97.

Plakandaras, V., Bouri, E. and Gupta, R., 2021. Forecasting Bitcoin Returns: Is there a Role for the US–China Trade War? *Journal of Risk, 23(3).*

Psychoyios, Dimitris., Dotsis, George. and Markellos, Raphael N., 2010. A jump diffusion model for VIX volatility options and futures. *Review of Quantitative Finance and Accounting, 35(3),* pp. 245-269.

Rhoads, Russel., 2011. *Trading VIX Derivatives: Trading and Hedging Strategies Using VIX Futures, Options, and Exchange-traded Notes.* John Wiley & Sons.

Rombouts, J.V. and Stentoft, L., 2011. Multivariate option pricing with time varying volatility and correlations. *Journal of Banking & Finance, 35(9),* pp. 2267-2281.

Sebastião, H. and Godinho, P., 2019. Bitcoin futures: An effective tool for hedging cryptocurrencies. *Finance Research Letters.*

Shahzad, S.J.H., Bouri, E., Roubaud, D., Kristoufek, L. and Lucey, B., 2019. Is Bitcoin a better safe-haven investment than gold and commodities? *International Review of Financial Analysis, 63,* pp. 322-330.

Shi, S. and Shi, Y., 2019. Bitcoin futures: trade it or ban it? *The European Journal of Finance,* pp. 1-16.

Shreve, S.E., 2004. *Stochastic Calculus for Finance II: Continuous-Time Models.* Springer Science & Business Media.

Siu, T.K. and Elliott, R.J., 2021. Bitcoin option pricing with a SETAR-GARCH model. *The European Journal of Finance, 27(6),* pp. 564-595.

Soczo, C., 2003. Estimation of future volatility. *Periodica Polytechnica Social and Management Sciences, 11(2),* pp. 201-214.

Trimborn, S. and Härdle, W.K., (2018). CRIX an Index for cryptocurrencies. *Journal of Empirical Finance, 49,* pp. 107-122.

Venter, P.J. and Maré, E., 2020. GARCH Generated Volatility Indices of Bitcoin and CRIX. *Journal of Risk and Financial Management, 13(6),* p.121.

Venter, P.J. and Maré, E., 2020. GARCH option pricing models in a South African equity context. *ORiON, 36(1),* pp. 1-17.

Venter, P.J. and Maré, E., 2021. GARCH option pricing and implied FX volatility indices. *Studies in Economics and Econometrics,* pp. 1-11.

Venter, P.J. and Maré, E., 2021. Price discovery in the volatility index option market: A univariate GARCH approach. *Finance Research Letters,* 102069.

Venter, P.J. and Maré, E., 2021. Univariate and Multivariate GARCH Models Applied to Bitcoin Futures Option Pricing. *Journal of Risk and Financial Management, 14(6),* p.261.

Venter, P.J. and Maré, E., 2022. Pricing collateralised options in the presence of counterparty credit risk: An extension of the Heston–Nandi model. *South African Statistical Journal, 56(1),* pp.37-51.

Venter, P.J., Maré, E. and Pindza, E., 2020. Price discovery in the cryptocurrency option market: A univariate GARCH approach. *Cogent Economics & Finance, 8(1),* 1803524.

Von Boetticher, S.T., 2017. The Piterbarg framework for option pricing (Doctoral dissertation, University of Johannesburg).

Wang, X., 2017. Analytical valuation of vulnerable options in a discrete-time framework. *Probability in the Engineering and Informational Sciences, 31(1),* pp. 100-120.

Wang, X., 2020. Valuation of Asian options with default risk under GARCH models. *International Review of Economics & Finance, 70,* pp. 27-40.

Wang, X., 2018. Valuing executive stock options under correlated employment shocks. *Finance Research Letters, 27,* pp. 38-45.

Wang, Tianyi., Shen, Yiwen., Jiang, Yueting. and Huang, Zhuo., 2017. Pricing the CBOE VIX futures with the Heston–Nandi GARCH model. *Journal of Futures Markets, 37(7),* pp. 641-659.

Wang, Zhiguang., and Daigler, R.T., 2011. The performance of VIX option pricing models: empirical evidence beyond simulation. *Journal of Futures Markets, 31(3),* pp. 251-281.

Whaley, Robert E., 1993. Derivatives on market volatility: Hedging tools long overdue. *The Journal of Derivatives, 1(1),* pp. 71-84.

Wilmott, P., 2007. *Paul Wilmott introduces quantitative finance.* John Wiley & Sons.

Zhang, J.E. and Zhu, Y., 2006. VIX futures. *Journal of Futures Markets: Futures, Options, and Other Derivative Products, 26(6),* pp. 521-531.

Zhu, Song-Ping., and Lian, Guang-Hua., 2012. An analytical formula for VIX futures and its applications. *Journal of Futures Markets, 32(2),* pp. 166-190.

# Appendix A

# Proof of Theorem 6

The proof of Theorem 6 is outlined below. The proof follows Wang (2017) closely. However, Wang (2017) derived expressions for the required probabilities in the Black-Scholes framework (measure $Q$). This relies on the existence of a unique risk-free rate. To extend the model to the Piterbarg framework (multiple interest rates to account for the presence of collateral), it is necessary to derive expressions for the probabilities under the $Q_{r_R}$ measure.

*Proof.* To evaluate the integral $I_1$, it is necessary to define a new probability measure,

$$Q_{r_R}^{(1)}(y) = \frac{\mathbb{E}_t^{Q_{r_R}}\left[\left(1_{\{y\}}\right) S_T\left(1_{\{\tilde{\tau}>T\}}\right)\right]}{\mathbb{E}_t^{Q_{r_R}}\left[S_T\left(1_{\{\tilde{\tau}>T\}}\right)\right]},$$

for any event $y \in \mathcal{F}_T$. The characteristic function of $x_T$ under $Q_{r_R}^{(1)}$ is given by,

$$\begin{aligned}
f^{(1)}(t, i\phi_1) &= \mathbb{E}_t^{Q_{r_R}^{(1)}}\left[e^{i\phi_1 x_T}\right] \\
&= \frac{\mathbb{E}_t^{Q_{r_R}}\left[e^{i\phi_1 x_T} S_T\left(1_{\{\tilde{\tau}>T\}}\right)\right]}{\mathbb{E}_t^{Q_{r_R}}\left[S_T\left(1_{\{\tilde{\tau}>T\}}\right)\right]} \\
&= \frac{\mathbb{E}_t^{Q_{r_R}}\left[e^{(i\phi_1+1)x_T}\left(1_{\{\tilde{\tau}>T\}}\right)\right]}{\mathbb{E}_t^{Q_{r_R}}\left[S_T\left(1_{\{\tilde{\tau}>T\}}\right)\right]} \\
&= \frac{\mathbb{E}_t^{Q_{r_R}}\left[e^{(i\phi_1+1)x_T} e^{-\sum_{s=t}^{T}\kappa_s}\right]}{\mathbb{E}_t^{Q_{r_R}}\left[e^{x_T-\sum_{s=t}^{T}\kappa_s}\right]} \\
&= \frac{f_{PD}^*(t, i\phi_1+1, -1)}{f_{PD}^*(t, 1, -1)}
\end{aligned}$$

In this case, standard probability theory applies (Kendall and Stuart, 1977), the distribu-

tion function corresponding to $f^{(1)}$ is given by,

$$F^{(1)}(x_T;x) = \frac{1}{2} - \frac{1}{\pi}\int_0^{-\infty} \mathrm{Re}\left[\frac{e^{i\phi_1 x} f^{(1)}(t,i\phi_1)}{i\phi_1}\right] d\phi_1,$$

this implies that

$$\begin{aligned} Q_{r_R}^{(1)}(x_T \geq \ln K) &= 1 - F^{(1)}(x_T;\ln K) \\ &= \frac{1}{\pi}\int_0^{-\infty} \mathrm{Re}\left[\frac{e^{i\phi_1 \ln K} f^{(1)}(t,i\phi_1)}{i\phi_1}\right] d\phi_1 + \frac{1}{2}. \end{aligned}$$

By using the definition of $Q_{r_R}^{(1)}$, we have that,

$$Q_{r_R}^{(1)}(x_T \geq \ln K) = \frac{\mathbb{E}_t^{Q_{r_R}}\left[\left(1_{\{x_T \geq \ln K\}}\right) S_T\left(1_{\{\tilde{\tau}>T\}}\right)\right]}{\mathbb{E}_t^{Q_{r_R}}\left[S_T\left(1_{\{\tilde{\tau}>T\}}\right)\right]},$$

which implies,

$$\begin{aligned} \mathbb{E}_t^{Q_{r_R}}\left[\left(1_{\{x_T \geq \ln K\}}\right) S_T\left(1_{\{\tilde{\tau}>T\}}\right)\right] &= Q_{r_R}^{(1)}(x_T \geq \ln K) \times \mathbb{E}_t^{Q_{r_R}}\left[S_T\left(1_{\{\tilde{\tau}>T\}}\right)\right] \\ &= \left(\frac{1}{\pi}\int_0^{-\infty} \mathrm{Re}\left[\frac{e^{i\phi_1} f^{(1)}(t,i\phi_1)}{i\phi_1}\right] d\phi_1 + \frac{1}{2}\right) f_{PD}^*(t,1,-1) \\ &= \Pi_1(t,T) + \frac{1}{2} f_{PD}^*(t,1,-1), \end{aligned}$$

which is an explicit expression for $I_1$.

For $I_2$ a similar process is required. Define the following probability measure,

$$Q_{r_R}^{(2)}(y) = \frac{\mathbb{E}_t^{Q_{r_R}}\left[\left(1_{\{y\}}\right)\left(1_{\{\tilde{\tau}>T\}}\right)\right]}{\mathbb{E}_t^{Q_{r_R}}\left[\left(1_{\{\tilde{\tau}>T\}}\right)\right]}.$$

The characteristic function of $x_T$ takes the following form,

$$\begin{aligned} f^{(2)}(t,i\phi_1) &= \mathbb{E}_t^{Q_{r_R}^{(2)}}\left[e^{i\phi_1 x_T}\right] \\ &= \frac{\mathbb{E}_t^{Q_{r_R}}\left[e^{i\phi_1 x_T}\left(1_{\{\tilde{\tau}>T\}}\right)\right]}{\mathbb{E}_t^{Q_{r_R}}\left[\left(1_{\{\tilde{\tau}>T\}}\right)\right]} \\ &= \frac{\mathbb{E}_t^{Q_{r_R}}\left[e^{i\phi_1 x_T}\left(1_{\{\tilde{\tau}>T\}}\right)\right]}{\mathbb{E}_t^{Q_{r_R}}\left[\left(1_{\{\tilde{\tau}>T\}}\right)\right]} \\ &= \frac{\mathbb{E}_t^{Q_{r_R}}\left[e^{i\phi_1 x_T} e^{-\sum_{s=t}^T \kappa_s}\right]}{\mathbb{E}_t^{Q_{r_R}}\left[e^{\sum_{s=t}^T \kappa_s}\right]} \\ &= \frac{f_{PD}^*(t,i\phi_1,-1)}{f_{PD}^*(t,0,-1)}. \end{aligned}$$

The corresponding distribution function is given by,

$$F^{(2)}(x_T; x) = \frac{1}{2} - \frac{1}{\pi}\int_0^{-\infty} \text{Re}\left[\frac{e^{i\phi_1 x} f^{(2)}(0, i\phi_1)}{i\phi_1}\right] d\phi_1,$$

which implies,

$$\begin{aligned} Q^{(2)}_{r_R}(x_T \geq \ln K) &= 1 - F^{(2)}(x_T; \ln K) \\ &= \frac{1}{\pi}\int_0^{-\infty} \text{Re}\left[\frac{e^{i\phi_1 \ln K} f^{(2)}(t, i\phi_1)}{i\phi_1}\right] d\phi_1 + \frac{1}{2}. \end{aligned} \tag{A.1}$$

By using Equation A.1 above and the definition of $Q^{(2)}_{r_R}$ it is possible to derive an expression for $I_2$,

$$\begin{aligned} I_2 &= \mathbb{E}_t^{Q_{r_R}}\left[\left(1_{\{\tilde{\tau}>T, S_T \geq K\}}\right)\right] \\ &= Q^{(2)}_{r_R}(x_T \geq \ln K) \times Q_{r_R}(\tilde{\tau} > T) \\ &= Q^{(2)}_{r_R}(x_T \geq \ln K) \times \mathbb{E}_t^{Q_{r_R}}\left[e^{\sum_{s=1}^{T}\kappa_s}\right] \\ &= Q^{(2)}_{r_R}(x_T \geq \ln K) \times f^*_{PD}(t, 0, -1) \\ &= \Pi_2(t, T) + \frac{1}{2} f^*_{PD}(t, 0, -1) \end{aligned}$$

For the derivation of $I_3$, the following probability measure is defined,

$$Q^{(3)}_{r_R}(y) = \frac{\mathbb{E}_t^{Q_{r_R}}\left[\left(1_{\{y\}} S_T\right)\right]}{\mathbb{E}_t^{Q_{r_R}}\left[S_T\right]},$$

and the characteristic function of $x_T$ under $Q^{(3)}_{r_R}$,

$$\begin{aligned} f^{(3)}(t, i\phi_1) &= \mathbb{E}_t^{Q^{(3)}_{r_R}}\left[e^{i\phi_1 x_T}\right] \\ &= \frac{\mathbb{E}_t^{Q_{r_R}}\left[e^{i\phi_1 x_T}\right]}{\mathbb{E}_t^{Q_{r_R}}\left[S_T\right]} \\ &= \frac{f^*_{PD}(t, i\phi_1 + 1, 0)}{f^*_{PD}(t, 1, 0)}. \end{aligned}$$

It is possible to show that,

$$Q^{(3)}_{r_R}(x_T \geq \ln K) = \frac{1}{\pi}\int_0^{-\infty} \text{Re}\left[\frac{e^{i\phi_1 \ln K} f^{(3)}(t, i\phi_1)}{i\phi_1}\right] d\phi_1 + \frac{1}{2},$$

which implies

$$\begin{aligned} I_3 &= Q^{(3)}_{r_R}(x_T \geq \ln K) \times \mathbb{E}_t^{Q_{r_R}}[S_T] \\ &= Q^{(3)}_{r_R}(x_T \geq \ln K) \times f^*_{PD}(t,1,0) \\ &= \Pi_3(t,T) + \frac{1}{2} f^*_{PD}(t,1,0). \end{aligned}$$

Finally,

$$\begin{aligned} I_4 &= \mathbb{E}_t^{Q_{r_R}}\left[\left(1_{\{S_T \geq K\}}\right)\right] \\ &= Q_{r_R}(x_T \geq \ln K) \\ &= 1 - Q_{r_R}(x_T \leq \ln K) \\ &= \frac{1}{\pi}\int_0^{-\infty} \mathrm{Re}\left[\frac{e^{i\phi_1 \ln K} f^*_{PD}(t, i\phi_1, 0)}{i\phi_1}\right] d\phi_1 + \frac{1}{2} \\ &= \Pi_4(t,T) + \frac{1}{2}. \end{aligned}$$

This implies,

$$\begin{aligned} \tilde{V}_t^{(FC)} &= (1-\theta)e^{r_C(T-t)}(I_1 - KI_2) + \theta e^{r_C(T-t)}(I_3 - KI_4) \\ &= (1-\theta)e^{r_C(T-t)}\left(\Pi_1(t,T) + \frac{1}{2}f^*_{PD}(t,1,-1) - K\left(\Pi_2(t,T) + \frac{1}{2}f^*_{PD}(t,0,-1)\right)\right) \\ &+ \theta e^{r_C(T-t)}\left(\Pi_3(t,T) + \frac{1}{2}f^*_{PD}(t,1,0) - K\left(\Pi_4(t,T) + \frac{1}{2}\right)\right), \end{aligned}$$

and

$$\begin{aligned} \tilde{V}_t^{(ZC)} &= (1-\theta)e^{r_F(T-t)}(I_1 - KI_2) + \theta e^{r_F(T-t)}(I_3 - KI_4) \\ &= (1-\theta)e^{r_F(T-t)}\left(\Pi_1(t,T) + \frac{1}{2}f^*_{PD}(t,1,-1) - K\left(\Pi_2(t,T) + \frac{1}{2}f^*_{PD}(t,0,-1)\right)\right) \\ &+ \theta e^{r_F(T-t)}\left(\Pi_3(t,T) + \frac{1}{2}f^*_{PD}(t,1,0) - K\left(\Pi_4(t,T) + \frac{1}{2}\right)\right), \end{aligned}$$

which completes the proof. □

# Index